# RIGA TECHNICAL UNIVERSITY

**Faculty of Computer Science and Information Technology**

**Department of Engineering Mathematics**

**IMAD CHADDAD**

Ph.D student of the Mathematical Modeling program

## THE INFLUENCE OF SURFACE ROUGHNESS ON THE STRUCTURE OF MAGNETOHYDRODYNAMIC FLOWS AND STABILITY OF SHALLOW WATER FLOWS

**Scientific supervisors :**

**Dr. habil.phys ,**

**Professor M.Ya.Antimirov**

**(Till 20.03.2005)**

**Dr. Math Professor Kolishkin.A**

**RIGA 2008**

# ABSTRACT

The main topic of the PhD thesis is the analysis of the factors that influence the structure and stability of magnetohydrodynamic (MHD) flows and shallow water flows. In particular, we shall concentrate of the effect of the roughness of the boundary. Methods of analysis are based on analytic solutions which are found for some MHD flows over the roughness elements in strong magnetic fields in rectangular ducts. The MHD solutions described in our work facilitate the investigation of the redistribution of the fluid in a region where the magnetic field is strong ( the Hartmann number is large) . The analysis of the behavior of MHD flows at high Hartmann numbers is a topic of increasing interest since it is mainly applicable to MHD devices such as pumps, and MHD generators. The main features of MHD liquid-metal flows at large Hartmann number are as follows: A ‘ flat’ velocity profile in the core of a channel and thin boundary layers near the boundaries. Electric currents induced in the fluid modify the field of the flow. Knowing the path of these currents then it is possible to predict the flow structure. In our analytical solution of the MHD problems where wall roughness is taken into account, the length of the sidewalls of the channel is considered infinitely long and that is why the Hartmann number (Ha) is taken to be sufficiently large and even sometimes the boundary limits approaches $+\infty$.

Hydraulic engineers are effectively using Chezy formula to estimate the “lumped” effect of turbulent flows such as computation of flow rate and losses in channels or pipes and design of open channels. The roughness of the boundary is taken care of by using empirical friction coefficients. These coefficients are related by several empirical formulas with the Reynolds number of the flow as well as with the roughness of the boundary. The coherent structures in wake flows are believed to appear as a final product of hydrodynamic instability of the flow. Methods of weakly nonlinear theory have been applied in the past to different flows and usually lead to amplitude evolution equations for the most unstable mode. One of such equations is the complex Ginzburg-Landau equation. Weakly nonlinear theory is applied to quasi-two-dimensional flows in [22] with Rayleigh friction (internal friction is assumed to be linearly related to the velocity distribution). It is shown in [22] that the coefficients of the Ginzburg-Landau equation for the case where the internal friction is represented by a linear function of the velocity strongly depend on the shape of the base flow profile. As a result it was concluded in [22] that weakly nonlinear models cannot be used for such cases since it is impossible to determine experimentally the base flow velocity distribution with high accuracy and, therefore, one cannot use reliable values of the coefficients of the Ginzburg-Landau equation in the analysis. However, in Part **3** of our work we show that small variations of linear stability characteristics do not lead to large changes in the Landau constant (the Landau constant is the

real part of one of the coefficients of the Ginzburg-Landau equation) when a nonlinear Chezy formula is used to model bottom friction.

This work consists of four parts. All of the parts are theoretical while the fourth part is practical dealing with corrosion of EUROFER steel in the Pb17Li flow and its application to D-T ( Deutrium-tritium ) plasma confinement in a reactor.

In the first part we state the principles of MHD flows and then we describe the influence of the surface roughness on the MHD flow of a conducting metal and state the governing equations. Since MHD flow problems are widely studied in channels of various forms and different boundary conditions, the results of such studies have direct applications in different fields of the magnetohydrodynamics [29], [38], and [58]. Since magnetohydrodynamics studies the motion of electrically conducting fluids in the presence of magnetic fields, it is obvious that the magnetic field influences the fluid motion. Usually in MHD problems electromagnetic force is added to the equation of motion and the magnetic field (through Ohm's law) changes the fluid motion. We describe some MHD flow problems in ducts over the roughness elements in a strong magnetic field and analytical solutions of such problems are obtained using of the Dirac delta function (see [3], [4], [6], [7], [12] and [13]).

Asymptotic analysis of these problems is performed for the case of strong magnetic fields and graphs of the z-components of the current are shown for different Hartmann numbers. Different boundary layers for the field velocity and for the z-components of the currents at large Hartmann numbers are analyzed. The MHD problem for fully developed flow is solved for the cases of a uniform and non-uniform external magnetic field where the surface roughness is taken into account. The distribution of fluid velocity, induced current $\varphi(y,z)$ with its potential and external magnetic field are derived (see the following references for the analysis of similar problems [2], [5], [11]-[13], [17], [18], [30], [31], [42], [50], [53], [54], [57], [59], [65], [69], & [74]).

The purpose of this part is to study and examine the induced magnetic profiles and get a clearer idea about the behavior of such flows of an electrically conducting fluid through channels (or ducts) .In fact, this problem is directly applicable to other MHD problems such as MHD generators, pumps, accelerators, and flowmeters [in flowmeter, a conducting fluid passes through an insulating pipe (duct) across which a uniform magnetic field is applied]. A potential gradient is created and can be measured by probes embedded in the walls of the pipe (this technique is used to measure the flow of blood in human bodies). In addition, the influence of the surface roughness on the MHD flow of a conducting metal may be useful for the techniques used

to set up the cooling system of the Tokamak reactor ( Tokamak is an acronym from the Russian words for toroidal magnetic confinement) .

The second part of our work is devoted to the calculation of some classes of improper oscillatory integrals. It is shown that oscillatory integrals in some cases can be transformed to integrals of non-oscillating functions. Such integrals have direct applications to MHD flows analyzed in the thesis. These results are applied in order to transform the solution of some MHD problems arising in half space $z \geq 0$ as a result of the roughness of the surface z=0 for various boundary layers (see [3], [4], [6], [7], [17], [21] , [72] & [74]).

During my seven year stay in Riga, LATVIA (one the main MHD application centers in EUROPE), I had the opportunity to visit some interesting sites related to MHD study such as the Physics Institute in Salaspils where I have seen the three recently planned experimental sessions (each 2000 hours long) which have been finished successfully. Results gained in these investigations demonstrated essential influence of magnetic field on the corrosion processes both in the intensity of corrosion and its character. New results concerning the profile of corrosion are obtained [55] & [56]. Such studies have an important implication on how to confine and control the burning D-T plasmas by a strong drag of magnetic fields inside a reactor [1], [9], [20], [55], [56], [70] and [73]. In addition, I had the opportunity to participate in some PAMIR MHD International Conferences ($4^{th}$ , $5^{th}$ and $7^{th}$ PAMIR International Conferences) . As a result of these activities the third part of the thesis describing practical aspects related to the effect of surface roughness on MHD flows ([1], [9], [20], [32]-[37], [39], [40], [48], [49], [55]-[57], [60], [64], [68], [70] and [73]) was written.

The fourth part is devoted to the analysis of shallow water flow in a weakly nonlinear regime using the complex Ginzburg-Landau equation (CGLE). It is shown in the previous studies [22] related to weakly nonlinear analysis of quasi-two-dimensional flows (shallow water flow is one of the examples considered in [22]) that the values of the Landau's constant differ by a factor of 3 for two different velocity profiles with linear stability characteristics (differing by not more that 20%). In other words, the Landau's constant was found to be quite sensitive to the shape of the base flow profile. In Part four of the thesis the bottom friction is modeled by a nonlinear Chezy formula [64]. The analysis of data presented in Table 1 and Table 2 shows that for a one-parametric family of shallow wake flows the changes in the linear stability characteristics resulted in even smaller changes in the coefficients of the CGLE. As a result, it is plausible to conclude that the complex Ginzburg-Landau equation can be used for the analysis of

shallow wake flows in a weakly nonlinear regime (see [8], [10], [14]-[16], [19], [22]-[24], [26], [43]-[47], and [67]) for the application of weakly nonlinear models to different flows in fluid mechanics..

# ANOTATION

# CONTENTS

# INTRODUCTION

Magnetohydrodynamics is a part of fluid mechanics which analyzes the dynamics of electrically conducting fluids and their interactions with magnetic fields. Examples of such fluids include plasmas and liquid metals.

The main set of equations which describes magnetohydrodynamics (MHD) is a combination of the Navier-Stokes equations of fluid dynamics and Maxwell's equations of electromagnetism (see [26], [27], and [50]). The corresponding differential equations have to be solved simultaneously. In fact, this is too complex to be done symbolically at all, except for the most trivial cases. For real world problems, numerical solutions are found using super computers. Since MHD is a fluid theory, it cannot treat kinetic phenomena (see [18], [50]). The interaction of a flow of an electrically conducting fluid with external magnetic field results in changes in the flow characteristics. These changes depend on the structure of the flow, the presence of conducting or non-conducting walls, the orientation of the magnetic field with respect to the flow and some other minor factors. For example, the presence of a magnetic field leads to larger pressure losses since in this case the pressure drop depends mainly on the Hartmann number (see [5], [28], and [53] &[54]).

Some studies of MHD problems in liquid metal flows have concentrated on the determination of the pressure drop in the flows in straight pipes perpendicular to the magnetic field [50], and [59]. One of the main problems in MHD that is important in applications is pressure losses in pipe bends. Some local variations in pipe bend and special conditions of fluids are used to reduce such pressure losses (see [50], [53], and [59]).

It is known that the velocity distribution in a liquid metal blanket exerts a decisive influence on heat and mass transport. Therefore, since knowledge of this distribution is required, studies in the corrosion and tritium transport field have been conducted (see [1], [55] and [56]). We mention here the latest study of MHD problems in liquid metal blankets of fusion reactor done by I. Micheal [52] and the very recent one done by the European Fusion Development Agreement ( EFDA) concerning the European fusion research programme that outlooks the infra-structures needed towards DEMO [37].

Other experiments were conducted to investigate the single phase convective heat transfer in a compact heat sink consisting of 26 rectangular microchannels of 300 μ m width and 800 μ m depth. The relative roughness is estimated to be 4-6 %. Dionized water was used as the working fluid. Tests were performed with the Reynolds number range of 162 and 1257. The inlet

liquid temperature of 30, 50, and 70ºC and the heating powers of 140 to 450 w were investigated (see [5], [57] and [65]). The platform area was $5.0 \times 1{,}53\,\mathrm{cm}^2$. It is found that the friction factors significantly depart from those of conventional theories, possibly attributable to the surface roughness. The temperature is actually dependent on the fluid physical properties which also influences the heat transfer characteristics to some extent. Correlations were provided for the friction factors. Such pressure losses have also been discussed in pipe bends and in magnetic field subject to local variations. For instance, in both of the papers [57] and [65] channel flows with transverse magnetic field were considered. As can be seen from the cited references, it is important to know the influence of surface roughness on the structure of MHD flows.

The main results obtained in this thesis are briefly summarized below. The principles of MHD flows are described in the first part of the thesis. The governing equations are presented for the case of a conducting fluid moving in a magnetic field perpendicular to the flow of the form:

$$\mathbf{B}^{\mathrm{e}} = \mathrm{B}_0 \mathbf{e}_z \text{ with the boundary } \tilde{z} = 0 \tag{0.1}$$

along with the governing equations of Magnetohydrodynamics (MHD). These equations represent a combination of the Euler's equations of fluid dynamics and the Maxwell's equations of electrodynamics:

$$\frac{\partial \vec{v}}{\partial t} + (\vec{v}\nabla)\vec{v} = -\frac{1}{\rho}\nabla p + \nu \Delta \vec{v} + \frac{1}{\rho}\left(\vec{j} \times \vec{B}\right) \tag{0.2}$$

$$\frac{\partial \vec{B}}{\partial t} = curl\left(\vec{v} \times \vec{B}\right) + \nu_m \Delta \vec{B} \tag{0.3}$$

$$div\,\vec{v} = 0 \tag{0.4}$$

$$div\vec{B} = 0 \tag{0.5}$$

Previous works concerning linear approximation to the flow over roughness elements in a strong magnetic field [2], [28], and [50] are generalized for the case of the roughness of the surface considered in the form

$$\tilde{z} = \tilde{\chi}_0 \cos(\pi\tilde{x} / 2L) \tag{0.6}$$

where the conducting fluid is located in the half space $\tilde{z} > 0, -\infty < \tilde{x}, \tilde{y} < +\infty$ and the external magnetic field is of the form $B^c = B_0 e_z$ and the boundary $\tilde{z} = 0$ is non conducting. We assume a steady current flow with the density $\tilde{\mathbf{j}} = j_0 \mathbf{e}_x$ in the direction of the x-axis. In this case, if the surface $\tilde{z} = 0$ is ideally smooth then the flow is absent because electromagnetic force $\vec{F} = \vec{\tilde{j}} \times \vec{B}$ is constant and $rot\vec{F} = 0$. Suppose that the roughness on the surface $\tilde{z} = 0$ has the rectangular form (see Fig.1):

$$\tilde{z} = \tilde{\chi}_0 \ \tilde{f}(\tilde{x}) = \tilde{\chi}_0 \left[\eta(\tilde{x} + L) - \eta(\tilde{x} - L)\right] = \begin{cases} \tilde{\chi}_0, & -L < \tilde{x} < L, \\ 0, & |\tilde{x}| > L, \end{cases} \qquad (0.7)$$

We started part 1 of our work from the result obtained in monograph [71] where MHD flow of an incompressible fluid in an infinitely long plane channel with the constant cross section with the walls parallel to the y-axis is considered. The problem discussed in [71] is generalized in our work for the case of the surface roughness in the form:

$$\tilde{z} = \begin{cases} \tilde{f}(\tilde{x}), -L \le \tilde{x} \le L, -\infty < \tilde{y} < +\infty, \\ 0, \tilde{x} \notin (-L, L). \end{cases} \qquad (0.8)$$

We consider dimensionless MHD equations for the fluid velocity $V_y(y,z)$, and the potential for the induced current $\Phi(y,z)$ in the form:

$$\Delta V_y - Ha^2 V_y + Ha \frac{\partial \Phi}{\partial x} = 0, \qquad (0.9)$$

$$\Delta \Phi = Ha \frac{\partial V_y}{\partial x}, \qquad (0.10)$$

where Ha denotes the Hartmann number.

We note here that the fully developed MHD flow is considered in the direction of the y-axis while the external magnetic field and the given external current have only x and z components which do not depend on the y variable. There is also here the external current, which is parallel to boundary z=0 , and that is the case if the roughness is absent.

Using the equation of continuity we obtain the following relationship

$$\int_0^{\infty} j_x(x_0, z)dz \to \frac{\pi D}{2} \text{ as } Ha \to \infty. \qquad (0.11)$$

It is shown in the thesis that when $Ha \to \infty$ almost all of this full current flow through the cross section of Hartmann boundary layer $x = x_0 > 0$, $0 \le z < Ha^{-1}$, so that

$$\int_0^{Ha^{-1}} j_x(x_0.z)dz = \frac{\pi D}{4} Ha \int_0^{Ha^{-1}} \psi(x_0, z) e^{-zHa} dz \approx \frac{\pi D}{2} Ha \int_0^{Ha^{-1}} e^{-zHa} dz = \frac{\pi D}{2}\left(1 - e^{-1}\right). \qquad (0.12)$$

The roughness of an infinitely long prism is considered ( parallel to y as $V_y(x,z)\vec{e}_y$ with constant arbitrary cross-section. Besides, we assert the Bio-savare law which states that the case of induced magnetic field does not depend on the variable y. An analytical solution of the problem about MHD flow of a conducting fluid in the half space ( z > 0 ) with a special form of roughness on boundary z = 0 is obtained.[2], [5], [12] & [13]. Besides, the results of numerical calculations and streamlines of induced current are presented by graphs. In more

details, we investigate the asymptotic of functions $V_y(x,z)$ , $j_x(x,z)$ $j_z(x,z)$. As a result, several boundary layers of functions $V_y(x,z)$ and $j_z(x,z)$ as $Ha \to \infty$ are obtained. Besides, for the evaluation of Hartmann numbers at which the asymptotic formulae (3.11)-(3.14) are correct we compare the numerical results for the component $j_z(x,z)$, obtained by exact formula (2.31) and by asymptotic formula (2.70). These numerical results for Hartmann numbers Ha =10, 30 , 50 are shown on Fig.3 . For Hartmann numbers $Ha \geq 10$ the results obtained by exact formula (2.31) and by asymptotic formula (2.70) practically coincide. The package "Mathematica" is used here.

The streamlines of the current $j(x,z)$ are calculated by the formula:

$$\frac{dz}{dx} = \frac{j_z(x,z)}{j_x(x,z)} \qquad (0.13)$$

Calculations are done for the Hartmann numbers Ha=5 and Ha=10 and for various values of initial conditions $z(0)$.

The solutions of certain problems in MHD flow of conducting fluid in the half space ( z > 0 ) are expressed in terms of improper integrals of the product of some meromorphic function and the function $\exp(-a\sqrt{\lambda^2+b^2}\cos\lambda\cos\lambda x)$ where a > 0 , b > 0 and x > 0 which is the x-coordinate in the Cartesian coordinate system. It is difficult to calculate these integrals numerically since the integrands are strongly oscillating at the large x. Methods of calculation of such integrals are discussed in part **2** of our work.

We considered the improper integral having the form:

$$\int_0^\infty \frac{P_n(\lambda^2)}{Q_m(\lambda^2)} e^{-a\sqrt{\lambda^2+b^2}} \frac{\cos\lambda\cos\lambda x}{\lambda^2 - \frac{\lambda^2}{4}} d\lambda \qquad (0.14)$$

It is assumed that all the zeros of polynomial $Q(\lambda^2)$ are simple and have the form:

$$\lambda_k{}^2 = -a_k{}^2,\ k = 1, 2, \cdots 3, ..., n. \qquad (0.15)$$

Using the Fourier cosine transform of the form

$$F_c(\lambda) = \sqrt{\frac{2}{\pi}} \int_0^\infty f(x)\cos\lambda x dx \qquad (0.16)$$

and evaluating the integral, we obtain

$$\int_0^\infty \frac{e^{-a\sqrt{\lambda^2+b^2}}}{\sqrt{\lambda^2+b^2}} \cos\lambda x\, d\lambda = K_0(b\sqrt{a^2+x^2}) \qquad (0.17)$$

where $K_0$(z) is the modified Bessel function of order zero of the second kind.

Differentiating (0.17) and making suitable substitutions, we get :

$$I_2 = \sqrt{\frac{2}{\pi}} \int_0^{\infty} e^{-a\sqrt{\lambda^2+b^2}} \cos \lambda x \, d\lambda = \sqrt{\frac{2}{\pi}} \frac{K_1(b\sqrt{a^2+x^2})}{\sqrt{a^2+x^2}} = f(x) \qquad (0.18)$$

It is shown in part 2 of the thesis that integrals (0.14) are transformed into integrals of monotone functions using the convolution theorem for product of two Fourier cosine transforms and the formulas (0.17) and (0.18). Similar examples and other applications to some MHD problems are provided (see [3], [6], [7], [11] and [27]). We proceed to examine the solution of this problem through the use of asymptotic evaluation for different Hartmann numbers with their corresponding graphs to showing numerical results of the current's components.

Linear approximation to the flow over roughness elements in a strong magnetic field is a subject of increasing interest nowadays especially for the fact that this study is directly linked to other MHD phenomena such as the MHD studies on the EUROFER corrosion of Pb17-Li at 550°C. Three experimental sessions had been recently done in the Physics Institute in Salaspils and had been completed successfully this year [56]. The surface of the corroded metal on the wall is described by a simplest periodic structure that reads:

$$Z = Z(y) = \chi_0 \cos(\pi Y / L) \qquad (0.19)$$

where $\chi_0$ and L represent the scales of the considered roughness ([18], [23], [55] and [56]). Results gained in these investigations demonstrated essential influence of magnetic field on the corrosion processes both in the intensity of corrosion and its character. New results concerning the profile of corrosion are obtained [55], [56]. Note that the results of this study can be used to decide how to control the Deuterium-Tritium (D-T) burning plasmas by a strong magnetic field drag inside of a reactor [1], [55], [56], [70] and [73]. Recent results are reported as well in the fourth section of this work.

This Deuterium-Tritium (D-T) Cycle is:

$$D + T \rightarrow n + \alpha + 17.58 MeV \qquad (0.20)$$

The components along with the consequences of this important equation are briefly explained in the following papers ( [1], [9], [20], [28] ,[32]-[37], [40], [49], [56], [64], [70] and [73]).

Many works and experiments were done in the purpose of reducing pressure losses in MHD duct channels, two concepts are considered ideally practical for diminishing the pressure losses. The first is determined by an advantageous channel routing and the other relies on the reduction of the electrical conductivity of the channel. Because of the fact that an advantageous channel routing is depending mainly on the corrosion rate of the channel's wall, for this reason and on third part of our work we overlook the investigation of corrosion phenomena in EUROFER steel

in Pb17-Li stationary flow exposed to a magnetic field as for being one of the candidate materials used for fusion reactors[1], [9], [20], [28], [32]-[37] , [40] , [49] , [51], [55] , [56] , [62] , [70] and [73]

The fourth part is devoted to the analysis of shallow water flow in a weakly nonlinear regime using the Ginzburg-Landau equation. One of the major reasons that led to the study of this part is the analysis performed in [22] for different quasi-two-dimensional flows (one of the examples of such flows is shallow water flow). Calculations presented in [22] showed that the values of the Landau's constants differ by a factor of 3 for two different velocity profiles with very similar linear stability characteristics. The analysis in [22] is performed under the assumption that the internal friction is a linear function of the velocity. In particular, for quasi-two-dimensional flows [20] the internal friction was modelled in [19] by means of the Rayleigh's formula

$$\vec{f}_R = -\lambda_R \vec{u} \tag{0.21}$$

In our work we show that for the case where the friction force is a nonlinear function of the velocity the changes in the linear stability characteristics resulted in even smaller changes in the coefficients of the CGLE. As a result, it is plausible to conclude that the complex Ginzburg-Landau equation can be used for the analysis of shallow wake flows in a weakly nonlinear regime ( [8], [10], [14], [15], [16], [19], [23], [26], [43]-[47], [66] and [67]).

It is assumed here that the CGLE (Complex Ginzberg-Landau equation) can be used to describe spatio-temporal dynamics of shallow wake flows. We consider the base flow of the form

$$\vec{U} = (U(y),0) \tag{0.22}$$

where

$$U(y) = 1 - \frac{2R}{1-R}\frac{1}{\cosh^2(\alpha y)}. \tag{0.23}$$

We adopt in the present study the profile of the base flow which is suggested in [61] after careful analysis of available experimental data for deep water flows behind circular cylinders. The parameter $R$ is the velocity ratio: $R = (U_m - U_a)/(U_m + U_a)$, where $U_m$ is the wake centerline velocity and $U_a$ is the ambient velocity, and $\alpha = \sinh^{-1}(1)$. It is shown in [10] that under the rigid-lid assumption the linear stability of wake flows in shallow water is described by the following eigenvalue problem:

$$\varphi_1''(U-c+SU)+SU_y\varphi_1'+\left(k^2-U_{yy}-k^2U-\frac{S}{2}kU\right)\varphi_1=0 \tag{0.24}$$

$$\varphi_1(\pm\infty)=0, \tag{0.25}$$

where the perturbed stream function of the flow, $\psi(x,y,t)$, is assumed to be of the form

$$\psi(x,y,t)=\varphi_1(y)\exp[ik(x-ct)]+c.c. \tag{0.26}$$

Using $T_k(r)$ is the Chebyshev polynomial of degree $k$, then the collocation points $r_j$ are

$$r_j=\cos\frac{\pi j}{N},\ j=0,1,...,N. \tag{0.27}$$

Applying the collocation method we obtain the following equation:

$$(B-\lambda C)a=0 \tag{0.28}$$

where $B$ and $C$ are complex-valued matrices and

$a=(a_1a_2...a_N)^T$.

Then our problem is solved numerically by means of the IMSL routine DGVCCG. The critical values of the stability parameters $k,S$ and $c$ for different values of $R$ are given in Table I (here $S_c=\max_k S$). Next, we perform weakly nonlinear analysis in the neighborhood of the critical point. As a result, calculations presented in our paper demonstrate that the coefficients of the CGLE are not so sensitive to the variation of the parameter $R$ of the base flow and not only the Landau constant is not so sensitive to the changes in the profile but all the coefficients of the CGLE do not vary too much. The results that support such conclusions are shown in Tables 1 and 2. This contradicts to what was concluded in [22] that it would be impossible to apply methods of weakly nonlinear theory in practice since the base flow profile cannot be determined very precisely in experiments.

After so many works and experiments were done in the purpose of reducing pressure losses in MHD duct channels, two concepts are considered ideally practical for diminishing the pressure losses. The first is determined by an advantageous channel routing and the other relies on the reduction of the electrical conductivity of the channel. Because of the fact that an advantageous channel routing is depending mainly on the corrosion rate of the channel's wall, for this reason and on fourth part of our work we overlook the investigation of corrosion phenomena in EUROFER steel in Pb17-Li stationary flow exposed to a magnetic field as for being one of the candidate materials used for fusion reactors[1], [9], [20], [28], [32]-[37] , [40] , [49] , [51], [55] , [56] , [62] , [70] and [73]

# 1. FLOW OVER THE ROUGHNESS ELEMENTS IN A STRONG MAGNETIC FIELD

## 1.1 PRINCIPLES OF MHD FLOWS

The main MHD equations can be derived from the Navier-Stokes equations of fluid dynamics and the Maxwell equations. These MHD equations describe the complex couplings between the flow variables, i.e. the density, the velocity, the total energy, the pressure tensor, the gravitational force, and the magnetic field. As a matter of fact, MHD ( magnetohydrodynamics) has a vast range of practical applications such as control over motion of liquid metal in ducts and creation of new MHD pumps which do not contain movable elements. In addition to that, MHD has also a very important application in astrophysics for the explanation of the nature of the earth's magnetic field presence .[21] & [29]

The main principles that govern MHD flows are:

1. Electric eddy currents flow in a plane perpendicular to the main direction of the flow. They cause the thickness of the wall boundary layer to decrease and wall friction to Increase, i.e. the Hartmann effects.
2. If the channel wall is electrically conducting, the eddy currents are back-circuited via this wall. This gives rise to the electromagnetic volume forces contracting the fluid motion. ( We consider here in our case that the channel wall is not electrically conducing to reduce the MHD pressure losses ).
3. When the channel flow enters and leaves the homogeneous magnetic field zone, i.e., the field boundary zones, eddy currents are generated which likewise cause pressure losses counteracting the flow.
4. Another effect occurring both in the fluid flowing transversally and in the fluid flowing parallel to the magnetic field causes turbulence suppression, this laminarization leads to a big increase in the critical Reynolds number. Here, we expand some important comments on how to reduce the MHD pressure losses

The first concept is guaranteed when the coolant flow to be transformed from the poloidal flow direction, characterized by slow velocity, to a toroidal flow in narrower channels surmounting the original channels and characterized by a higher velocity . The flow in the poloidal direction is almost perpendicular to the direction of the magnetic flux density of the plasma holding field and is associated with MHD pressure losses. The higher flow velocity guarantees a good heat transfer. The abrupt change of flow direction (poloidal-toroidal-poloidal) in the magnetic field has two characteristics : Firstly, this elbow constitutes the point of the maximum loading of the

first wall. Secondly, the sharp deflection in the elbow might cause de-attachement of flow accompanied by the formation of hot spots. To counteract this process, guide plates of baffles could be installed in the deflection zone. [29], [57] and [65] .

The second concept is insulation between liquid and wall both the required pumping power and the mechanical stresses in the channel wall might become inadmissibly high. Reduction in stress by increasing the wall thickness is not possible because in non-insulated walls the pressure loss in a first approximation increases linearly with the wall thickness. A way out of this problem could consist in providing an electric insulation between the liquid metal and the supporting wall. Two methods are eligible. The most obvious idea would be to coat the inner side of the channel wall with an insulating material. However, no suitable material and coating technique have been found till this day to achieve an adequate service life if wall is in contact with the liquid metal. Therefore, the second method is more promising under which the wall is given a sandwich structure. The liquid metal is in contact with a thin (about 1 mm thick) wall supported via an electric insulator by the load carrying channel wall. This technique is applied above all for the supply and return manifolds of the blanket because the radiation exposure of the insulator is negligibly small in these manifolds. Two mathematical models for MHD-flows in a fusion reactor blanket have been considered. The first one describes fully-developed flows and the second governs non-uniform and non-steady-state flows. This model is derived from 3-D Navier-Stokes-Maxwell equations by their integration along the direction of the applied magnetic field. [1], [29], [55], [56], [57] and [65] .

## 1.2 THE FORM OF MAGNETIC FIELD AND MHD EQUATIONS FOR FULLY DEVELOPED MHD FLOW CAUSED BY THE ROUGHNESS OF THE BOUNDARY

The MHD flow of an incompressible fluid in an infinitely long channel with the constant cross section when the wall is taken parallel to the $\tilde{y}$ axis is considered in [71]. It is proved that the velocity of a fully developed flow in such channel is:

$$\vec{V} = V_y(x,z)\vec{e}_y, \tag{1.1}$$

and the magnetic field $\vec{B}$ is of the form

$$\vec{B} = \vec{B}_\perp(x,z) + B_y(x,y,z)\vec{e}_y, \tag{1.2}$$

where

$$\vec{B}_\perp(x,z) = B_x(x,z)\,\vec{e}_x + B_z(x,z)\vec{e}_z \tag{1.3}$$

Then by substituting (1.2) into the equation div $\vec{B} = 0$, we get :

$$\frac{\partial B_y}{\partial y} = 0 \text{ , i.e. } B_y = B_y(x,z) = b(x,z) + y\theta(x,z) \tag{1.4}$$

at the condition that

$$div\,\vec{B}_\perp = -\theta(x,z) \tag{1.5}$$

Further analysis shows that

$$\theta(x,z) = C = const, \quad C = 0 \text{ or } C \neq 0 \tag{1.6}$$

and that $B_y(x,z)\vec{e}_y$ is the induced magnetic field, $\vec{B}_\perp(x,z)$ is the given external magnetic field. We consider a similar problem about the MHD flow in half-space $\tilde{z} \geq 0$ caused by the roughness of the boundary $\tilde{z} = 0$ . In contrast to what is done in monograph [71] it is assumed here at the first that the induced magnetic field $\vec{B}^i$ has the x, y and z components. After that the symmetry of the flow is used and it is proved that the induced magnetic field has a single y-component, i.e. has the form of (1.4) with $\theta = 0$. We consider uniform external magnetic field in subsection 1.2.1 and non uniform magnetic field in subsection 1.2.2.

### 1.2.1 THE PROBLEM IN THE CASE OF A UNIFORM EXTERNAL MAGNETIC FIELD

The geometry of the flow is given on Fig. 1.

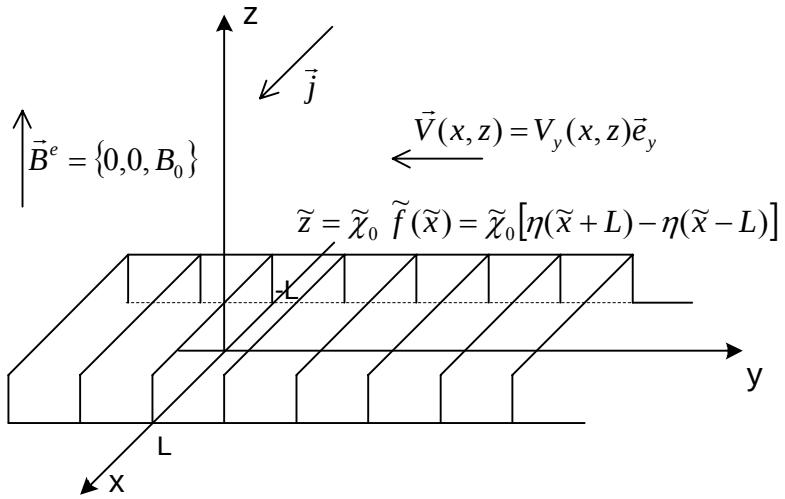


***Figure 1*. The geometry of the flow in rectangular form.**

The conducting fluid is located in the half-space $\tilde{z}>0$ , $-\infty<\tilde{x},\tilde{y}<+\infty$. The external magnetic field is of the form :

$$\vec{B}^e = B_0\,\vec{e}_z \tag{1.7}$$

A steady current flows with the density $\vec{j}_0 = j_0\,\vec{e}_x$ in the direction of the x-axis. If the surface $\tilde{z}=0$ is ideally smooth, then the flow is absent because the electromagnetic force $\vec{F}=\vec{j}\times\vec{B}^e$ is constant and rot $\vec{F}=0$. Suppose further that on the surface $\tilde{z}=0$ the roughness is of the form :

$$\tilde{z}=\begin{cases}\tilde{f}(\tilde{x}), -L\le\tilde{x}\le L, -\infty<\tilde{y}<+\infty,\\ 0, \tilde{x}\notin(-L,L).\end{cases} \tag{1.8}$$

In this case the full current is equal to $\vec{j}=\vec{j}_0+\vec{j}(\tilde{x},\tilde{z})$ and the flow of the fluid with velocity

$$\vec{V}_y = \tilde{V}_y(\tilde{y},\tilde{z})\,\vec{e}_y \tag{1.9}$$

arises in the opposite direction of the $\tilde{y}$-axis (see Fig.1)

We will prove that the induced magnetic field $\vec{B}^i$ in this case has the form

$$\tilde{\vec{B}}^i = \tilde{B}^i(\tilde{x},\tilde{z})\vec{e}_y \tag{1.10}$$

and the MHD equations for the fluid velocity $V_y(y,z)$ and for the potential of the induced current $\Phi(y,z)$, using the dimensionless variables, have the form

$$\Delta V_y - Ha^2 V_y + Ha\frac{\partial \Phi}{\partial x} = 0, \tag{1.11}$$

$$\Delta\Phi = Ha\frac{\partial V_y}{\partial x}, \tag{1.12}$$

where $\Delta = \partial^2/\partial x^2 + \partial^2/\partial z^2$, $Ha = B_0 L\sqrt{\sigma/\rho\nu}$ is the Hartmann number and where $\sigma,\rho,\nu$ are, respectively, the conductivity, the density and the viscosity of the fluid. We use the MHD equation of incompressible fluid and the Ohm's law (see[29], [50] and [58]) :

$$\left(\tilde{\vec{V}}\nabla\right)\tilde{\vec{V}} = -\frac{1}{\rho}grad\tilde{P} + \nu\Delta\tilde{\vec{V}} + \frac{1}{\rho}\left(\tilde{\vec{j}}\times\tilde{\vec{B}}\right), \tag{1.13}$$

$$\tilde{\vec{j}} = \sigma\left(\tilde{\vec{E}} + \tilde{\vec{V}}\times\tilde{\vec{B}}\right) = \sigma\left(-grad\tilde{\Phi} + \tilde{\vec{V}}\times\tilde{\vec{B}}\right), \tag{1.14}$$

where $\Delta = \frac{\partial^2}{\partial\tilde{x}^2} + \frac{\partial^2}{\partial\tilde{y}^2} + \frac{\partial^2}{\partial\tilde{z}^2}$, $\tilde{\vec{V}}\nabla = V_x\frac{\partial}{\partial\tilde{x}} + V_y\frac{\partial}{\partial\tilde{y}} + V_z\frac{\partial}{\partial\tilde{z}}$.

In our case

$$\tilde{\vec{V}} = \tilde{V}_y(x,z)\vec{e}_y, \tag{1.15}$$

$$\vec{B} = \tilde{\vec{B}}^i(\tilde{x},\tilde{z}) + \vec{B}^e, \tag{1.16}$$

where $\tilde{\vec{B}}^i$ is the induced magnetic field.

First , we prove that

$$\tilde{\vec{B}}^i(\tilde{x},\tilde{z}) = B^i(\tilde{x},\tilde{z})\vec{e}_y \tag{1.17}$$

at the condition that the vector of the induced current has the form

$$\tilde{\vec{j}}(\tilde{x},\tilde{z}) = j_x(\tilde{x},\tilde{z})\vec{e}_x + j_z(\tilde{x},\tilde{z})\vec{e}_z \tag{1.18}$$

and it will be shown as the corollary that the vector of fluid velocity is given by (1.15). For this purpose we use the Bio-Savare law, according to which the induced magnetic field vector $d\vec{B}$ created by an element $d\vec{l}$ of infinitely thin wire directed along the current $\vec{I}$ is equal to

$$d\vec{\tilde{B}} = I\frac{d\vec{l}\times\vec{r}_{M'M}}{\left|\vec{r}_{M'M}\right|^3}, \tag{1.19}$$

where $\vec{r}_{M'M}$ is a radius vector connecting the point $M'(\tilde{x}',\tilde{y}',\tilde{z}')\in d\vec{l}$ and the point of observation $M(\tilde{x},\tilde{y},\tilde{z})$ (see Fig. 2):

$$\vec{r}_{M'M} = (\tilde{x}-\tilde{x}')\vec{e}_x + (\tilde{y}-\tilde{y}')\vec{e}_y + (\tilde{z}-\tilde{z}')\vec{e}_z. \tag{1.20}$$

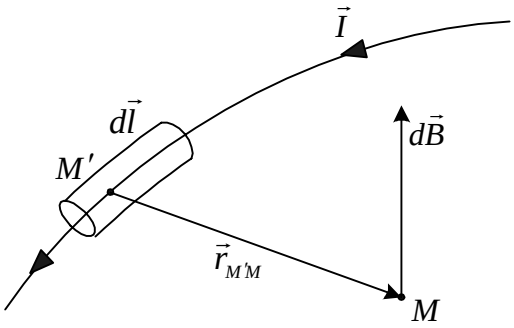


Figure 2. Magnetic induction $d\vec{B}$ caused by elementary current $Id\vec{l}$ .

Without loss of generality we can choose the point of observation *M (0, 0, 0)* in the origin. For each point $M'(\tilde{x}',\tilde{y}',\tilde{z}')$ in the fluid we always can choose the symmetric point $N'(\tilde{x}',-\tilde{y}',\tilde{z}')$ with respect to point *M (0, 0, 0).* We consider the magnetic induction $d\vec{B}$ caused by elementary current $Id\vec{l}$ passing through the point $M'(\tilde{x}',\tilde{y}',\tilde{z}')$ and by elementary current $I_1 d\vec{l}$ passing through the symmetric point $N'(\tilde{x}',-\tilde{y}',\tilde{z}')$. ( see figure 3) Here $\vec{I}$ and $\vec{I}_1$ are the currents with density $\vec{\tilde{j}}(\tilde{x},\tilde{z})$ given by formula(1.18).

Since vector $\vec{\tilde{j}}(\tilde{x},\tilde{z})$ doesn't depend of variable $\tilde{y}$ we have in our case that $\vec{I}_1 = \vec{I}$

Then according to formula(1.19) we have

$$d\vec{B}\Big|_M = Dd\vec{l}\times\left(\vec{r}_{M'M} + \vec{r}_{N'M}\right) \tag{1.21}$$

where $D = I\left|r_{MM'}\right|^{-3}$, $d\vec{l} = dl_x\vec{e}_x + dl_z\vec{e}_z$, (1.22)

$$\vec{r}_{M'M} = -\left(\tilde{x}'\vec{e}_x + \tilde{y}'\vec{e}_y + \tilde{z}'\vec{e}_z\right),\ \vec{r}_{N'M} = -\left(\tilde{x}'\vec{e}_x - \tilde{y}'\vec{e}_y + \tilde{z}'\vec{e}_z\right). \quad (1.23)$$

Substituting (1.22) , (1.23) into (1.21) we obtain:

$$d\vec{B} = -D\left(dl_x\vec{e}_x + dl_z\vec{e}_z\right)\times\left(2\tilde{x}'\vec{e}_x + 2\tilde{z}'\vec{e}_z\right)$$

or

$$d\vec{B} = D\left(2\tilde{z}'dl_x - 2\tilde{x}'dl_z\right)\vec{e}_y\,. \quad (1.24)$$

Summing formula (1.24) over the whole elements $d\vec{l}$ in the fluid we obtain formula (1.17), which completes the proof.

In order to obtain equations (1.11), (1.12) we substitute vectors $\tilde{\vec{V}}$ and $\tilde{\vec{B}}^i$ from (1.15), (1.16) and (1.17) into equations(1.13), and (1.14). We get :

$$\tilde{\vec{V}} = \tilde{V}_y(x,z)\vec{e}_y\,,\ \ \tilde{\vec{B}}(\tilde{x},\tilde{z}) = B_0\vec{e}_z + \tilde{B}^i(\tilde{x},\tilde{z})\vec{e}_y\,. \quad (1.25)$$

Consequently

$$\tilde{\vec{V}}\times\tilde{\vec{B}} = \tilde{V}_y(x,z)\vec{e}_y\times\left(B_0\vec{e}_z + \tilde{B}^i(\tilde{x},\tilde{z})\vec{e}_y\right) = B_0\tilde{V}_y(x,z)\vec{e}_x\,, \quad (1.26)$$

$\tilde{\vec{j}}\times\tilde{\vec{B}} = \sigma\left(-\,grad\tilde{\Phi} + B_0\tilde{V}_y\vec{e}_x\right)\times\left(B_0\vec{e}_z + \tilde{B}^i\vec{e}_y\right)$, i.e.

$$\tilde{\vec{j}}\times\tilde{\vec{B}} = \sigma\left\{B_0\frac{\partial\tilde{\Phi}}{\partial\tilde{x}}\vec{e}_y - \frac{\partial\tilde{\Phi}}{\partial\tilde{x}}\tilde{B}^i\vec{e}_z + \frac{\partial\tilde{\Phi}}{\partial\tilde{z}}\tilde{B}^i\vec{e}_x - {B_0}^2\tilde{V}_y\vec{e}_y + B_0\tilde{V}_y\tilde{B}^i\vec{e}_z\right\}, \quad (1.27)$$

$$\left(\tilde{\vec{V}}\nabla\right)\tilde{\vec{V}} = 0\,. \quad (1.28)$$

Substituting (1.27) and (1.28) into (1.13) and projecting on the y axis we obtain :

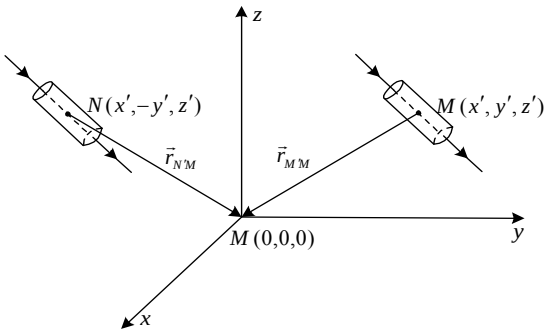


Figure 3. Symmetric representation needed to the proof of formula (1.24) [71]

$$0 = -\frac{1}{\rho}\frac{\partial \tilde{P}(\tilde{x},\tilde{y},\tilde{z})}{\partial \tilde{y}} + \nu\left(\frac{\partial^2}{\partial \tilde{x}^2} + \frac{\partial^2}{\partial \tilde{z}^2}\right)\tilde{V}_y(\tilde{x},\tilde{z}) + \frac{\sigma}{\rho}\left[B_0\frac{\partial \tilde{\Phi}(\tilde{x},\tilde{z})}{\partial \tilde{x}} - B_0^2\tilde{V}_y(\tilde{x},\tilde{z})\right]. \qquad (1.29)$$

Since all of the terms in equation (1.29) except for the term $\partial\tilde{P}/\partial\tilde{y}$, do not depend on variable $\tilde{y}$ then term $\partial\tilde{P}/\partial\tilde{y}$ also must not depend on variable $\tilde{y}$, i.e. it must be

$$\frac{\partial \tilde{P}}{\partial \tilde{y}} = F_1(\tilde{x},\tilde{z}) \Rightarrow \tilde{P} = F_1(\tilde{x},\tilde{z})\tilde{y} + F_2(\tilde{x},\tilde{z}), \qquad (1.30)$$

where $F_1$ and $F_2$ are the arbitrary functions.

Substituting (1.30) and (1.27) into (1.13) and projecting on the x and z axis we obtain the following two equations:

$$0 = -\frac{\tilde{y}}{\rho}\frac{\partial F_1}{\partial \tilde{x}} - \frac{1}{\rho}\frac{\partial F_2}{\partial \tilde{x}} + \frac{\sigma}{\rho}\frac{\partial \tilde{\Phi}}{\partial \tilde{z}}B^i, \qquad (1.31)$$

$$0 = -\frac{\tilde{y}}{\rho}\frac{\partial F_1}{\partial \tilde{z}} - \frac{1}{\rho}\frac{\partial F_2}{\partial \tilde{z}} + B^i\left(-\frac{\partial \tilde{\Phi}}{\partial \tilde{x}} + B_0 V_y\right). \qquad (1.32)$$

Since all the terms located on the right hand sides of equations (1.31) and (1.32) except the first ones do not depend on $\tilde{y}$, then the first terms in these equations also do not depend on $\tilde{y}$, i.e. it must be

$$\frac{\partial F_1}{\partial \tilde{x}} = 0, \quad \frac{\partial F_1}{\partial \tilde{z}} = 0 \Rightarrow \quad F_1 = C = const. \qquad (1.33)$$

Consequently, equations (1.30)-(1.32) are of the form:

$$\frac{\partial \tilde{P}}{\partial \tilde{y}} = C \ \ (C \text{ is a constant}) \qquad (1.34)$$

$$\Rightarrow \tilde{P}(\tilde{x}.\tilde{z}) = C\tilde{y} + F_2(\tilde{x}.\tilde{z}), \qquad (1.35)$$

$$\frac{\partial F_2(\tilde{x},\tilde{z})}{\partial \tilde{x}} = \sigma\frac{\partial \tilde{\varphi}}{\partial \tilde{z}}B^i, \qquad (1.36)$$

$$\frac{\partial F_2(\tilde{x},\tilde{z})}{\partial \tilde{z}} = \rho B^i\left(\frac{\partial \tilde{\Phi}}{\partial \tilde{x}} - B_0\tilde{V}_y\right). \qquad (1.37)$$

Since in the case of our problem the external gradient of pressure is absent, then

in equation(1.34) and (1.35) we must have :

$$C = 0,\ \widetilde{P}(\widetilde{x},\widetilde{z}) = F_2(\widetilde{x},\widetilde{z}). \tag{1.38}$$

So, equation (1.29) becomes now of the form:

$$\nu\left(\frac{\partial^2}{\partial\widetilde{x}^2}+\frac{\partial^2}{\partial\widetilde{z}^2}\right)\widetilde{V}(\widetilde{x},\widetilde{z})+\frac{\sigma}{\rho}\left[B_0\frac{\partial\widetilde{\Phi}(\widetilde{x},\widetilde{z})}{\partial\widetilde{x}}-B_0{}^2\widetilde{V}_y(\widetilde{x},\widetilde{z})\right]=0. \tag{1.39}$$

We use now the dimensionless quantities by taking the values $L, \nu/L, B_0, \nu\sqrt{\rho\nu/\sigma}, \nu\sqrt{\rho\nu/\sigma}/L^2$ as the scales of length, velocity, magnetic field, potential and current, respectively.

To obtain equation (1.12) , it is enough to apply operation of divergence to equation (1.14)

and use the equation of continuity $div\,\vec{\tilde{j}}=0$ and equation (1.26):

$$0 = -\Delta\widetilde{\Phi} + B_0 div\widetilde{V}_y(\widetilde{x},\widetilde{z})\vec{e}_y\ , \tag{1.40}$$

i.e.

$$\Delta\widetilde{\Phi} = B_0\frac{\partial\widetilde{V}_y}{\partial\widetilde{y}}\ . \tag{1.41}$$

Passing in formulae (1.41) to the dimensionless variables, we obtain equation (1.12).

To obtain pressure $\widetilde{P}(\widetilde{x},\widetilde{z})$ we must know function $F_2(\widetilde{x},\widetilde{z})$, i.e. we must use a system of the nonlinear equations (1.36) and (1.37). First, we can solve the linear system of equations (1.11) and (1.12) with the corresponding boundary conditions and obtain functions $\widetilde{V}_y(\widetilde{x},\widetilde{z})$ and $\widetilde{\Phi}(\widetilde{x},\widetilde{z})$. After that we can obtain the induced magnetic field $B^i$, using equations $rotB^i = grad\widetilde{\Phi}$, $divB^i = 0$. As a result, the right hand sides of equations (1.36) and (1.37) will be known functions and we get the function $\widetilde{P}(\widetilde{x},\widetilde{z}) = F_2(\widetilde{x},\widetilde{z})$ from the system (1.36) and (1.37) up to an arbitrary constant.

### 1.2.2 THE PROBLEM IN THE CASE OF A NON UNIFORM EXTERNAL MAGNETIC FIELD

Assume that the external magnetic field can be represented in the form:

$$\vec{B^e} = \vec{B^i}_{\perp}\ (\tilde{x},\tilde{z}) = B_x(\tilde{x},\tilde{z})\vec{e}_x + B_z(\tilde{x},.\tilde{z})\vec{e}_z \tag{1.42}$$

Since vector $\vec{B^e}$ does not depend on the y variable, the formula for $\vec{B^i}\ (\tilde{x},\tilde{z})$ has the same form as in section 1.3.1:

$$\vec{B}^i\ (\tilde{x},\tilde{z}) = B^i\ (\tilde{x},\tilde{z})\ \vec{e}_y\,. \tag{1.43}$$

In this section only the MHD equations and pressure $\tilde{P}(\tilde{x},\tilde{z})$ are changed.

We have

$$\tilde{\vec{V}} = \tilde{V}_y(\tilde{y},\tilde{z})\vec{e}_y\,, \tag{1.44}$$

$$\tilde{\vec{B}} = \vec{B}^i(\tilde{x},\tilde{z}) + \tilde{B}_x(\tilde{x},\tilde{z})\vec{e}_x + \tilde{B}_z(\tilde{x},\tilde{z})\vec{e}_z\,. \tag{1.45}$$

Consequently

$$\tilde{\vec{V}}\times\tilde{\vec{B}} = \tilde{V}_y\ (\tilde{x},\tilde{z})\left[-\tilde{B}_x(\tilde{x},\tilde{z})\vec{e}_z + \tilde{B}_z(\tilde{x},\tilde{z})\vec{e}_x\right], \tag{1.46}$$

$$\tilde{\vec{j}}\times\tilde{\vec{B}} = \sigma(-grad\tilde{\Phi} + \tilde{\vec{V}}\times\tilde{\vec{B}})\times\tilde{\vec{B}}, \tag{1.47}$$

i.e.

$$\tilde{\vec{j}}\times\tilde{\vec{B}} = \sigma\left\{\left(\frac{\partial\tilde{\Phi}}{\partial\tilde{z}} + B_x\tilde{V}_y\right)\tilde{B}^i\,\vec{e}_x + \left[\frac{\partial\tilde{\Phi}}{\partial\tilde{x}}B_z - \frac{\partial\tilde{\Phi}}{\partial\tilde{z}}B_x - \left(B_x{}^2 + B_z{}^2\right)\tilde{V}_y\right]\vec{e}_y + \left(B_z - \frac{\partial\tilde{\Phi}}{\partial\tilde{x}}\right)\tilde{B}^i\,\vec{e}_z\right\}. \tag{1.48}$$

Substituting (1.44), (1.45) and (1.48) into (1.13) and projecting the resulting equation on the y axis, we obtain:

$$0 = -\frac{1}{\rho}\frac{\partial \tilde{P}}{\partial \tilde{y}} + \nu\left(\frac{\partial^2}{\partial \tilde{x}^2} + \frac{\partial^2}{\partial \tilde{z}^2}\right)\tilde{V}_y + \frac{\sigma}{\rho}\left[\frac{\partial \tilde{\Phi}}{\partial \tilde{x}}B_z - \frac{\partial \tilde{\Phi}}{\partial \tilde{z}}B_x - (B_x{}^2 + B_z{}^2)\tilde{V}_y\right]. \tag{1.49}$$

As in section 1.2.1, it follows from (1.49) that

$$\frac{\partial \tilde{P}}{\partial \tilde{y}} = F_3(\tilde{x},\tilde{z}) \Rightarrow \tilde{P} = F_3(\tilde{x},\tilde{z})\,\tilde{y} + F_4(\tilde{x},\tilde{z}), \tag{1.50}$$

where $F_3$ and $F_4$ are arbitrary functions. Substituting (1.44), (1.45) and (1.50) into (1.13) and projecting the resulting equations on the x and z axes, respectively, we obtain:

$$0 = --\tilde{y}\frac{\partial F_3}{\partial \tilde{x}} - \frac{\partial F_4}{\partial \tilde{x}} + \sigma\left(\frac{\partial \tilde{\Phi}}{\partial \tilde{z}} + B_x\tilde{V}_y\right)\tilde{B}^i, \tag{1.51}$$

$$-\tilde{y}\frac{\partial F_3}{\partial \tilde{z}} - \frac{\partial F_4}{\partial \tilde{z}} + \sigma\left(\frac{\partial \tilde{\Phi}}{\partial \tilde{x}}B_z - \frac{\partial \tilde{\Phi}}{\partial \tilde{z}}B_x - \left|\vec{B}_\perp\right|^2\tilde{V}_y\right). \tag{1.52}$$

It follows from (1.51) and (1.52) that

$$\frac{\partial F_3}{\partial \tilde{x}} = 0, \frac{\partial F_3}{\partial \tilde{z}} = 0 \Rightarrow F_3 = C = const. \tag{1.53}$$

Consequently, equations (1.50)-(1.52) are of the form:

$$\frac{\partial \tilde{P}}{\partial \tilde{y}} = C \Rightarrow \tilde{P}(\tilde{x},\tilde{z}) = C\,\tilde{y} + F_4(\tilde{x},\tilde{z}), \tag{1.54}$$

$$\frac{\partial F_4}{\partial \tilde{x}} = \sigma\left(\frac{\partial \tilde{\Phi}}{\partial \tilde{z}} + B_x\tilde{V}_y\right)\tilde{B}^i, \tag{1.55}$$

$$\frac{\partial F_4}{\partial \tilde{z}} = \sigma\left(\frac{\partial \tilde{\Phi}}{\partial \tilde{x}}B_z - \frac{\partial \tilde{\Phi}}{\partial \tilde{z}}B_x - \left|\vec{B}_\perp\right|^2\tilde{V}_y\right). \tag{1.56}$$

As in section 1.2.1 the constant C = 0, i.e.

$$\tilde{P}(\tilde{x},\tilde{z}) = F_4(\tilde{x},\tilde{z}). \tag{1.57}$$

Equation (1.49) can be rewritten in the form:

$$\nu\left(\frac{\partial^2}{\partial\tilde{x}^2}+\frac{\partial^2}{\partial\tilde{z}^2}\right)\tilde{V}_y+\sigma\left[\frac{\partial\tilde{\Phi}}{\partial\tilde{x}}B_z-\frac{\partial\tilde{\Phi}}{\partial\tilde{z}}B_x-\left(B_x{}^2+B_z{}^2\right)\tilde{V}_y\right]=0. \qquad (1.58)$$

To obtain the second equation it is sufficient to apply the operation of divergence to equation (1.14) and use the equation of continuity $div\tilde{\vec{j}}=0$:

$$0=-\Delta\tilde{\Phi}+div\left[\tilde{V}_y\left(B_z\,\vec{e}_x-B_x\,\vec{e}_z\right)\right] \qquad (1.59)$$

or $$\Delta\tilde{\Phi}=B_z\frac{\partial\tilde{V}_y}{\partial\tilde{x}}-B_x\frac{\partial\tilde{V}_y}{\partial\tilde{z}}+\tilde{V}_y\left(\frac{\partial B_z}{\partial\tilde{x}}-\frac{\partial B_x}{\partial\tilde{z}}\right). \qquad (1.60)$$

The linear system (1.58)-(1.60) with corresponding boundary conditions on the boundary $\tilde{z}=0$ has a unique solution. For a certain form of the given functions $B_x(\tilde{x},\tilde{z})$ and $B_z(\tilde{x},\tilde{z})$ one can find an analytic form of this solution. In general case, this solution may be obtained only by numerical methods. In this section we have considered the fully developed MHD flow in the direction of the y axis. The external magnetic field and the given external current has only x and z components, which do not depend on the variable y. The pressure gradient is absent in the y-direction. It is proved, using the symmetry of the flow in this case, that induced magnetic field has only a y-component. The system of MHD equations for the velocity of fluid and for the potential of the induced current is obtained. Also the equations for the x and z components of pressure gradient are obtained. It is also proved that the pressure of fluid in the given case is a function depending on the x and z variables.

## 1.3 ANALYTICAL SOLUTION OF THE MHD PROBLEM TO THE FLOW OVER THE ROUGHNESS ELEMENTS USING THE DIRAC DELTA FUNCTION

In the designing of the present reactor Tokamak the value of the Hartmann boundary layer in a strong magnetic field becomes commensurable with the size of the roughness of the surface of a channel's wall. Therefore, it is needed to study the influence of the roughness of the surface on the MHD flow of the conducting metal, which is planned to use in the system of the cooling of the reactor.

The MHD problem on the flow of conducting fluid in the half space, arising due to the roughness of the surface in the form $\tilde{z} = \tilde{\chi}_0 \tilde{f}(\tilde{x})$ with the conditions that the values $\left|\tilde{f}(\tilde{x})\right|$ and $\left|\tilde{f}'(\tilde{x})\right|$ are small is solved in [5]. These assumptions allow one to transfer the boundary condition for potential of the current $\tilde{\Phi}(\tilde{x},\tilde{z})$ from the surface $\tilde{z} = \tilde{\chi}_0 \tilde{f}(\tilde{x})$ to the plane $\tilde{z} = 0$ and neglect the term $\tilde{f}'(\tilde{x})\partial\tilde{\Phi}(\tilde{x},0)/\partial\tilde{x}$ in the boundary condition. Without this simplification one obtains an integral equation for unknown function $\partial\tilde{\Phi}(\tilde{x},0)/\partial\tilde{x}$, which can be solved only numerically. In this section this problem is solved for the case when the roughness of surface $\tilde{z} = \tilde{\chi}_0 \tilde{f}(\tilde{x})$ has the rectangular form: $\tilde{z} = \tilde{\chi}_0$, if $\tilde{x} \in (-L, L)$ and $\tilde{z} = 0$, if $\tilde{x} \notin [-L, L]$. As a result the derivative $\tilde{f}'(\tilde{x})$ in the boundary condition is expressed through the Dirac delta function and instead of an integral equation for the function $\tilde{f}'(\tilde{x})\partial\tilde{\Phi}(\tilde{x},0)/\partial\tilde{x}$ an unknown constant $\partial\tilde{\Phi}(L,0)/\partial\tilde{x}$ appears in the process of solution. This fact allows one to solve this problem analytically and estimate the error due to the neglected term $\tilde{f}'(\tilde{x})\partial\tilde{\Phi}(\tilde{x},0)/\partial\tilde{x}$ in above mentioned boundary condition. In addition, the asymptotic of this problem in a strong magnetic field is obtained.

### 1.3.1 THE STATEMENT OF THE PROBLEM

The geometry of the flow is shown on Fig.4. The conducting fluid is located in the half space $\tilde{z} > 0$, $-\infty < \tilde{x}, \tilde{y} < +\infty$. The external magnetic field has the form

$$\mathbf{B}^{e} = \mathrm{B}_0 \mathbf{e}_z . \tag{1.61}$$

The boundary $\tilde{z} = 0$ is not conducting. A steady current flows with the density $\tilde{\mathbf{j}} = j_0 \mathbf{e}_x$ in the direction of the x-axis. If the surface $\tilde{z} = 0$ is ideally smooth then the flow is absent because

the electromagnetic force $\vec{F} = \vec{\tilde{j}} \times \vec{B}$ is constant and $rot\vec{F} = 0$. Suppose that on the surface $\tilde{z} = 0$ there is the roughness of the rectangular form (see Fig.4):

$$\tilde{z} = \tilde{\chi}_0 \, \tilde{f}(\tilde{x}) = \tilde{\chi}_0 [\eta(\tilde{x} + L) - \eta(\tilde{x} - L)] = \begin{cases} \tilde{\chi}_0, & -L < \tilde{x} < L, \\ 0, & |\tilde{x}| > L, \end{cases} \tag{1.62}$$

where $\eta(\tilde{x})$ is the Heaviside step function: $\eta(\tilde{x}) = \begin{cases} 0, \tilde{x} < 0, \\ 1, \tilde{x} > 0. \end{cases}$ (1.63)

In this case the full current is equal to $\mathbf{j} = \mathbf{j}_0 + \mathbf{j}(\tilde{x}, \tilde{z})$ and the flow of the fluid with the velocity $\mathbf{V} = \tilde{V}_y(\tilde{y}, \tilde{z})\mathbf{e}_y$ arises in the direction opposite to the $\tilde{y}$ axis (Fig.1).

We will deduce the boundary condition for the potential $\tilde{\Phi}(\tilde{x}, \tilde{y})$ of an electrical field on the surface $\tilde{z} = \tilde{\chi}_0 \tilde{f}(\tilde{x})$. The normal component of the current on this surface must be equal to zero because the boundary $\tilde{z} = \tilde{\chi}_0 \tilde{f}(\tilde{x})$ is not conducting, i.e. it must be $\mathbf{j} \cdot \mathbf{n} = 0$ on the surface ($\mathbf{n}$ is the unit normal to the surface).

Using formula $\mathbf{n} = grad[\tilde{z} - \tilde{\chi}_0 \tilde{f}(\tilde{x})] / \sqrt{1 + \tilde{\chi}_0^{\,2} \tilde{f}'^2(\tilde{x})}$ we obtain

$$\mathbf{n} = \left[ - \tilde{\chi}_0 \tilde{f}'(\tilde{x}) \mathbf{e}_x + \mathbf{e}_z \right] / \sqrt{1 + \tilde{\chi}_0^{\,2} \tilde{f}'^2(\tilde{x})}, \tag{1.64}$$

where

$$\tilde{f}'(\tilde{x}) = [\delta(\tilde{x} + L) - \delta(\tilde{x} - L)], \tag{1.65}$$

$\delta(\tilde{x})$ is the Dirac delta function.

Substituting $\mathbf{n}$ from (1.64) and $\tilde{\mathbf{j}} = \left( j_0 + \tilde{j}_x(\tilde{x}, \tilde{z}) \right) \mathbf{e}_x + \tilde{j}_z(\tilde{x}, \tilde{z}) \mathbf{e}_z$ into $\tilde{\mathbf{j}} \cdot \mathbf{n} = 0$ and using formula $\tilde{\mathbf{j}} = \sigma \left[ - grad \tilde{\Phi} + \tilde{\mathbf{V}} \times \tilde{\mathbf{B}} \right]$, i.e. $\tilde{j}_x = -\sigma \, \partial \tilde{\Phi} / \partial \tilde{x}$, $\tilde{j}_z = -\sigma \, \partial \tilde{\Phi} / \partial \tilde{z}$ on the surface, where $\tilde{\mathbf{V}} = 0$, we obtain the boundary condition for the potential $\tilde{\Phi}(\tilde{x}, \tilde{z})$:

$$\tilde{z} = \tilde{\chi}_0 \tilde{f}(\tilde{x}): \quad - \sigma \frac{\partial \tilde{\Phi}}{\partial \tilde{z}} = \tilde{\chi}_0 \left[ j_0 \tilde{f}'(\tilde{x}) \; - \sigma \frac{\partial \Phi}{\partial \tilde{x}} \tilde{f}'(\tilde{x}) \right], \tag{1.66}$$

where function $\tilde{f}'(\tilde{x})$ is given by (1.65).

The only approximation which is made in this section is the following: we transfer the boundary condition (1.66) from the surface $\tilde{z} = \tilde{\chi}_0 \tilde{f}(\tilde{x})$ to the plane $\tilde{z} = 0$, i.e. we only assume that the value $\tilde{\chi}_0 \left| \tilde{f}(\tilde{x}) \right|$ is small. As a result, we obtain the boundary condition for the potential in the form

$$\tilde{z}=0:\quad \partial\tilde{\Phi}/\partial\tilde{z}=\tilde{\chi}_0\left[-j_0\sigma^{-1}+\partial\tilde{\Phi}/\partial\tilde{x}\right]\cdot\left[\delta(\tilde{x}+L)-\delta(\tilde{x}-L)\right]. \qquad (1.67)$$

We do not neglect the term $\partial\tilde{\Phi}/\partial\tilde{x}$ in the boundary condition (1.67) and as a result we obtain the new coefficient in the solution used in paper [4].

We use the following dimensionless quantities using the values L, $\nu/\mathrm{L}$, $B_0$, $\nu\sqrt{\rho\nu/\sigma}/L$, $\nu\sqrt{\rho\nu\sigma}/L^2$ as scales of length, velocity, magnetic field, potential and current, respectively. Here $\sigma$, $\rho$, $\nu$ are, respectively, the conductivity, the density and the viscosity of the fluid. Then the MHD equations and the boundary conditions have the form (see [28]):

$$\Delta \mathrm{V_y}-\mathrm{Ha}^2\mathrm{V_y}+\mathrm{Ha}\cdot\partial\Phi/\partial\mathrm{x}=0,\quad \Delta\Phi=\mathrm{Ha}\cdot\partial\mathrm{V_y}/\partial\mathrm{x}\ , \qquad (1.68),(1.69)$$

$$\mathrm{z}=0:\quad \mathrm{V_y}=0,\quad \partial\Phi/\partial z=\chi_0\left[-A+F(x,0)\right]\cdot\left[\delta(x+1)-\delta(x-1)\right], \qquad (1.70),(1.71)$$

$$\sqrt{\mathrm{x}^2+\mathrm{z}^2}\to\infty:\quad \mathrm{V_y}\to 0,\ \Phi\to 0, \qquad (1.72)$$

where $\Delta=\partial^2/\partial x^2+\partial^2/\partial z^2$, $Ha=B_0L\sqrt{\sigma/\rho\nu}$ is the Hartmann number, $A=j_0L^2/(\nu\sqrt{\rho\nu\sigma})$, $\chi_0=\tilde{\chi}_0/L$ and $F(x,0)=\left.\dfrac{\partial\Phi}{\partial x}\right|_{z=0}$. (1.73)

### 1.3.2 THE SOLUTION OF PROBLEM (1.68)-(1.72)

In order to solve problem (1.68)-(1.72) we use the symmetry of this problem with respect to x: the function $\mathrm{V_y}(\mathrm{x,z})$ is an even function, $\Phi(x,z)$ is an odd function with respect to x. This means that the functions $\mathrm{V_y}(\mathrm{x,z})$ and $\Phi(x,z)$ satisfy additional boundary conditions:

$$z=0:\quad \frac{\partial V_y}{\partial x}=0,\ \Phi(x,0)=0. \qquad (1.74)$$

Therefore, problem (1.68)-(1.72) can be solved by means of Fourier cosine and Fourier sine transforms (see[5]). Namely, we apply the Fourier cosine transform with respect to x to equation (1.68) and to $\mathrm{V_y}$ in boundary condition (1.70) and the Fourier sine transform to equation (1.69) and to $\partial\Phi/\partial z$ in boundary condition (1.71), that means, by substituting:

$$V_y^{\,c}(\lambda,z)=\sqrt{\frac{2}{\pi}}\int_0^{\infty}V_y(x,z)\cos\lambda x\,dx\,, \tag{1.75}$$

$$\Phi^s(\lambda,z)=\sqrt{\frac{2}{\pi}}\int_0^{\infty}\Phi(x,z)\sin\lambda x\,dx\,. \tag{1.76}$$

We obtain the following system of ordinary differential equations for unknown functions $V_y^{\,c}(\lambda,z)$, $\Phi^s(\lambda,z)$:

$$-\lambda^2 V_y+\frac{d^2V_y^{\,c}}{dz^2}-Ha^2V_y^{\,c}+Ha\lambda\Phi^s=0\,, \tag{1.77}$$

$$-\lambda^2\Phi^s+\frac{d^2\Phi^s}{dz^2}+Ha\lambda V_y^{\,c}=0\,. \tag{1.78}$$

We apply also transforms (1.75) and (1.76) to boundary conditions (1.70) and (1.71):

$$z=0:\ \ V_y^{\,c}=0,\ \ \frac{d\Phi^s}{dz}=\chi_0\left[A-F(1,0)\right]\sqrt{\frac{2}{\pi}}\sin\lambda\,;\ z\to\infty: V_y^{\,c},\Phi^s\to 0, \tag{1.79),(1.80}$$

where $\quad F(1,0)=\dfrac{\partial\Phi}{\partial x}$ at x=1, z=0 (1.81)

is an unknown constant. The solution of the problem (1.77)-(1.80) has the form:

$$\Phi^s(\lambda,z)=\chi_0\sqrt{\frac{2}{\pi}}\left[-F(1,0)+A\right]\frac{\sin\lambda}{2\lambda^2}\left(k_1e^{k_2z}+k_2e^{k_1z}\right)\,, \tag{1.82}$$

$$V^c(\lambda,z)=\chi_0\sqrt{\frac{2}{\pi}}\left[-F(1,0)+A\right]\frac{\sin\lambda}{2\lambda}\left(e^{k_1z}-e^{k_2z}\right), \tag{1.83}$$

where

$$k_1=-(\sqrt{\lambda^2+\mu^2}+\mu)\,,\ k_2=-(\sqrt{\lambda^2+\mu^2}-\mu)\,,\ 2\mu=Ha\,. \tag{1.84}$$

Applying the inverse Fourier sine and cosine transforms to formulae (1.82), (1.83), we obtain the solution of problem (1.68)-(1.72), containing unknown constant $F(1,0)$:

$$\Phi(x,z)=\frac{\chi_0}{\pi}\left[-F(1,0)+A\right]\int_0^{\infty}\left(k_1e^{k_2z}+k_2e^{k_1z}\right)\frac{\sin\lambda}{\lambda^2}\sin\lambda x\,d\lambda\,, \tag{1.85}$$

$$V_y(x,z)=\frac{\chi_0}{\pi}\left[-F(1,0)+A\right]\int_0^{\infty}\left(e^{k_1z}-e^{k_2z}\right)\frac{\sin\lambda}{\lambda}\cos\lambda x\,d\lambda\,. \tag{1.86}$$

The components $j_x$ and $j_z$ of the induced current density are obtained from the formula

$$\widetilde{\mathbf{j}} = \sigma\left[-\,grad\widetilde{\Phi}(\widetilde{x},\widetilde{z}) + \widetilde{\mathbf{V}} \times \widetilde{\mathbf{B}}\right], \tag{1.87}$$

where $\widetilde{\mathbf{V}} = \widetilde{V}_y(\widetilde{x},\widetilde{z})\mathbf{e}_y$, $\widetilde{\mathbf{B}} = \widetilde{B}_y^i(\widetilde{x},\widetilde{z})\mathbf{e_y} + B_0\mathbf{e_z}$. (1.88)

In the dimensionless quantities formula (1.87) has the form

$$\mathbf{j} = -grad\Phi(x,z) + Ha\mathbf{V} \times \mathbf{B}, \tag{1.89}$$

where $\mathbf{V} = V_y(x,z)\mathbf{e}_y$, $\mathbf{B} = B_y^i(x,z)\mathbf{e_y} + \mathbf{e_z}$. (1.90)

Substituting (1.90) into (1.89) we obtain

$$\mathbf{j} = -grad\Phi(x,z) + HaV_y(x,z)\mathbf{e_x}. \tag{1.91}$$

It follows from (1.91) that

$$j_x = -\frac{\partial\Phi}{\partial x} + HaV_y(x,z), \quad j_z = -\frac{\partial\Phi}{\partial z} \tag{1.92}$$

or, using formulae (1.85), (1.86) and (1.84),

$$j_x = -D\int_0^\infty \left(k_1 e^{k_1 z} + k_2 e^{k_2 z}\right)\frac{\sin\lambda\cos\lambda x}{\lambda}d\lambda, \tag{1.93}$$

$$j_z = -D\int_0^\infty \left(e^{k_1 z} + e^{k_2 z}\right)\sin\lambda\sin\lambda x d\lambda, \tag{1.94}$$

$$D = \frac{\chi_0}{\pi}\left[A - F(1,0)\right]. \tag{1.95}$$

For the evaluation of unknown constants F(1,0) and D in formulae (1.85), (1.86), (1.93) and (1.94) it is necessary to use integral (1.85) and evaluate the limit

$$\mathrm{F(1,0)}= D\lim_{z\to+0}\int_0^\infty \left(k_1 e^{k_2 z} + k_2 e^{k_1 z}\right)\frac{\sin\lambda\cos\lambda}{\lambda}d\lambda. \tag{1.96}$$

Differentiation with respect to $x$ under the integral sign in (1.85) is correct in the region $0 < z_0 \le z < +\infty, 0 \le x < +\infty$ because this integral , also as the corresponding integral (1.96) of partial derivative with respect to $x$ of integrand in (1.85) is majorized in this region. However, if we substitute $z = 0$ using the integral sign in (1.96), we obtain the divergence of the integral, which converges only in the sense of Abel (see [5]):

$$I \equiv \int_0^\infty \sqrt{\lambda^2+\mu^2}\,\frac{\sin 2\lambda}{\lambda}d\lambda = \lim_{\delta\to+0}\int_0^\infty e^{-\delta\lambda}\,\sqrt{\lambda^2+\mu^2}\,\frac{\sin 2\lambda}{\lambda}d\lambda \qquad (1.97)$$

or, after evident transformations

$$I \equiv l\ \underset{\delta\to+0}{im}\int_0^\infty e^{-\delta\lambda}\,\frac{\mu^2}{\sqrt{\lambda^2+\mu^2}+\lambda}\,\frac{\sin 2\lambda}{\lambda}d\lambda + \lim_{\delta\to+0}\int_0^\infty e^{-\delta\lambda}\sin 2\lambda d\lambda. \qquad (1.98)$$

The first integral on the right hand side of (1.98) converges in the usual sense, but the second integral converges only in the sense of Abel and equal to ½ (see [5]). However, such a method gives the solution, which tends to zero as Hartmann number Ha tends to infinity. The last contradicts to the physical sense of the problem. Therefore, it is needed to transform integral (1.85) to such form that, after passing to the limit as $z\to+0$ we would obtain the integral converging in the usual sense. For this purpose we use the formulae:[74]

$$\int_0^\infty e^{-z\sqrt{\lambda^2+\mu^2}}\cos a\lambda d\lambda = \frac{\mu z}{\sqrt{z^2+a^2}}K_1\left(\mu\sqrt{z^2+a^2}\right), \qquad (1.99)$$

$$\int_0^\infty \sqrt{\lambda^2+\mu^2}\,e^{-z\sqrt{\lambda^2+\mu^2}}\cos a\lambda d\lambda = \frac{\mu}{\sqrt{z^2+a^2}}\left[\frac{\mu z^2}{\sqrt{z^2+a^2}}K_2\left(\mu\sqrt{z^2+a^2}\right) - K_1\left(\mu\sqrt{z^2+a^2}\right)\right], \qquad (1.100)$$

where $a\ge 0$, $z>0$ and $K_\nu(z)$ is the modified Bessel function of the second kind of order $\nu$ ($\nu$=1, 2). As a result, we obtain (the details are found in [4]):

$$V_y(x,z) = -D\cdot\mu z\cdot sh\mu z\int_{x-1}^{x+1}\frac{K_1\left(\mu\sqrt{z^2+t^2}\right)}{\sqrt{z^2+t^2}}dt, \qquad (1.101)$$

$$j_x(x,z) = D\cdot ch\mu z\left[F(1+x)-F(1-x)\right] + \mu V_y(x,z), \qquad (1.102)$$

where

$$F(a) = \int_0^a \frac{\mu}{\sqrt{z^2+t^2}}\left[\frac{\mu z^2}{\sqrt{z^2+t^2}}K_2\left(\mu\sqrt{z^2+t^2}\right) - K_1\left(\mu\sqrt{z^2+t^2}\right)\right]dt. \qquad (1.103)$$

The evaluation of integral (1.94) gives:

$$j_z(x,z) = D\mu z\cdot ch\mu z\left[\frac{K_1\left(\mu\sqrt{z^2+(1-x)^2}\right)}{\sqrt{z^2+(1-x)^2}} - \frac{K_1\left(\mu\sqrt{z^2+(1+x)^2}\right)}{\sqrt{z^2+(1+x)^2}}\right]. \qquad (1.104)$$

We transform $\partial\Phi/\partial x$, using formulae (1.85), (1.99) and (1.100):

$$\left.\frac{\partial\Phi}{\partial x}\right|_{x=1} = -D\left\{ch\mu z\int_0^2 \frac{\mu}{\sqrt{z^2+t^2}}\left[\frac{\mu z^2}{\sqrt{z^2+t^2}}K_2\left(\mu\sqrt{z^2+t^2}\right)-K_1\left(\mu\sqrt{z^2+t^2}\right)\right]dt+\right.$$

$$\left.+\mu^2 z\cdot sh\mu z\int_0^2 \frac{1}{\sqrt{z^2+t^2}}K_1\left(\mu\sqrt{z^2+t^2}\right)dt\right\}. \qquad (1.105)$$

The integrals on the right hand side of (1.105) diverge if $z=0$. To overcome this difficulty, we perform the following transformation. First we use the substitution

$$t = z\xi,\quad dt = zd\xi. \qquad (1.106)$$

Then it follows from formula (1.105) that

$$\left.\frac{\partial\Phi}{\partial x}\right|_{x=1} = -D\left\{ch\mu z\int_0^{\frac{2}{z}} \frac{\mu}{\sqrt{1+\xi^2}}\left[\frac{\mu z}{\sqrt{1+\xi^2}}K_2\left(\mu z\sqrt{1+\xi^2}\right)-K_1\left(\mu z\sqrt{1+\xi^2}\right)\right]d\xi+\right.$$

$$\left.+\mu\cdot sh\mu z\int_0^{\frac{2}{z}} \frac{\mu z}{\sqrt{1+\xi^2}}K_1\left(\mu z\sqrt{1+\xi^2}\right)d\xi\right\}. \qquad (1.107)$$

In order to pass to the limit as $z\to+0$ in (1.107) we use the formula

$$K_n(z)\approx\frac{1}{2}(n-1)!\left(\frac{2}{z}\right)^n,\ n=1,2,3,...\ \text{at}\ z\to+0,$$

i.e. $$K_1(z)\approx\frac{1}{z},\ K_2(z)\approx\frac{2}{z^2}\ \text{at}\ z\to+0. \qquad (1.108)$$

As a result we obtain from formula (1.107) that

$$\lim_{z\to+0}\left.\frac{\partial\Phi}{\partial x}\right|_{x=1} = -D\lim_{z\to+0}\frac{1}{z}\int_0^{\frac{2}{z}}\left[\frac{2}{\left(1+\xi^2\right)^2}-\frac{1}{1+\xi^2}\right]d\xi - D\lim_{z\to+0}\mu\cdot sh\mu z\int_0^{\frac{2}{z}}\frac{1}{1+\xi^2}d\xi. \qquad (1.109)$$

The second limit in the right hand side of formula (1.109) is equal to zero, but the first limit gives undefined expression of the form $\frac{0}{0}$ because

$$\int_0^{\infty}\left[\frac{2}{\left(1+\xi^2\right)^2}-\frac{1}{1+\xi^2}\right]d\xi = \int_0^{\infty}\frac{2}{\left(1+\xi^2\right)^2}d\xi-\frac{\pi}{2}=0. \qquad (1.110)$$

Consequently, from formula (1.109) we obtain

$$\lim_{z\to+0}\left.\frac{\partial\Phi}{\partial x}\right|_{x=1} = -D\lim_{z\to+0}\frac{1}{z}\int_0^{\frac{2}{z}}\left[\frac{2}{\left(1+\xi^2\right)^2}-\frac{1}{1+\xi^2}\right]d\xi = = -D\lim_{z\to+0}\left[\frac{2}{\left(1+\frac{4}{z^2}\right)^2}-\frac{1}{1+\frac{4}{z^2}}\right]\left(-\frac{2}{z^2}\right) = -\frac{D}{2}. \tag{1.111}$$

It follows from (1.111) and (1.95) that

$$F(1,0) = -\frac{1}{2}D, \text{ i.e. } F(1,0) = -\frac{\chi_0}{2\pi}\left[A - F(1,0)\right] \tag{1.112}$$

We obtain the unknown constant F(1,0) from equation (1.112):

$$F(1,0) = -\frac{\chi_0}{2\pi}A\frac{1}{1-\frac{\chi_0}{2\pi}}. \tag{1.113}$$

Consequently, the coefficient D, which is the unknown coefficient in the (1.101), (1.102) and (1.104), is given by

$$D = \frac{\chi_0}{\pi}\left[A - F(1,0)\right] = \frac{\chi_0}{\pi}A\frac{1}{1-\frac{\chi_0}{2\pi}} > 0 \text{ if } \chi_0 < 2\pi. \tag{1.114}$$

We remind that $\chi_0 = \widetilde{\chi}_0 / L$ is the single small parameter in our problem. The inequality $\chi_0 < 2\pi$ gives the natural restriction at which the y-component of the velocity $V_y(x,z)$ in formula (1.86) is negative, (that is, corresponds to the physical sense of this problem (see Fig.4).

It is important to note that if we would neglect the term $\partial\Phi/\partial x$ in boundary condition (1.67), the way it was done in paper [4] for function f(x) of arbitrary form, we obtain the same solution of this problem but at the condition that coefficient D would be equal to $D = A\chi_0/\pi$ instead of formula (1.114). It gives us the opportunity to evaluate the error which occurs if the term $\partial\Phi/\partial x$ is neglected in boundary condition (1.67). For example, if $\chi_0/2\pi = 0.1$, then the error $\delta$ is equal to $\delta = (1/0.9 - 1)\cdot 100\%$, i.e. $\delta = 11\%$.

### 1.3.3 THE ASYMPTOTIC ANALYSIS OF THE PROBLEM AND NUMERICAL RESULTS

It follows from formula (1.86) that at $Ha \to \infty$ we have $k_1 z \to -\infty$, $k_2 z \to 0$ ( everywhere except the regions $0 \le z \le Ha^{-1}$ and $z > Ha$, respectively ).

Consequently, at $Ha \to \infty$ in region $Ha^{-1} \le z \le Ha$ we obtain from formula (1.86) that

$$\lim_{Ha\to\infty} V_y(x,z) \equiv V_c = -\frac{\pi}{2}[\eta(1-x)+\eta(1+x)] = \begin{cases} -\dfrac{\pi D}{2}, x \in (-1,1), \\ 0, \qquad x \notin (-1,1), \end{cases} \tag{1.115}$$

where $V_c$ =constant is the core velocity.

The region $0 \le z \le Ha^{-1}$ is the Hartmann boundary layer, where the velocity of fluid is changed from zero to the velocity of the flow core $V_c$ = constant, but the region $Ha < z < +\infty$ is the distant wake, where the velocity is changed from $V_c$ to zero: (see Figure 4):

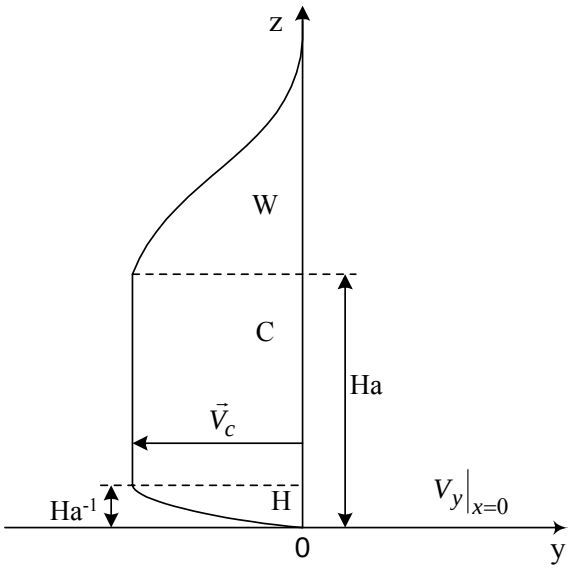


***Figure 4.*** **The regions of the flow in the cross-section x=0 at** $Ha \to \infty$ **:**

**H- the Hartmann layer,** $0 < z < Ha^{-1}$ **;**

**C- the flow core,** $Ha^{-1} < z < Ha$ **;**

**W- the distant wake,** $Ha < z < +\infty$ **.**

It is necessary to note that at large Hartmann numbers the velocity $V_c$ in the core of flow is constant and does not depend on Ha. At $Ha \to +\infty$ only the height of core region $Ha^{-1} < z < Ha$ is increased. The asymptotic of the current's component $j_x(x,z)$ in the region $Ha^{-1} < z < +\infty$ is obtained from formula (1.93):

$$\lim_{Ha\to\infty} j_x = 0, \quad Ha^{-1} < z < +\infty . \tag{1.116}$$

The asymptotic of the current component $j_z(x,z)$ at $Ha \to +\infty$ is obtained by the exact formula (1.104). For this purpose we use the formula that holds when $\mu \to \infty$, $z > 0$, $l > 0$:

$$ch\mu z \approx 0.5 e^{\mu z}, \quad K_1(\mu l) \approx \sqrt{\frac{\pi}{\mu l}} e^{-\mu l}. \tag{1.117}$$

Then, according to (1.104), the component $j_z(x,z)$ exponentially tends to zero at $\mu \to \infty$ everywhere, except for the two regions, bounded by the parabolas:

$$\mu\sqrt{z^2 + (x-1)^2} - \mu z = 1 \text{ and } \mu\sqrt{z^2 + (x+1)^2} - \mu z = 1, \tag{1.118}$$

i.e. bounded by the parabolas:

$$z + \frac{1}{2\mu} = 0.5\mu(x+1)^2 \quad \text{and} \quad z + \frac{1}{2\mu} = 0.5\mu(x-1)^2 \tag{1.119}$$

and we can put $\frac{1}{2\mu} \approx 0$ at $\mu \to \infty$ in formula (1.119). Inside of the two regions, bounded by parabolas (1.119), component $j_z(x,z)$ tends to infinity as $\mu \to \infty$ by the law

$$j_z \approx \sqrt{\mu / z}, \tag{1.120}$$

because it follows from (1.104), (1.117), (1.118) as $\mu \to \infty$ that

$$\ell \equiv \sqrt{z^2 + (1-x)^2} = (1 + \mu z)/z \approx \mu, \quad \mu l - \mu z = 1, \tag{1.121}$$

$$\mu z ch\mu z l^{-1} K_1(\mu l) \approx 0.5\mu e^{\mu(z-\ell)} (\pi/(2\mu z))^{0.5} = \mathrm{e}^{-1} \left(\pi/8\right)^{0.5} \left(\mu/z\right)^{0.5}. \tag{1.122}$$

The asymptotic of functions of the functions $V_y(x,z)$, $j_x(x,z)$ $j_z(x,z)$ are obtained from integrals (1.86), (1.93) and (1.94), using the formula, which holds at $\mu \to \infty$:

$$-k_1 = \left(\sqrt{\lambda^2 + \mu^2} - \mu\right) + 2\mu = 2\mu + \frac{\lambda^2}{\sqrt{\lambda^2 + \mu^2} + \mu} \approx 2\mu + \frac{\lambda^2}{2\mu}, \tag{1.123}$$

$$-k_2 = \sqrt{\lambda^2 + \mu^2} - \mu \approx \frac{\lambda^2}{2\mu}, \quad 2\mu = Ha. \tag{1.124}$$

Substituting (1.123) and (1.124) into integrals (1.86), (1.93), (1.94) and using the Poisson

integral (see [5]), we obtain the asymptotic formulae, which holds for the whole region $0 < z < +\infty$ as $Ha \to \infty$:

$$V_y(x,z) = -\frac{\pi}{4} D\left(1 - e^{-zHa}\right)\psi(x,z), \tag{1.125}$$

$$\psi(x,z) = erf\left[\beta\frac{1+x}{\sqrt{z}}\right] + erf\left[\beta\frac{1-x}{\sqrt{z}}\right],\ \beta = 0.5\sqrt{Ha}\ , \tag{1.126}$$

$$j_x = D\left\{\frac{\pi}{4} Hae^{-zHa}\psi(x,z) + \frac{\beta}{z\sqrt{\pi z}}\left(1 + \frac{\pi}{4}e^{-zHa}\right)\left[(1+x)e^{\frac{-\beta^2(1+x)^2}{z}} + (1-x)e^{\frac{-\beta^2(1-x)^2}{z}}\right]\right\}, \tag{1.127}$$

$$j_z = -\frac{1}{2} D\beta\sqrt{\frac{\pi}{z}\left(1 + e^{-zHa}\right)}\left[e^{\frac{-\beta^2(1-x)^2}{z}} - e^{\frac{-\beta^2(1+x)^2}{z}}\right]. \tag{1.128}$$

We see from formula (1.125) that at $Ha \to \infty$ we have:

1) Component $V_y = \frac{-\pi}{2} D$ = constant in region $Ha^{-1} < z < Ha$.

2). Component $V_y$ is changed from 0 till $V_y = \frac{-\pi}{2} D = V_c$ in region $0 < z < Ha^{-1}$.

3). Component $V_y$ is changed from $V_c$ till zero in region $Ha < z < +\infty$.

In addition, it follows from formula (1.125) that on the lines $x = \pm 1$, $0 < z < +\infty$ the component $V_y \to 0.5V_c$ as $Ha \to \infty$. That means that the two new boundary layers exist in the regions:

$$-\varepsilon < \beta\frac{1-x}{\sqrt{z}} < \varepsilon \text{ and } -\varepsilon < \beta\frac{1+x}{\sqrt{z}} < \varepsilon, \tag{1.129}$$

where $\varepsilon$ is some small positive number. In these regions component $V_y$ is changed between $-V_c$ and zero. It is impossible to get these two new boundary layers from formula (1.86).

Similarly, we see from (1.128) that at $Ha \to \infty$:

1. Component $j_z$ exponentially tends to zero everywhere except for the two regions, lying inside parabolas (1.119), because in this case both the exponent in the square bracket of formula (1.128) tends to zero.
2. Inside the region bounded by the first or second parabola in (1.119), where one of the exponents in the square bracket of (1.128) does not equal to zero, component $j_z \approx \sqrt{\mu/z}$, i.e. tends to infinity as $\mu \to \infty$.
3. Finally, we see from formula (1.127) that at $Ha \to \infty$ the current component $j_x(x,z)$ tends to zero everywhere except for the region $0 < z < Ha^{-1}$ because in this region

$\exp(-zHa) \neq 0$ and the function $\psi(x,z)$ tends to 2 everywhere except for the two regions in formula (1.129).

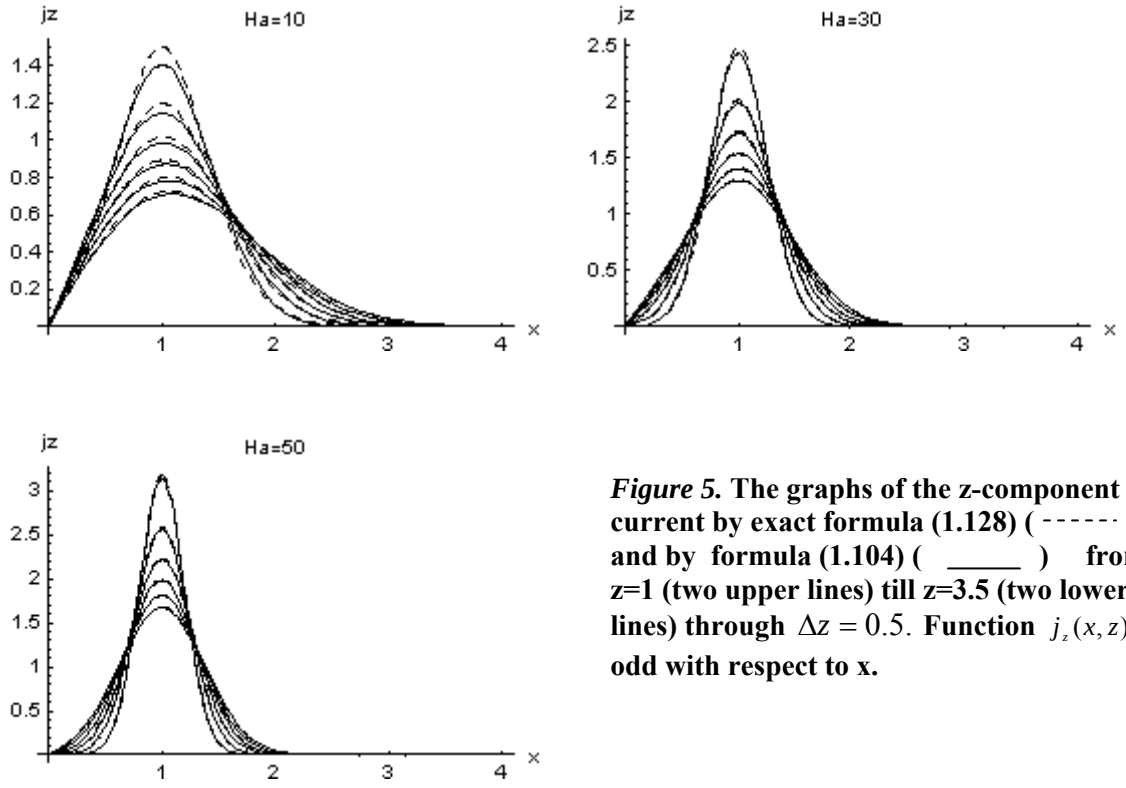


***Figure 5.*** **The graphs of the z-component of current by exact formula (1.128) ( - - - - - - ) and by formula (1.104) ( _____ ) from z=1 (two upper lines) till z=3.5 (two lower lines) through $\Delta z = 0.5$. Function $j_z(x,z)$ is odd with respect to x.**

For the evaluation of Hartmann numbers at which the asymptotic formulae (1.125)-(1.128) are correct we compare the numerical results for the component $j_z(x,z)$, obtained by exact formula (1.104) and by asymptotic formula (1.128). These numerical results for Hartmann numbers Ha =10 , 30 , 50 are shown on Fig.6 . For Hartmann numbers $Ha \geq 10$ the results obtained by exact formula (1.104) and by asymptotic formula (1.128) practically coincide. Calculations for functions $V_y(x,z)$ and $j_x(x,z)$ by exact formulae (1.86) , (1.93) and by asymptotic formulae (1.125) , (1.127) give coincidence at the same Hartmann numbers .

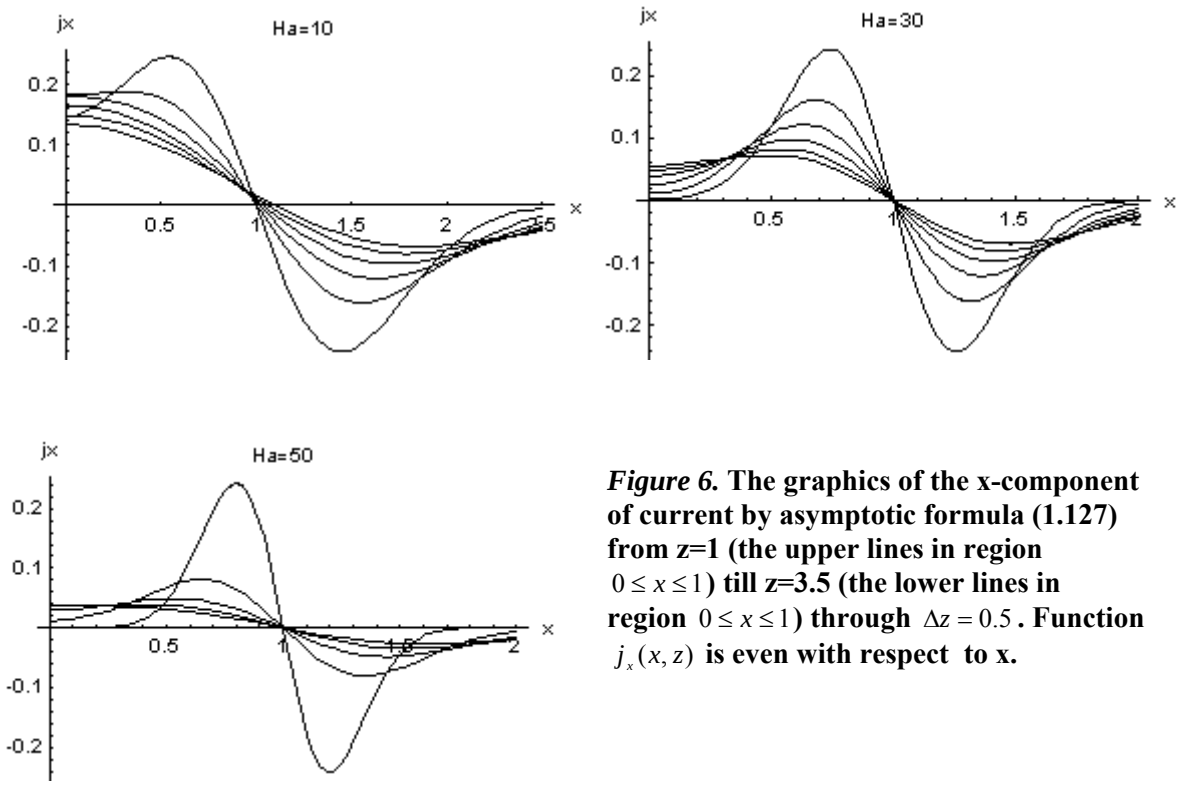


***Figure 6.*** **The graphics of the x-component of current by asymptotic formula (1.127) from z=1 (the upper lines in region $0 \le x \le 1$) till z=3.5 (the lower lines in region $0 \le x \le 1$) through $\Delta z = 0.5$. Function $j_x(x,z)$ is even with respect to x.**

On Fig.7 the numerical results of calculation of the current's component $j_x(x,z)$ by asymptotic formula (1.127) for Hartmann numbers Ha=10, 30 and 50 are shown. We can see, that the sign of the function $j_x(x,z)$ is changed in the neighbourhood of the line $x=1$, $0 < z < +\infty$. It means that the streamlines of current $\vec{j}(x,z)$ change their direction to the opposite in the neighbourhood of this line.

It follows from (1.128) that the full current through the cross section $z = z_0$=constant is equal to

$$\int_0^\infty j_z(x,z_0)dx = -\frac{\pi D}{2}\left(1+e^{-z_0 Ha}\right)erf\frac{Ha}{2z_0} \to -\frac{\pi D}{2} \text{ as } Ha \to \infty. \qquad (1.130)$$

The same full current flow through the cross section $x = x_0$, $0 < z < +\infty$ that follows from (1.127) and also from the equation of continuity:

$$\int_0^\infty j_x(x_0,z)dz \to \frac{\pi D}{2} \text{ as } Ha \to \infty. \qquad (1.131)$$

One can see also from (1.27) that at $Ha \to \infty$ almost all of this full current flow through the cross section of Hartmann boundary layer $x = x_0 > 0$, $0 \le z < Ha^{-1}$:

$$\int_0^{Ha^{-1}} j_x(x_0.z)dz = \frac{\pi D}{4} Ha \int_0^{Ha^{-1}} \psi(x_0, z) e^{-zHa} dz \approx \frac{\pi D}{2} Ha \int_0^{Ha^{-1}} e^{-zHa} dz = \frac{\pi D}{2}\left(1 - e^{-1}\right). \qquad (1.132)$$

On Fig.8 the streamlines of current $\vec{j}(x, z)$, obtained by formula

$$\frac{dz}{dx} = \frac{j_z(x, z)}{j_x(x, z)} \qquad (1.133)$$

for Hartmann numbers Ha=5 and Ha=10 and for various values of initial conditions $z(0)$ are shown. The package "Mathematica" is used. Since the function $j_x(x, z)$ is equal to zero in the neighbourhood of the point x =1 the results of calculations on Fig.8 in region $0 \le x \le 1$ are shown . One can see from Fig.8 that when Hartmann number increases then the full current is concentrated near the plane z = 0.

For calculations of streamlines in region $1 \le x \le +\infty$ we use the differential equation

$$\frac{dx}{dz} = \frac{j_x(x, z)}{j_z(x, z)}. \qquad (1.134)$$

The streamlines of current in this region are shown on Fig.9 for the same Hartmann numbers Ha=5 and Ha=10 . One can see from Fig.9 that in the neighbourhood of point x =1 the streamlines change directions to the opposite direction in the neighbourhood of this point.

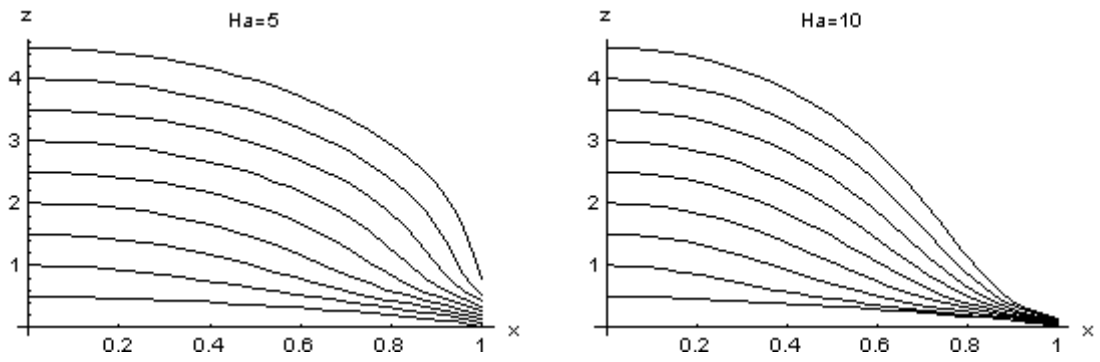


***Figure 7.*** **The streamlines of current $\vec{j}(x, z)$ in region $0 \le x \le 1$ at Ha=5 and at Ha=10.**

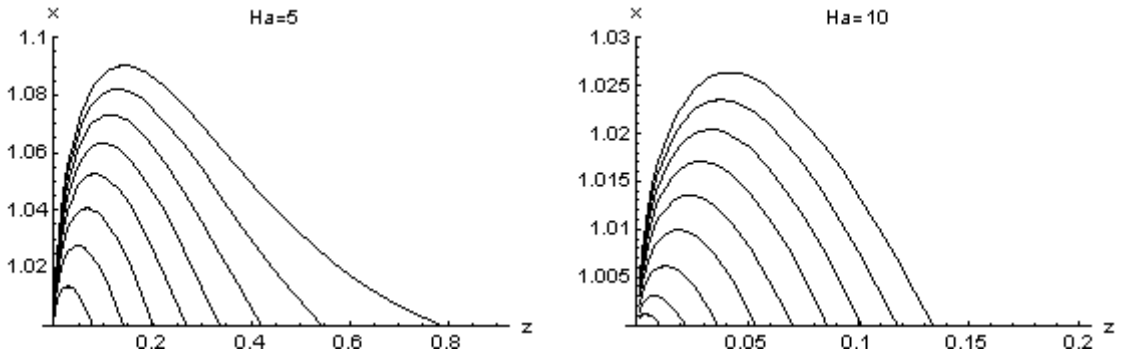


***Figure 8.*** **The streamlines of current $\vec{j}(x,z)$ in region $1 \le x \le +\infty$ at Ha=5 and at Ha=10.**

## CONCLUSIONS

1. The analytical solution of the two dimensional problem on the MHD flow in half space $z \ge 0$ due to the roughness of the boundary of special form is obtained. The roughness with constant rectangular cross section is located along the y axis. In this case the external current flows parallel to x axis and the external magnetic field is parallel to z axis. The two dimensional MHD flow in the direction opposite to y axis arises, only if the roughness of the boundary is present.

2. The analytical solution is obtained at the single approximate assumption that the height of the roughness is small .The solutions for the y component of the velocity of the fluid and for the x component of the induced current are obtained in the form of improper integrals of elementary functions. On the other hand, the z component of the induced current is expressed through the Bessel function.

3. The asymptotic solution of the problem at Hartmann number $Ha \to \infty$ is obtained in the form of elementary functions. For Hartmann numbers Ha ≥ 10 the exact and the asymptotic solutions practically coincide.

4. Several boundary layers for the velocity of the fluid and for the x and z components of the current at large Hartmann numbers are found.

5. The velocity of the fluid in the core at large Hartmann numbers is constant; that means it does not depend on Ha. With the increase of Hartmann number only the height of the core region $Ha^{-1} < z < Ha$ is increased.

6. Using the package "Mathematica" the streamlines of electrical current are presented. The induced current at large Hartmann numbers flow only in Hartmann boundary layer $0 < z < Ha^{-1}$ and along the lines $x = \pm 1$, which are the vertical boundaries of the roughness.

## 1.4 ANALYTICAL SOLUTION OF THE MHD PROBLEM TO THE FLOW OVER THE ROUGHNESS ELEMENTS IN THE FORM OF A STEP FUNCTION

In section **1.3** the MHD problem on the flow of conducting fluid in the half space, arising due to the roughness of the surface in the form $\tilde{z} = \tilde{\chi}_0 \tilde{f}(\tilde{x})$ with the conditions that the values $\left|\tilde{f}(\tilde{x})\right|$ and $\left|\tilde{f}'(\tilde{x})\right|$ are small is solved. In this section similar problem for the constant cross-section of prism bounded by step-function form is solved [3].

### 1.4.1 THE PROBLEM OVER THE ROUGHNESS ELEMENTS IN A STRONG MAGNETIC FIELD

In this section we assume that the roughness of the surface $\tilde{z} = 0$ has the form of the step-function (see Fig.10):

$$\tilde{z} = \tilde{F}(\tilde{x}) = \begin{cases} \tilde{\chi}_1, & |\tilde{x}| < L_1 \\ \tilde{\chi}_0, & L_1 < |\tilde{x}| < L \\ 0, & |\tilde{x}| > L \end{cases} \tag{1.135}$$

or $\tilde{z} = \tilde{F}(\tilde{x}) = \tilde{\chi}_0 \ \tilde{f}_1(\tilde{x}) + (\tilde{\chi}_1 - \tilde{\chi}_0) \ \tilde{f}_2(\tilde{x})$, (1.136)

where $\tilde{f}_1(\tilde{x}) = \eta(\tilde{x} + L) - \eta(\tilde{x} - L)$, $\tilde{f}_2(\tilde{x}) = \eta(\tilde{x} + \tilde{L}_1) - \eta(\tilde{x} - \tilde{L}_1)$. (1.137)

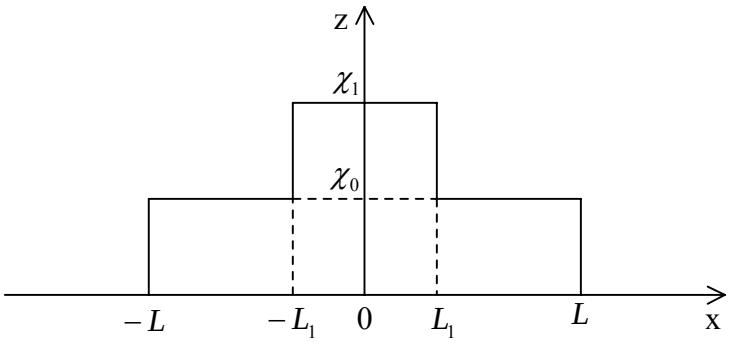


**Figure 9. The constant cross-section of the roughness in this part**

We will deduce the boundary condition for the potential $\widetilde{\Phi}(\widetilde{x},\widetilde{z})$ of an electrical field on the surface $\widetilde{z}=\widetilde{F}(\widetilde{x})$. The normal component of the current on this surface must be equal to zero because the boundary $\widetilde{z}=\widetilde{\chi}_0\widetilde{f}(\widetilde{x})$ is not conducting, i.e. it must be $\mathbf{j}\cdot\mathbf{n}=0$ on the surface (**n** is the unit vector of the normal to the surface).

Using formula $\mathbf{n}=grad[\widetilde{z}-\widetilde{F}(\widetilde{x})]/\sqrt{1+\widetilde{F}^2(\widetilde{x})}$ we obtain

$$\mathbf{n}=\left[\widetilde{F}'(\widetilde{x})\mathbf{e}_x+\mathbf{e}_z\right]/\sqrt{1+\widetilde{F}'^2(\widetilde{x})}, \tag{1.138}$$

where

$$\widetilde{F}'(\widetilde{x})=\widetilde{\chi}_0\left[\delta(\widetilde{x}+L)-\delta(\widetilde{x}-L)\right]+(\widetilde{\chi}_1-\widetilde{\chi}_0)\left[\delta(\widetilde{x}+\widetilde{L}_1)-\delta(\widetilde{x}-\widetilde{L}_1)\right], \tag{1.139}$$

$\delta(\widetilde{x})$ is the Dirac delta function.

Substituting the value of **n** from (1.138) and $\widetilde{\mathbf{j}}=\left(j_0+\widetilde{j}_x(\widetilde{x},\widetilde{z})\right)\mathbf{e}_x+\widetilde{j}_z(\widetilde{x},\widetilde{z})\mathbf{e}_z$ into $\widetilde{\mathbf{j}}\cdot\mathbf{n}=0$ and using formula $\widetilde{\mathbf{j}}=\sigma\left[-grad\widetilde{\mathbf{\Phi}}+\widetilde{\mathbf{V}}\times\widetilde{\mathbf{B}}\right]$, i.e. $\widetilde{j}_x=-\sigma\,\partial\widetilde{\Phi}/\partial\widetilde{x}$, $\widetilde{j}_z=-\sigma\,\partial\widetilde{\Phi}/\partial\widetilde{z}$ on the surface, where $\widetilde{\mathbf{V}}=0$, we obtain the boundary condition for the potential $\widetilde{\Phi}(\widetilde{x},\widetilde{z})$:

$$\widetilde{z}=\widetilde{F}(\widetilde{x}):\quad -\sigma\frac{\partial\widetilde{\Phi}}{\partial\widetilde{z}}=\widetilde{F}'(\widetilde{x})\left[j_0-\sigma\frac{\partial\widetilde{\Phi}}{\partial\widetilde{x}}\right], \tag{1.140}$$

where function $\widetilde{F}'(\widetilde{x})$ is given by (1.139).

As in the previous section we transfer the boundary condition (1.140) from the surface $\widetilde{z}=\widetilde{F}(\widetilde{x})$ to the plane $\widetilde{z}=0$, i.e. we suppose that only the value $\left|\widetilde{F}(\widetilde{x})\right|$ is small. As a result, we obtain the boundary condition for the potential in the form

$$\widetilde{z}=0:\quad \partial\widetilde{\Phi}/\partial\widetilde{z}=\left[-j_0\sigma^{-1}+\partial\widetilde{\Phi}/\partial\widetilde{x}\right]\widetilde{F}'(\widetilde{x}). \tag{1.141}$$

We do not neglect the term $\partial\widetilde{\Phi}/\partial\widetilde{x}$ in boundary condition (1.140) and as a result we obtain the new coefficient in the solution used in paper [4].

We use the following dimensionless quantities where we use the values L, $\nu/\mathrm{L}$, $B_0$, $\nu\sqrt{\rho\nu/\sigma}/L$, $\nu\sqrt{\rho\nu\sigma}/L^2$ as scales of length, velocity, magnetic field, potential and current, respectively. Here $\sigma$, $\rho$, $\nu$ are, respectively, the conductivity, the density and the viscosity of the fluid.

Then the MHD equations and the boundary conditions have the form (see [3]):

$$\Delta \mathrm{V_y} - \mathrm{Ha}^2 \mathrm{V_y} + \mathrm{Ha}\cdot\partial\Phi/\partial\mathrm{x} = 0, \tag{1.142}$$

$$\Delta\Phi = \mathrm{Ha}\cdot\partial \mathrm{V_y}/\partial\mathrm{x}, \tag{1.143}$$

$$z = 0 : V_y = 0 \tag{1.144}$$

$$\partial\Phi/\partial z = [-A + F(x,0)]F'(x), \tag{1.145}$$

$$F'(x) = \chi_0[\delta(x+1) - \delta(x+1)] + (\chi_1 - \chi_0)[\delta(x+L_1) - \delta(x-L_1)], \tag{1.146}$$

$$\sqrt{\mathrm{x}^2 + \mathrm{z}^2} \to \infty : \quad \mathrm{V_y} \to 0, \Phi \to 0, \tag{1.147}$$

where $\Delta = \partial^2/\partial x^2 + \partial^2/\partial z^2$, $Ha = B_0 L\sqrt{\sigma/\rho\nu}$ is the Hartmann number, $A = j_0 L^2/(\nu\sqrt{\rho\nu\sigma})$, $\chi_0 = \widetilde{\chi}_0/L$, $\chi_1 = \widetilde{\chi}_1/L$ and

$$F(x,0) = \left.\frac{\partial\Phi}{\partial x}\right|_{z=0}. \tag{1.148}$$

### 1.4.2 The solution of the problem over the roughness in a strong magnetic field

In order to solve problem (1.142)-(1.147) we use the symmetry of this problem with respect to x: the function $\mathrm{V_y}(\mathrm{x,z})$ is an even function, $\Phi(x,z)$ is an odd function with respect to x. This means that functions $\mathrm{V_y}(\mathrm{x,z})$ and $\Phi(x,z)$ satisfy additional boundary conditions:

$$z = 0 : \quad \frac{\partial V_y}{\partial x} = 0, \Phi(x,0) = 0. \tag{1.149}$$

Therefore problem (1.142)-(1.147) can be solved by means of Fourier cosine and Fourier sine transforms (see[4]). We apply the Fourier cosine transform with respect to x to equation (1.142) and to $\mathrm{V_y}$ in boundary condition (1.144) and the Fourier sine transform to equation (1.143) and to $\partial\Phi/\partial z$ in boundary condition (1.145), substituting:

$$V_y{}^c(\lambda,z)=\sqrt{\frac{2}{\pi}}\int_0^\infty V_y(x,z)\cos\lambda x dx\,, \tag{1.150}$$

$$\Phi^s(\lambda,z)=\sqrt{\frac{2}{\pi}}\int_0^\infty \Phi(x,z)\sin\lambda x dx\,. \tag{1.151}$$

As a result we obtain the following system of ordinary differential equations for unknown functions $V_y{}^c(\lambda,z)$, $\Phi^s(\lambda,z)$:

$$-\lambda^2 V_y+\frac{d^2V_y{}^c}{dz^2}-Ha^2V_y{}^c+Ha\lambda\Phi^s=0\,, \tag{1.152}$$

$$-\lambda^2\Phi^s+\frac{d^2\Phi^s}{dz^2}+Ha\lambda V_y{}^c=0\,. \tag{1.153}$$

We apply also transforms (1.150) and (1.151) to boundary conditions (1.144) and (1.145):

$$z=0:\quad V_y{}^c=0,\quad \frac{d\Phi^s}{dz}=\sqrt{2\pi}D_1\sin\lambda+\sqrt{2\pi}D_2\sin\lambda L_{1,}\,; \tag{1.154}$$

$$z\to\infty: V_y{}^c,\Phi^s\to 0, \tag{1.155}$$

where $D_1=\frac{\chi_0}{\pi}[A-F(1,0)], D_2=\frac{\chi_1-\chi_0}{\pi}[A-F(L_1,0),$ (1.156)

$F(L_1,0)=\frac{\partial\Phi}{\partial x}$ at $x=L_1$, z=0, $F(1,0)=\frac{\partial\Phi}{\partial x}$ at x=1, z=0, (1.157)

are the unknown constants.

The solution of the problem (1.152)-(1.155) is represented in the form:

$$\Phi^s(\lambda,z)=\frac{1}{2\lambda^2}\left(k_1e^{k_2z}+k_2e^{k_1z}\right)\,[\sqrt{2\pi}D_1\sin\lambda+\sqrt{2\pi}D_2\sin\lambda L_{1,}], \tag{1.158}$$

$$V^c(\lambda,z)=\frac{1}{2\lambda}\left(e^{k_1z}-e^{k_2z}\right)[\sqrt{2\pi}D_1\sin\lambda+\sqrt{2\pi}D_2\sin\lambda L_{1,}]\,, \tag{1.159}$$

where

$$k_1=-(\sqrt{\lambda^2+\mu^2}+\mu) \tag{1.160}$$

$$k_2=-(\sqrt{\lambda^2+\mu^2}-\mu)\,, \tag{1.161}$$

and $2\mu = Ha$. (1.162)

Applying the inverse Fourier sine and cosine transforms to formulae (1.158) and (1.159), we obtain the solution of problem (1.142)-(1.147), containing unknown constants $F(1,0)$ and $F(L_1,0)$ as :

$$\Phi(x,z) = D_1\int_0^\infty \left(k_1 e^{k_2 z} + k_2 e^{k_1 z}\right)\frac{\sin\lambda}{\lambda^2}\sin\lambda x d\lambda +$$

$$+ D_2\int_0^\infty \left(k_1 e^{k_2 z} + k_2 e^{k_1 z}\right)\frac{\sin\lambda L_1}{\lambda^2}\sin\lambda x d\lambda , \quad (1.163)$$

$$V_y(x,z) = D_1\int_0^\infty \left(e^{k_1 z} - e^{k_2 z}\right)\frac{\sin\lambda}{\lambda}\cos\lambda x d\lambda +$$

$$+ D_2\int_0^\infty \left(e^{k_1 z} - e^{k_2 z}\right)\frac{\sin\lambda L_1}{\lambda}\cos\lambda x d\lambda . \quad (1.164)$$

The components $j_x$ and $j_z$ of the induced current density are obtained using the formula:

$$\widetilde{\mathbf{j}} = \sigma\left[-grad\widetilde{\Phi}(\widetilde{x},\widetilde{z}) + \widetilde{\mathbf{V}}\times\widetilde{\mathbf{B}}\right], \quad (1.165)$$

where $\widetilde{\mathbf{V}} = \widetilde{V}_y(\widetilde{x},\widetilde{z})\mathbf{e}_y$ , and (1.166)

$$\widetilde{\mathbf{B}} = \widetilde{B}_y^i(\widetilde{x},\widetilde{z})\mathbf{e_y} + B_0\mathbf{e_z}. \quad (1.167)$$

In the dimensionless quantities, formula (1.165) is of the form :

$$\mathbf{j} = -grad\Phi(x,z) + Ha\mathbf{V}\times\mathbf{B}, \quad (1.168)$$

where $\mathbf{V} = V_y(x,z)\mathbf{e}_y$ (1.169)

and $\mathbf{B} = B_y^i(x,z)\mathbf{e_y} + \mathbf{e_z}$. (1.170)

Substituting (1.169) and (1.170) into (1.168) we get:

$$\mathbf{j} = -grad\Phi(x,z) + HaV_y(x,z)\mathbf{e_x}. \quad (1.170)$$

It follows from (1.168), (1.169) and (1.170 ) that

$$j_x = -\frac{\partial\Phi}{\partial x} + HaV_y(x,z) \quad (1.171)$$

and $j_z = -\frac{\partial\Phi}{\partial z}$ (1.178)

Now using formulae (1.160), (1.161), (1.162), (1.163) , (1.164) and (1.171) we get:

$$j_x = -D_1 \int_0^{\infty} \left(k_1 e^{k_1 z} + k_2 e^{k_2 z}\right) \frac{\sin\lambda \cos\lambda x}{\lambda} d\lambda - D_2 \int_0^{\infty} \left(k_1 e^{k_1 z} + k_2 e^{k_2 z}\right) \frac{\sin\lambda L_1 \cos\lambda x}{\lambda} d\lambda, \quad (1.173)$$

and $$j_z = -D_1 \int_0^{\infty} \left(e^{k_1 z} + e^{k_2 z}\right) \sin\lambda \sin\lambda x d\lambda \; - D_2 \int_0^{\infty} \left(e^{k_1 z} + e^{k_2 z}\right) \sin\lambda L_1 \sin\lambda x d\lambda \,. \quad (1.174)$$

For the evaluation of unknown constants $F(1,0), F(L_1,0)$ or $D_1, D_2$ in formulae (1.163), (1.164) (1.173) and (1.174) it is necessary to use integral (1.163) and evaluate the limit as:

$$F(1,0) = D_1 \lim_{z \to +0} \int_0^{\infty} \left(k_1 e^{k_2 z} + k_2 e^{k_1 z}\right) \frac{\sin\lambda \cos\lambda}{\lambda} d\lambda + D_2 \lim_{z \to +0} \int_0^{\infty} \left(k_1 e^{k_2 z} + k_2 e^{k_1 z}\right) \frac{\sin\lambda L_1 \cos\lambda}{\lambda} d\lambda \quad (1.175)$$

and a similar limit for $F(L_1,0)$. Note that the partial derivatives with respect to $x$ to equation (1.163) can be obtained under the integral sign of (1.163) in the region $0 < z_0 \le z < +\infty, 0 \le x < +\infty$. This integral, also as corresponding to the integral (1.175) of partial derivative with respect to $x$ of integrand in (1.164) is majorized in this region. However, if we substitute $z = 0$ under the same integral sign in (1.175), we obtain the divergent integral. In fact this integral converges only in the sense of Abel (see [5]). For example, for the first integral in the right hand side in (1.175), we obtain:

$$I \equiv \int_0^{\infty} \sqrt{\lambda^2 + \mu^2}\, \frac{\sin 2\lambda}{\lambda} d\lambda = \lim_{\delta \to +0} \int_0^{\infty} e^{-\delta\lambda} \sqrt{\lambda^2 + \mu^2}\, \frac{\sin 2\lambda}{\lambda} d\lambda \quad (1.176)$$

or, after evident transformations

$$I \equiv \lim_{\delta \to +0} \int_0^{\infty} e^{-\delta\lambda} \frac{\mu^2}{\sqrt{\lambda^2 + \mu^2} + \lambda} \frac{\sin 2\lambda}{\lambda} d\lambda + \lim_{\delta \to +0} \int_0^{\infty} e^{-\delta\lambda} \sin 2\lambda d\lambda. \quad (1.177)$$

The first integral in the right hand side of (1.177) converge in the usual sense, but the second integral converge only in the sense of Abel and equal to ½ (see [5]). However, such method gives the solution, which tends to zero as Hartmann number Ha tends to infinity. But this contradicts the physical sense of the problem. Therefore, it is necessary to transform integral (1.163) to such form that after passing to the limit as $z \to +0$ we would obtain the convergence of this integral in the usual sense.

For this purpose we use the following formulae:

$$\int_0^{\infty} e^{-z\sqrt{\lambda^2+\mu^2}} \cos a\lambda d\lambda = \frac{\mu z}{\sqrt{z^2 + a^2}} K_1\left(\mu\sqrt{z^2 + a^2}\right), \quad (1.178)$$

$$\int_0^{\infty} \sqrt{\lambda^2 + \mu^2} e^{-z\sqrt{\lambda^2+\mu^2}} \cos a\lambda d\lambda = \frac{\mu}{\sqrt{z^2 + a^2}} \left[\frac{\mu z^2}{\sqrt{z^2 + a^2}} K_2\left(\mu\sqrt{z^2 + a^2}\right) - K_1\left(\mu\sqrt{z^2 + a^2}\right)\right], \quad (1.179)$$

where $a \geq 0$, $z > 0$ and $K_\nu(z)$ is the modified Bessel function of the second kind of order $\nu$ ($\nu$=1, 2). As a result, we obtain (for the full details see [6] and [7]):

$$V_y(x,z) = -\mu z \cdot sh\mu z[D_1 \int_{x-1}^{x+1} \frac{K_1\left(\mu\sqrt{z^2+t^2}\right)}{\sqrt{z^2+t^2}}dt + D_2 \int_{x-L_1}^{x+L_1} \frac{K_1\left(\mu\sqrt{z^2+t^2}\right)}{\sqrt{z^2+t^2}}dt], \quad (1.180)$$

$$j_x(x,z) = ch\mu z\{D_1[F(1+x)-F(1-x)]+D_2[F(L_1+x)-F(L_1-x)]\}+\mu V_y(x,z), \quad (1.181)$$

where

$$F(a) = \int_0^a \frac{\mu}{\sqrt{z^2+t^2}}\left[\frac{\mu z^2}{\sqrt{z^2+t^2}}K_2\left(\mu\sqrt{z^2+t^2}\right) - K_1\left(\mu\sqrt{z^2+t^2}\right)\right]dt\,. \quad (1.182)$$

The evaluation of integral (1.174) gives:

$$j_z(x,z) = \mu z \cdot ch\mu z[D_1 G(x,z,1) + D_2 G(x,z,L_1)], \quad (1.183)$$

*where*

$$G(x,z,L_1) = \frac{K_1\left(\mu\sqrt{z^2+(L_1-x)^2}\right)}{\sqrt{z^2+(L_1-x)^2}} - \frac{K_1\left(\mu\sqrt{z^2+(L_1+x)^2}\right)}{\sqrt{z^2+(L_1+x)^2}}. \quad (1.184)$$

*We transform ∂Φ/∂x, using formulae* (1.174), (1.178), and (1.179) :

$$\left.\frac{\partial\Phi}{\partial x}\right|_{x=1} = -D_1\left\{ch\mu z\int_0^2 \frac{\mu}{\sqrt{z^2+t^2}}\left[\frac{\mu z^2}{\sqrt{z^2+t^2}}K_2\left(\mu\sqrt{z^2+t^2}\right) - K_1\left(\mu\sqrt{z^2+t^2}\right)\right]dt + \right.$$

$$\left. + \mu^2 z \cdot sh\mu z\int_0^2 \frac{1}{\sqrt{z^2+t^2}}K_1\left(\mu\sqrt{z^2+t^2}\right)dt\right\} -$$

$$- D_2\left\{ch\mu z\int_{L_1-1}^{L_1+1} \frac{\mu}{\sqrt{z^2+t^2}}\left[\frac{\mu z^2}{\sqrt{z^2+t^2}}K_2\left(\mu\sqrt{z^2+t^2}\right) - K_1\left(\mu\sqrt{z^2+t^2}\right)\right]dt + \right.$$

$$\left. + \mu^2 z \cdot sh\mu z\int_{L_1-1}^{L_1+1} \frac{1}{\sqrt{z^2+t^2}}K_1\left(\mu\sqrt{z^2+t^2}\right)dt\right\}. \quad (1.185)$$

The integrals located to the right hand side of formula (1.185) diverge if $z = 0$.

In order to overcome this difficulty, we perform the following transformation. First we use the following substitution:

$$t = z\xi, \quad dt = zd\xi. \tag{1.186}$$

Then from formula (1.185) it follows that :

$$\left.\frac{\partial\Phi}{\partial x}\right|_{x=1} = -D_1\left\{ch\mu z\int_0^{\frac{2}{z}}\frac{\mu}{\sqrt{1+\xi^2}}\left[\frac{\mu z}{\sqrt{1+\xi^2}}K_2\left(\mu z\sqrt{1+\xi^2}\right)-K_1\left(\mu z\sqrt{1+\xi^2}\right)\right]d\xi+\right.$$

$$\left.+\mu\cdot sh\mu z\int_0^{\frac{2}{z}}\frac{\mu z}{\sqrt{1+\xi^2}}K_1\left(\mu z\sqrt{1+\xi^2}\right)d\xi\right\}-$$

$$-D_2\left\{ch\mu z\int_{\frac{L_1-1}{z}}^{\frac{L_1+1}{z}}\frac{\mu}{\sqrt{1+\xi^2}}\left[\frac{\mu z}{\sqrt{1+\xi^2}}K_2\left(\mu z\sqrt{1+\xi^2}\right)-K_1\left(\mu z\sqrt{1+\xi^2}\right)\right]d\xi\right.$$

$$\left.+\mu\cdot sh\mu z\int_{\frac{L_1-1}{z}}^{\frac{L_1+1}{z}}\frac{\mu z}{\sqrt{1+\xi^2}}K_1\left(\mu z\sqrt{1+\xi^2}\right)d\xi\right\}. \tag{1.187}$$

To pass to the limit at $z \to +0$ in formula (1.185) we now use the following formula :

$$K_n(z) \approx \frac{1}{2}(n-1)!\left(\frac{2}{z}\right)^n, \; n = 1,2,3,... \text{ at } z \to +0,$$

i.e.
$$K_1(z) \approx \frac{1}{z}, \; K_2(z) \approx \frac{2}{z^2} \text{ at } z \to +0. \tag{1.188}$$

As a result we obtain from formula (1.187) that

$$\lim_{z\to+0}\left.\frac{\partial\Phi}{\partial x}\right|_{x=1} = -D_1\lim_{z\to+0}\frac{1}{z}\int_0^{\frac{2}{z}}\left[\frac{2}{\left(1+\xi^2\right)^2}-\frac{1}{1+\xi^2}\right]d\xi - D_1\lim_{z\to+0}\mu\cdot sh\mu z\int_0^{\frac{2}{z}}\frac{1}{1+\xi^2}d\xi -$$

$$-D_2\lim_{z\to+0}\frac{1}{z}\int_{\frac{L_1-1}{z}}^{\frac{L_1+1}{z}}\left[\frac{2}{\left(1+\xi^2\right)^2}-\frac{1}{1+\xi^2}\right]d\xi - D_2\lim_{z\to+0}\mu\cdot sh\mu z\int_{\frac{L_1-1}{z}}^{\frac{L_1+1}{z}}\frac{1}{1+\xi^2}d\xi. \tag{1.189}$$

The second and the last limits on the right hand side of formula (1.189) are equal to zero, but the first and the third limits gives undefined expression of the form $\frac{0}{0}$ and that is mainly because of the following equality :

$$\int_0^{\infty}\left[\frac{2}{\left(1+\xi^2\right)^2}-\frac{1}{1+\xi^2}\right]d\xi=\int_0^{\infty}\frac{2}{\left(1+\xi^2\right)^2}d\xi-\frac{\pi}{2}=0. \tag{1.190}$$

Consequently, from formula (1.189) we get:

$$\lim_{z\to+0}\left.\frac{\partial\Phi}{\partial x}\right|_{x=1}=-D_1\lim_{z\to+0}\frac{1}{z}\int_0^{\frac{2}{z}}\left[\frac{2}{\left(1+\xi^2\right)^2}-\frac{1}{1+\xi^2}\right]d\xi-\quad D_2\lim_{z\to+0}\frac{1}{z}\int_{\frac{L_1-1}{z}}^{\frac{L_1+1}{z}}\left[\frac{2}{\left(1+\xi^2\right)^2}-\frac{1}{1+\xi^2}\right]d\xi=$$

$$=-D_1\lim_{z\to+0}\left[\frac{2}{\left(1+\frac{4}{z^2}\right)^2}-\frac{1}{1+\frac{4}{z^2}}\right]\left(-\frac{2}{z^2}\right)-D_2\lim_{z\to+0}\left[\frac{2}{\left(1+\frac{(L_1+1)^2}{z^2}\right)^2}-\frac{1}{1+\frac{(L_1+1)^2}{z^2}}\right]\left(-\frac{L_1+1}{z^2}\right)+$$

$$D_2\lim_{z\to+0}\left[\frac{2}{\left(1+\frac{(L_1-1)^2}{z^2}\right)^2}-\frac{1}{1+\frac{(L_1-1)^2}{z^2}}\right]\left(-\frac{L_1-1}{z^2}\right)=-\frac{D_1}{2}+\frac{2D_2}{1-L_1{}^2}. \tag{1.191}$$

It follows from(1.156) and (1.191) that :

$$F(1,0)=-\frac{1}{2}D+\frac{2D_2}{1-L_1{}^2}. \tag{1.192}$$

Similarly for $F(L_1,0)$ we obtain:

$$F(L_1,0)=\frac{2D_1}{1-L_1{}^2}-\frac{D_2}{2L_1}. \tag{1.193}$$

We remind that [see formula(1.156)]

$$D_1=\frac{\chi_0}{\pi}[A-F(1,0)],\ \ D_2=\frac{\chi_1-\chi_0}{\pi}[A-F(L_1,0)]. \tag{1.194}$$

Consequently formulae(1.192) and (1.193) represent the system of two equations for the two unknown constants $F(1,0)$ and $F(L_1,0)$, i.e. for the two unknown constants $D_1$ and $D_2$.
Substituting these constants into formulae (1.163), (1.164), (1.173) and (1.174), we obtain the solution of problem (1.142)-(1.147).

# 2. EVALUATION OF IMPROPER INTEGRAL

The solutions of certain problems about MHD flow of conducting fluid in the half space are expressed in terms of improper integrals of the product of some meromorphic function and the function $\exp(-a\sqrt{\lambda^2+b^2})\cos\lambda\cos\lambda x$. Here $a>0$ and $b>0$ are some parameters, $x>0$ is the x-coordinate in Cartesian coordinate system (see [7], [4]). It is difficult to calculate these integrals numerically since the integrands are strongly oscillating at large x.

In this chapter these integrals are transformed into integrals of monotone functions using the convolution theorem for product of two Fourier cosine transforms.

## 2.1 THE TRANSFORMATION OF INTEGRAL OF PRODUCT OF THE MONOTONE FUNCTION AND THE FUNCTION $\exp(-a\sqrt{\lambda^2+b^2})\cos\lambda\cos\lambda x$

We consider the improper integral of the form

$$\int_0^\infty \frac{P_n(\lambda^2)}{Q_m(\lambda^2)} e^{-a\sqrt{\lambda^2+b^2}} \frac{\cos\lambda\cos\lambda x}{\lambda^2-\frac{\pi^2}{4}}\,d\lambda, \tag{2.1}$$

where $P_n(\lambda^2)$, $Q_m(\lambda^2)$ are polynomials of degrees n and m, respectively, $m\ge n$, $a>0$, $b>0$, $x>0$ are some positive parameters. The point $\lambda=\pi/2$ is the removable singularity of the integrand in (2.1), because in the numerator of this integrand $\cos\lambda=0$ at $\lambda=\pi/2$. At large x the integrand in formula (2.1) strongly oscillate what make it difficult to calculate of this integral using package “Mathematica”.

We suppose that all zeros of polynomial $Q(\lambda^2)$ are simple and have the form: $\lambda_k{}^2=-a_k{}^2$, $k=1,2,\cdots 3,...,n$.

Let

$$F_c(\lambda)=\sqrt{\frac{2}{\pi}}\int_0^\infty f(x)\cos\lambda x dx \tag{2.2}$$

is the Fourier cosine transform of function f(x).

We use the theorem (see [23]):

if $F_c(\lambda)$ and $\Phi_c(\lambda)$ are the Fourier cosine transforms of functions $f(x)$ and $\varphi(x)$, respectively, then

$$\int_0^\infty F_c(\lambda)\Phi_c(\lambda)\cos\lambda x d\lambda = \frac{1}{2}\int_0^\infty \varphi(\xi)\left[f(|x-\xi|) + f(x+\xi)\right]d\xi . \tag{2.3}$$

in formula (2.3) we make the following substitution:

$$\frac{P_n(\lambda^2)}{Q_m(\lambda^2)}\frac{\cos\lambda}{\lambda^2 - \frac{\pi^2}{4}} = \Phi_c(\lambda), \quad e^{-a\sqrt{\lambda^2+b^2}} = F_c(\lambda). \tag{2.4}$$

To obtain the functions $\varphi(x)$, $f(x)$ it is necessary to evaluate the integrals:

$$I_1 = \sqrt{\frac{2}{\pi}}\int_0^\infty \frac{P_n(\lambda^2)}{Q_m(\lambda^2)}\frac{\cos\lambda\cos\lambda x\, d\lambda}{\lambda^2 - \frac{\pi^2}{4}} = \varphi(x), \tag{2.5}$$

$$I_2 = \sqrt{\frac{2}{\pi}}\int_0^\infty e^{-a\sqrt{\lambda^2+b^2}}\cos\lambda x\, d\lambda = f(x). \tag{2.6}$$

For evaluation of $I_2$ we use the known integral in the literature:

$$\int_0^\infty \frac{e^{-a\sqrt{\lambda^2+b^2}}}{\sqrt{\lambda^2+b^2}}\cos\lambda x\, d\lambda = K_0(b\sqrt{a^2+x^2}), \tag{2.7}$$

where $K_0(z)$ is the modified Bessel function of order 0 of the second kind.

Differentiating formula (2.7) with respect to a we evaluate integral $I_2$:

$$I_2 = \sqrt{\frac{2}{\pi}}\int_0^\infty e^{-a\sqrt{\lambda^2+b^2}}\cos\lambda x\, d\lambda = \sqrt{\frac{2}{\pi}}\frac{K_1(b\sqrt{a^2+x^2})}{\sqrt{a^2+x^2}} = f(x) \tag{2.8}$$

where $K_1(z)$ is the modified Bessel function of order 1 of the second kind.

For evaluation of integral $I_1$ we use the residue method (from [6]):

$$I_1 = \sqrt{\frac{2}{\pi}}\frac{1}{2}\mathrm{Re}\left\{\left(2\pi i\sum_{k=1}^{m}\operatorname*{Res}_{a_k i} + \pi i \operatorname*{Res}_{\pi/2}\right)\frac{P_n(z^2)}{Q_m(z^2)}\left[e^{iz(1-x)} + e^{iz(1+x)}\right]\right\}, \tag{2.9}$$

where

$$\operatorname*{Res}_{z_0}\frac{\varphi(z)}{\psi(z)} = \frac{\varphi(z_0)}{\psi'(z_0)}, \tag{2.10}$$

at the condition, that $\varphi(z)$ and $\psi(z)$ are the analytical functions in point $z_0$ and on some small neighborhood where $\psi(z_0)=0$, $\psi'(z_0)\neq 0$. It follows from (2.9), (2.10) that

$$I_1=\sqrt{\frac{2}{\pi}}\frac{\pi}{2}\sum_{k=1}^{m}\frac{P_n(-a_k^2)}{Q_m{}'(-a_k^2)}\left[e^{-a_k|1-x|}\,\mathrm{sign}(1-x)+e^{-a_k(1+x)}\right]+$$

$$+\frac{1}{2}\frac{P_n\left(\frac{\pi^2}{4}\right)}{Q_m{}'\left(\frac{\pi^2}{4}\right)}\left[\sin\left(\frac{\pi}{2}|1-x|\right)sign(1-x)+\sin\left(\frac{\pi}{2}|1+x|\right)\right]=\varphi(x), \qquad (2.11)$$

where $sign(1-x)$ means the sign of $(1-x)$.

Substituting (2.8) and (2.11) into (2.3), using (2.1) and (2.4) and taking into account that $|1-x|^2=(1-x)^2$, we transform integral (2.1) into integral of non-oscillating function:

$$\int_0^\infty \frac{P_n(\lambda^2)}{Q_m(\lambda^2)}e^{-a\sqrt{\lambda^2+b^2}}\cos\lambda\cos\lambda x d\lambda=$$

$$=\frac{ab}{\pi}\int_0^\infty\varphi(\xi)\left[\frac{K_1\left(b\sqrt{(x-\xi)^2+a^2}\right)}{b\sqrt{(x-\xi)^2+a^2}}+\frac{K_1\left(b\sqrt{(x+\xi)^2+a^2}\right)}{b\sqrt{(x+\xi)^2+a^2}}\right]d\xi, \qquad (2.12)$$

where $\varphi(\xi)$ is given by formula (2.11).

Similarly, we can transform each integral of the form

$$\int_0^\infty F_c(\lambda^2)e^{-b\sqrt{\lambda^2+a^2}}\cos\lambda\cos\lambda x\,d\lambda \qquad (2.13)$$

into the right-hand side of formula (2.12) under the condition, that integral (2.13) converges and

$$\sqrt{\frac{2}{\pi}}\int_0^\infty\varphi(x)\cos\lambda x\,dx=F_c(\lambda^2) \qquad (2.14)$$

For example, if we consider the integral

$$\int_0^\infty\frac{e^{-z\sqrt{\lambda^2+\mu^2}}}{\frac{\pi^2}{4}-\lambda^2}\cos\lambda\cos\lambda x d\lambda,\ (z\geq 0,\ x\geq 0), \qquad (2.15)$$

with oscillating function $\cos\lambda x$ at large x.

Here $x>0$, $z>0$ are some positive parameters. In this case it follows from

(2.4), (2.8), (2.11) that:

$$\Phi_c(\lambda)=\frac{\cos\lambda}{\frac{\pi^2}{4}-\lambda^2},\quad F_c(\lambda)=e^{-z\sqrt{\lambda^2+\mu^2}} \tag{2.16}$$

$$I_1=\sqrt{\frac{2}{\pi}}\int_0^\infty \frac{\cos\lambda\cos\lambda x}{\frac{\pi^2}{4}-\lambda^2}d\lambda=\sqrt{\frac{2}{\pi}}\cos\left(\frac{\pi}{2}x\right)\eta(1-x)=\varphi(x), \tag{2.17}$$

where $\eta(1-x)=\begin{cases}1, & |x|<1\\ 0, & |x|>1\end{cases}$

(2.18)

is the Heavy-side step function,

$$I_2=\sqrt{\frac{2}{\pi}}\int_0^\infty e^{-z\sqrt{\lambda^2+\mu^2}}\cos\lambda x d\lambda=\sqrt{\frac{2}{\pi}}\frac{\mu z}{\sqrt{z^2+x^2}}K_1\left(\mu\sqrt{z^2+x^2}\right)=f(x). \tag{2.19}$$

Substituting (2.16), (2.17) and (2.19) into (2.3) we obtain:

$$\int_0^\infty \frac{e^{-z\sqrt{\lambda^2+\mu^2}}}{\frac{\pi^2}{4}-\lambda^2}\cos\lambda\cos\lambda x d\lambda=$$

$$=\frac{2\mu z}{\pi}\int_0^1\left[\frac{K_1\left(\mu\sqrt{z^2+(x-\xi)^2}\right)}{\sqrt{z^2+(x-\xi)^2}}+\frac{K_1\left(\mu\sqrt{z^2+(x+\xi)^2}\right)}{\sqrt{z^2+(x+\xi)^2}}\right]\cos\frac{\pi}{2}\xi\, d\xi. \tag{2.20}$$

Integral (2.20) can be easily evaluated using package "Mathematica" for all values of the parameters $x\ge 0$ and $z\ge 0$. As it can be seen from formula (2.20), the advantages of these transformations are:

1. The parameter x goes from an argument of oscillating function cosine into the argument of the monotone Bessel function $K_1$;
2. The limits of the integration are changed in the bounded region $0\le\xi\le 1$.

**a. APPLICATIONS TO SOME MHD PROBLEMS**

The integrals (2.12) and (2.20) are used to evaluate or transform the solution of problems about MHD flows arising due to the roughness of the surface (see [4], [2]).

Consider the following problem.

The conducting fluid is located in the half space $\tilde{z} > 0, -\infty < \tilde{x}, \tilde{y} < +\infty$. The external magnetic field has the form

$$\vec{B}^e = B_0 \vec{e}_z . \tag{2.21}$$

The boundary $\tilde{z} = 0$ is not conducting. A steady current flows with the density $\vec{j} = j_0 \vec{e}_x$ in the direction of the x axis. If the surface $\tilde{z} = 0$ is ideally smooth then the flow is absent. Suppose that the roughness on the surface $\tilde{z} = 0$ has the form

$$\tilde{z} = \tilde{\chi}_0 \tilde{f}(\tilde{x}) \eta\left(L - |\tilde{x}|\right), \quad -\infty < \tilde{y} < +\infty , \tag{2.22}$$

where the height of the surface $\tilde{\chi}_0$ is small and $\eta(L - |x|)$ is the Heaviside step function (see Fig.1) where is shown the particular case of $\tilde{f}(\tilde{x})$ given by formula $\tilde{z} = \tilde{\chi}_0 \cos(\pi\tilde{x} / 2L) \cdot \eta(L - |x|)$). In this case the full current is equal to $\vec{j} = \vec{j}_0 + \vec{j}(\tilde{x},\tilde{z})$ and the flow of the fluid with the velocity $\vec{V} = V_y(y,z)\vec{e}_y$ arises in the direction opposite to the $\tilde{y}$ axis (see Fig.10.).

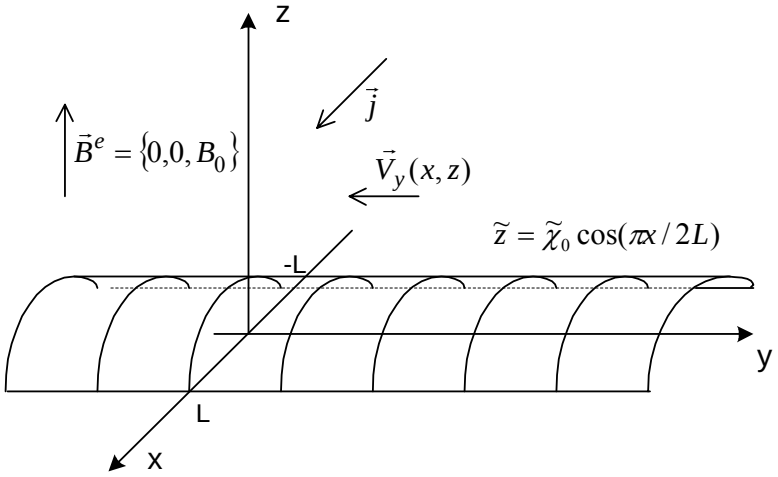


**Figure 10. The geometry of the flow in the case of full current**

In the dimensionless quantities the MHD equations and boundary conditions, which we transform from the surface $\tilde{z} = \tilde{f}(\tilde{x})$ to the surface $\tilde{z} = 0$ at the condition that $\tilde{\chi}_0$ is small, have the form (see [2]):

$$\Delta V_y - Ha^2 V_y + Ha \cdot \partial\Phi / \partial x = 0 , \tag{2.23}$$

$$\Delta\Phi = Ha \cdot \partial V_y / \partial x , \tag{2.24}$$

$$z = 0 : V_y = 0, \partial\Phi / \partial z = \chi_0 \left[ - A + F(x,0) \right] \cdot \left( df / dx \right), \tag{2.25}$$

$$\sqrt{x^2+z^2}\to\infty:\quad V_y\to 0,\ \Phi\to 0\,, \tag{2.26}$$

where $\Delta=\partial^2/\partial x^2+\partial^2/\partial z^2$, $\Phi(x,z)$ is the potential of current, $Ha=B_0L\sqrt{\sigma/\rho\nu}$ is the Hartmann number, $A=j_0L^2/(\nu\sqrt{\rho\nu\sigma})$, $\chi_0=\tilde{\chi}_0/L$ and $\sigma,\rho,\nu$ are, respectively, the conductivity, the density and the viscosity of the fluid and

$$F(x,0)=\left.\frac{\partial\Phi}{\partial x}\right|_{z=0}. \tag{2.27}$$

In paper [4]) the problem (2.23) – (2.26) is solved when neglecting the product function $F(x,0)df/dx$ in boundary condition (2.25), i.e. at the assumption that this product also is small. However, in the case when:

$$f(x)=\chi_0\cos(\pi x/2)\cdot\eta(1-|x|) \tag{2.28}$$

the solution has the form

$$V_y(x,z)=0.5A\chi_0\int_0^\infty\left(e^{k_1z}-e^{k_2z}\right)\frac{\cos\lambda\cos\lambda x}{\pi^2/4-\lambda^2}d\lambda\,, \tag{2.29}$$

$$\Phi(x,z)=-0.5A\int_0^\infty\left(k_1e^{k_2z}+k_2e^{k_1z}\right)\frac{\cos\lambda\sin\lambda x}{\lambda\left(\lambda^2-\pi^2/4\right)}d\lambda\,, \tag{2.30}$$

where $\quad k_1=-(\sqrt{\lambda^2+\mu^2}+\mu)$, $k_2=-(\sqrt{\lambda^2+\mu^2}-\mu)$, $\mu=0.5Ha$. (2.31)

It follows from (2.30) that the components of current $\vec{j}=-grad\Phi+HaV_y(x,z)\vec{e}_x$ have the form

$$j_x=-0.5A\chi_0\int_0^\infty\left(k_1e^{k_1z}+k_2e^{k_2z}\right)\frac{\cos\lambda\cos\lambda x}{\lambda^2-\pi^2/4}d\lambda\,, \tag{2.32}$$

$$j_z=-0.5A\chi_0\int_0^\infty\left(e^{k_1z}+e^{k_2z}\right)\frac{\lambda\cos\lambda\sin\lambda x}{\lambda^2-\pi^2/4}d\lambda\,. \tag{2.33}$$

We can transform $V_y(x,z)$, $j_x$ and $j_z$ using integral (2.20):

$$V_y(x,z)=-\frac{2\mu z}{\pi}A\chi_0\,\mathrm{sh}\,\mu z\int F(x,z,\xi)\cos\frac{\pi}{2}\xi d\xi\,, \tag{2.34}$$

where

$$F(x,z,\xi)=\frac{K_1\left(\mu\sqrt{z^2+(x-\xi)^2}\right)}{\sqrt{z^2+(x-\xi)^2}}+\frac{K_1\left(\mu\sqrt{z^2+(x+\xi)^2}\right)}{\sqrt{z^2+(x+\xi)^2}}, \tag{2.35}$$

$$j_x=\frac{2}{\pi}A\chi_0\mu\left\{ch\mu z\int_0^1\frac{\partial}{\partial z}\left[zF(x,z,\xi)\right]\cos\frac{\pi}{2}\xi d\xi\right\}-\mu zsh\mu z\int_0^1 F(x,z,\xi)\cos\frac{\pi}{2}\xi d\xi \tag{2.36}$$

$$j_z=-A\chi_0 ch\mu z\int_0^1\frac{\partial F(x,z,\xi)}{\partial x}\cos\frac{\pi}{2}\xi d\xi\,. \tag{2.37}$$

Integrals (2.34), (2.36), (2.37) are more suitable for calculations using package "Mathematica", than integrals (2.29), (2.32), (2.33).

In paper [2] the problem (2.23) – (2.26) is solved taking into account the product $F(x,0)df/dx$ in boundary condition (3.5) but for the case, that

$$f(x)=\chi_0\left[\eta(x+1)-\eta(x-1)\right]. \tag{2.38}$$

Then

$$f'(x)=\left[\delta(x+1)-\delta(x-1)\right], \tag{2.39}$$

where $\delta(\widetilde{x})$ is the Dirac delta function.

In this case the solution of the problem (2.23) – (2.26) has the form:

$$V_y(x,z)=D\int_0^\infty\left(e^{k_1z}-e^{k_2z}\right)\frac{\sin\lambda}{\lambda}\cos\lambda x d\lambda\,, \tag{2.40}$$

$$\Phi(x,z)=D\int_0^\infty\left(k_1e^{k_2z}+k_2e^{k_1z}\right)\frac{\sin\lambda}{\lambda^2}\sin\lambda x d\lambda\,, \tag{2.41}$$

where

$$D=\frac{\chi_0}{\pi}\frac{A}{1-\chi_0/\pi}\,. \tag{2.42}$$

Components of current $\vec{j}=-grad\Phi+HaV_y(x,z)\vec{e}_x$ has the form

$$j_x=-D\int_0^\infty\left(k_1e^{k_1z}+k_2e^{k_2z}\right)\frac{\sin\lambda\cos\lambda x}{\lambda}d\lambda\,, \tag{2.43}$$

$$j_z=-D\int_0^\infty\left(e^{k_1z}+e^{k_2z}\right)\sin\lambda\sin\lambda x d\lambda\,. \tag{2.44}$$

For transformation of given solution it is necessary use the integral which we obtain by differentiating formula (2.28) with respect to parameter a and substituting $a = z$, $b = \mu$, $x = a$:

$$\int_0^\infty \sqrt{\lambda^2 + \mu^2}\, e^{-z\sqrt{\lambda^2+\mu^2}} \cos a\lambda \, d\lambda = \frac{\mu}{\sqrt{z^2 + a^2}} \left[ \frac{\mu z^2}{\sqrt{z^2 + a^2}} K_2\left(\mu\sqrt{z^2 + a^2}\right) - K_1\left(\mu\sqrt{z^2 + a^2}\right) \right] \quad (2.45)$$

where $K_2(z)$ is the modified Bessel function of second kind.

substituting $a = t$ in (2.45) and integrating after that with respect to t from $t = 0$ till $t = a$, we obtain:

$$\int_0^\infty \sqrt{\lambda^2 + \mu^2}\, e^{-z\sqrt{\lambda^2+\mu^2}} \frac{\sin a\lambda}{\lambda} d\lambda = F(a), \quad (2.46)$$

where

$$F(a) = \int_0^a \frac{\mu}{\sqrt{z^2 + t^2}} \left[ \frac{\mu z^2}{\sqrt{z^2 + t^2}} K_2\left(\mu\sqrt{z^2 + t^2}\right) - K_1\left(\mu\sqrt{z^2 + t^2}\right) \right] dt. \quad (2.47)$$

Similar transformations with formula (2.28) give:

$$\int_0^\infty e^{-z\sqrt{\lambda^2+\mu^2}} \frac{\sin a\lambda}{\lambda} d\lambda = \mu z \int_0^a \frac{K_1(\mu\sqrt{z^2 + t^2})}{\sqrt{z^2 + t^2}} dt. \quad (2.48)$$

Using formulae (2.46), (2.48) we transform integrals (2.39), (2.43) to the form of integrals of non-oscillating functions:

$$V_y(x, z) = -D\mu z\, sh\mu z \int_{x-1}^{x+1} \frac{K_1(\mu\sqrt{z^2 + t^2})}{\sqrt{z^2 + t^2}} dt, \quad (2.49)$$

$$j_x(x, z) = Dch\mu z\left[F(1 + x) - F(1 - x)\right] + \mu V_y(x, z), \quad (2.50)$$

where $F(a)$ is given by formula (2.47). Using formula (2.28) one can evaluate integral (2.44):

$$j_z(x, z) = D\mu z\, ch\mu z \left[ \frac{K_1\left(\mu\sqrt{z^2 + (1 - x)^2}\right)}{\sqrt{z^2 + (1 - x)^2}} + \frac{K_1\left(\mu\sqrt{z^2 + (1 + x)^2}\right)}{\sqrt{z^2 + (1 + x)^2}} \right]. \quad (2.51)$$

Formula (2.51) gives an opportunity to obtain the asymptotic of component $j_z(x, z)$ at $\mu = 0.5Ha \to \infty$. We now use the formulae which hold at $\mu \to \infty$, $z > 0$, $l > 0$:

$$ch\mu z \approx 0.5e^{\mu z}, \quad K_1(\mu l) \approx \sqrt{\frac{\pi}{2\mu l}} e^{-\mu l}. \quad (2.52)$$

Then, according to (2.51), component $j_z(x,z)$ decreases at $\mu \to \infty$ everywhere, except two regions bounded by the parabolas:

$$\mu\sqrt{z^2+(x-1)^2}-\mu z=1;\quad \mu\sqrt{z^2+(x+1)^2}-\mu z=1, \tag{2.53}$$

i.e. by parabolas

$$z+\frac{1}{2\mu}=0.5\mu(x+1)^2;\qquad z+\frac{1}{2\mu}=0.5\mu(x-1)^2 \tag{2.54}$$

and we can replace $1/2\mu \approx 0$ at $\mu \to \infty$ in formula (2.54). Inside the regions bounded by parabolas (2.54), the component $j_z(x,z)$ tends to infinity in accordance with formula:

$$j_z \approx \sqrt{\mu / z}\,, \tag{2.55}$$

and it follows from (2.51) – (2.53) that:

$$l \equiv \sqrt{z^2+(1-x)^2} = (1+\mu z)/\mu \approx z\,,$$

$$\mu z \operatorname{ch} \mu z l^{-1} K_1(\mu l) \approx \mu \frac{1}{2} e^{\mu(z-l)} \sqrt{\frac{\pi}{2\mu z}} = e^{-1}\sqrt{\frac{\pi}{8}}\sqrt{\frac{\mu}{z}}\quad .$$

The convolution theorem for product of two Fourier cosine transforms can be used for transformation of one class of integrals containing oscillating functions to integrals of monotonic functions. These results are applied for transformation of solution of some MHD problems arising in half space $z \geq 0$ in the consequence of the roughness of the space z=0. The various boundary layers for induced current in a strong magnetic field are found in this problem.

# 3. CORROSION OF EUROFER STEEL AND MAGNETIC CONFINEMENT OF PLASMA IN REACTORS

Search of new energy sources draws the increasing attention of scientists of many countries and

that is why they are trying to drag and control the fusion of **D-T** (Deutrium-Tritium) plasma inside of a Tokamak-Reactor. (Tokamak is a device used in nuclear fusion research for magnetic confinement of plasma and it consists of a complex system of magnetic fields that

confine the plasma in a hollow doughnut-shaped container). The **D-T** reaction and its related use in reactors are briefly described.

During my seven year staying period in Riga, LATVIA ( One of the main MHD application centers currently existing in EUROPE), I have had access to some interesting sites related to MHD study such as the Physics Institute in Salaspils where I have seen the three recently planned experimental sessions (each 2000 hours long) which have been performed successfully. New results concerning the profile of corrosion are obtained. I had the opportunity to participate in some PAMIR MHD International Conferences ($4^{th}$ and $5^{th}$ and the $7^{th}$ PAMIR International Conferences). This led to the writing of the third section illustrating the mentioned above. [1], [32], [34], [35], [36], [37], [40], [49], [56] and [64]

### 3.1 Deuterium-Tritium reaction and its use in Reactors.

During this century, the world's population will double from six billion people and it will rise to ten billions by 2050. More importantly, a lot more energy will be used than we do today, energy consumption will probably be two times higher by the middle of the century with an even stronger increase in electricity consumption. ( Table 1 below)

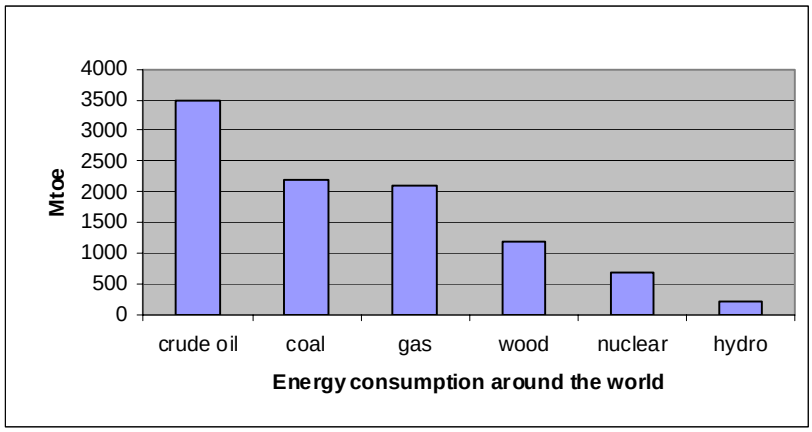


**Table 1. Energy consumption by the year 2007 [Mtoe (Million Tonnes Of Oil Equivalent)]**
**(The exact values are respectively 3500, 2200, 2100, 1200, 700, and 200)**

Fusion is the nuclear process that powers the sun and other stars. Under the very high temperature conditions, hydrogen atom becomes separated into its fundamental components-electrons and nuclei, and form a new state of matter called "Plasma". Finally the nuclei fuse producing Helium and giving energy. Scientists from all European member states and G8 countries associated with the EURATOM fusion program have been trying to reproduce this process on Earth. The fusion of Deutrium and Tritium, two Hydrogen isotopes would need a temperatue of 100 million ºC. This procedure can be done inside of a reactor using a ***Magnetic confinement*** that consists of heating on the Plasma by Joule effect and by injection of energetic

particle beams and radio-frequency waves into the plasma and its thermal isolation from the material walls by strong magnetic fields [1], [32], [33], [57], [49].

Mainly, three types of liquid metal blankets are proposed for this purpose:

1) ( SCLL), the Self-Cooled Lithium-Lead blanket

2) (WCLL), the Water-Cooled Lithium-Lead blanket

3) (HCLL), the Helium-Cooled Lithium-Lead blanket [1], [33], [57], [49].

EUROFER-97 steel has been tested as the best structural materials of the blanket in a reactor. It is supposed to be used as the basic construction material for the production of the HCLL **(Helium-Cooled Lithium-Lead**) Blanket.(Figure 13 below)

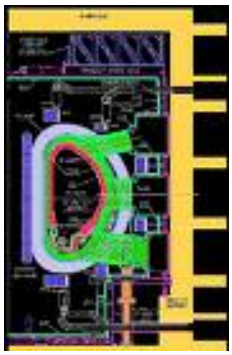

**Figure 11. HCLL Blanket image: 596 x 954 - 52k – jpg**

### 3.1.1 The Deuterium-Tritium (D-T) reaction and its products :

$$ {}^{2}_{1}\mathrm{H} + {}^{3}_{1}\mathrm{H} \rightarrow {}^{4}_{2}\mathrm{He} + {}^{1}_{0}\mathrm{n} + 17.6\ \mathrm{MeV} \qquad (3.1) $$

and simply represented in figure 12 below as:

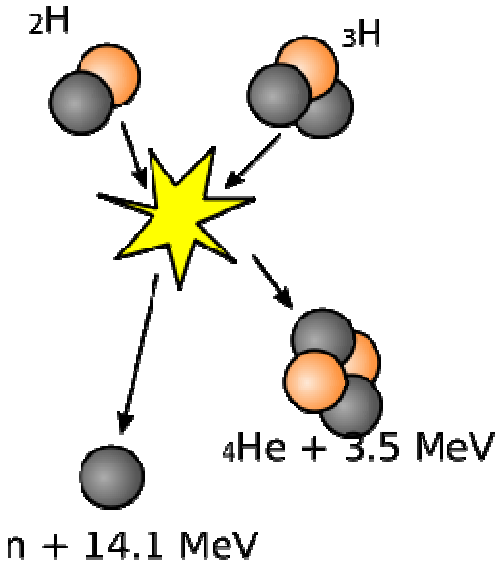


**Figure 12. Deuterium-Tritium (D-T) reaction and its products**

The fusion energy ( 17.6 MeV ) appears as Kinetic energy of neutrons (14.1 MeV ) that need to be saved inside of a reactor using lead, and of Alphas ( 3.5MeV ) that are evacuated as ashes from the chimney of a certain reactor [1], [36], [37], and [64].

Deutrium is generously present in seawater but Tritium is a radioactive element rarely existent naturally on Earth. However it can be bred inside the reactor using the reaction of the neutrons in a blanket containing lithium, an abundant light metal in the nature as:

$Li6 + n \text{ ---- } T + He4 + 4.8 \text{ MeV}$

(3.2)

$Li7 + n \text{ ---- } T + He4 - 2.5 \text{ MeV}$

(3.3)

Ten grams of deuterium which can be extrated from 500 litres of water and 15 gr of tritium produced from 30 gr the lithium would produce enough fuel for the lifetime electricity needs of a person in an industrialised country. In other words, these two resources are practically available. This is another advantage of D-T Fusion. [1], [29], [32], [39], [35], [49], [55], [56], [64]

3.1.2 Progress of the D-T plasmas confinement inside of Reactors.

Europe, the world leader in this field, has already undertaken several research and development projects dealing with Fusion. Among these, the **JET** project, for the Joint European Torus which is the largest Tokamak in the world constructed in Culham (UK). Despite the progress continuously achieved on JET, it is clear that a larger and more powerful device would be necessary to demonstrate the feasibility of nuclear fusion energy on a reactor scale. The future of fusion lies on **ITER** (The International Thermonuclear Experimental Reactor) whose purpose is to produce a detailed, complete, and fully integrated engineering design of ITER and all technical data necessary for future decisions and results that come out of ITER. [1], [22], [33], [34], [37], [57], [49], [64].

**ITER** will be constructed using the results of **JET** with the same concepts and the same Toroidal shape but on a much larger scale ( see figure 13 below).

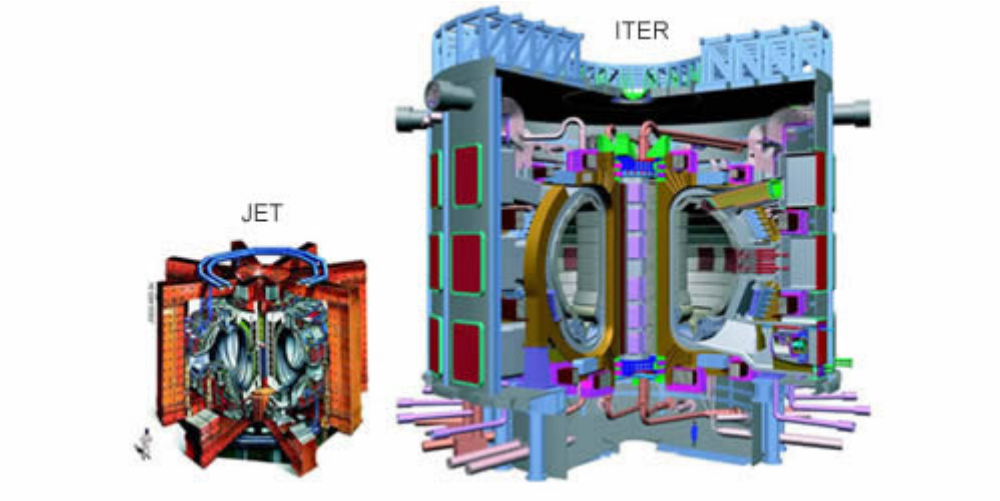


**Figure 13 The relative sizes of JET and ITER devices. [1]**

The plasma volume of **JET** and **ITER** are 100 $m^2$ and 800 $m^2$ respectively. In the case of **JET**, losses of energy are compensated by a source of outside energy. One of the advantages of **ITER** that it will not depend on power supply from the outside. The deuterium-tritium (D-T) experiments on the Tokamak Fusion Test Reactor (TFTR) have yielded unique information on the confinement, heating and alpha particle physics of reactor scale D-T plasmas as well as the first experience with tritium handling and D-T neutron activation in an experimental environment. **Toroidal and poloidal** field coils are used and these generate the strong magnetic field (typically about 5 tesla, which is about 100,000 times the earth's magnetic field) that confines the plasma and stops it touching the walls of the vacuum vessel. The D-T plasmas produced and studied in TFTR have peak fusion power of 10.7 MW with central fusion power densities of 2.8 $MWm^{-3}$ which is similar to the 1.7 $MWm^{-3}$ fusion power densities projected for 1,500 MW operation of (ITER). Detailed alpha particle measurements have confirmed alpha confinement and heating of the D-T plasma by alpha particles as expected. Advanced tokamak operating modes have been produced in TFTR which have the potential to double the fusion power to ~20 MW which would also allow the study of alpha particle effects under conditions very similar to those projected for ITER. TFTR is also investigating two new innovations, alpha channeling and controlled transport barriers, which have the potential to significantly improve the standard advanced tokamak.

This strategy included three steps beyond JET [35], [36], [37], [61]:

1) ITER, A Liquid lithium self-cooled breeding blanket aiming at demonstrating the controlled burn

of deuterium-tritium plasmas with steady state as an ultimate goal on a scale of a power plant and of

a number of key technologies. ITER project will be ready approximately by the end of year 2050 in Caradache, south of France.

2) DEMO, The water cooled blanket reactor aiming at the final demonstration of all the relevant technologies, tritium self-sufficiency and electricity production. Under the assumption that its design and construction would be started in 2035s and its operation in 2060s. A steady-state tokamak is minimized to have 5.8 m of major radius with 2.3 GW of fusion power with energy amplification Q exceeding 30.

3) PROTO, The first proto-type power station with complete reactor and ancillary systems that would include all the remaining technological developments as well as generating electricity on a commercial scale, under the assumption that its design and construction would be started in 2050s and its operation in 2070s. [1], [33], [35], [49], [49], [57], [64]

### 3.1.2 Major reasons of the use of fusion energy

Maybe at the end of this century, fusion would be considered as a new reliable long-term energy source that become a part of humans' lives with such important reasons:

**1.** The fuels are abundant everywhere and for a much very cheaper price in comparison to the present price.

**2.** The fusion process is very clean since it does not contribute to the greenhouse effect, to the spread of acid rain, or to radioactive particles that could take many years to remove.

**3. D-T** fusion power station can be made very safe due to two main reasons:

**(i)** a large uncontrolled release of energy would be impossible since the amounts of deuterium and tritium fuels inside the reactor will be very small;

**(ii)** the fusion reactions can be stopped in a very short time if an accident occurs, since the fuels are introduced inside the reactor while they are burned.

## 3.2 Analysis of MHD Phenomena Influence on the Corrosion of EUROFER Steel in the Pb-17Li Flow

In the second part of this thesis (section 2.2) the MHD flow with the roughness of the surface in the form $\tilde{z} = \tilde{\chi}_0 \cos(\pi\tilde{x}/2L)$ of a conducting fluid is located in the half space $\tilde{z} > 0, -\infty < \tilde{x}, \tilde{y} < +\infty$ is considered. The external magnetic field is $B^c = B_0 e_z$. Corrosion of EUROFER Steel in the Pb-17Li flow can be considered as a consequence of roughness on the surface of the walls where the Hartmann surfaces flows are perpendicular to the flow as well. The roughness is not smooth but its equation is of the form:

$$Z = Z(y) = \chi_0 \cos \alpha y, \qquad (3.4)$$

where $\chi_0$ is the amplitude, $\alpha = \pi a / L$ characterize the scale, L is the width of hills and depressions, and Ha is the Hartmann number. The value a=3 mm is chosen as a typical dimension. Here $\nu = 1.1 \times 10^{-7} m^2/s$; $\sigma = 0.73 \times 10^6 S/m$ and thus for the mass transfer problem $D_{Fe} = (6.4) \times 10^{-9} m^2/s$ more than $6 \times 10^{-9} m^2/s$ as it was assumed in [1], [55], and [56]) .

In spite of the fact that Corrosion of Steel in the Pb-17Li flow is a small but important part of the reactor work, we notify the importance and newest results attained of the corrosion process done in the Physics Institute-LATVIA [55], [56]. For instance, the first experimental 2000 hours' session for investigating the magnetic field influence on the corrosion of EUROFER steel in the flow of Pb-17Li has been completed successfully. During the whole session the following conditions were maintained at the experimental facility: the minimum temperature in the cold part of the loop $T_{min} = (350 \pm 20)\ ^0C$; the temperature in the test section $T_{TS} = (550 \pm 10)\ ^0C$; the mean flow velocity in the test section $U_{mean} = (5 \pm 0.5)$ cm/s; the magnetic field strength B = 1.7 T. The samples removed from the test section were washed off the residue of the melt in a pure Li melt at the temperature of $400^0C$ and further weighed. These measurements showed that mass losses for corroded samples located in the zone with a magnetic field are approximately over two times greater if compared with those located in the zone outside the magnetic field (B = 0) that evidences to a significant intensification of the corrosion by the magnetic field, see fig. 16. Moreover, it should be stressed that due to insufficient heat isolation of the test section the temperature of the molten metal varied over the length of the test section: at the zone (B = 0) inlet it was by ~ 15 °C higher than at the test section outlet with the magnetic

field, where T = 550 °C. This experiment was performed on different samples with flow velocities of 2,5 cm/s and 5cm/s and magnetic current of 0, 1,5 and 1.7 T. Results gained in these investigations demonstrated essential influence of magnetic field on the corrosion processes both in the intensity of corrosion and its character. ( Figure 14)

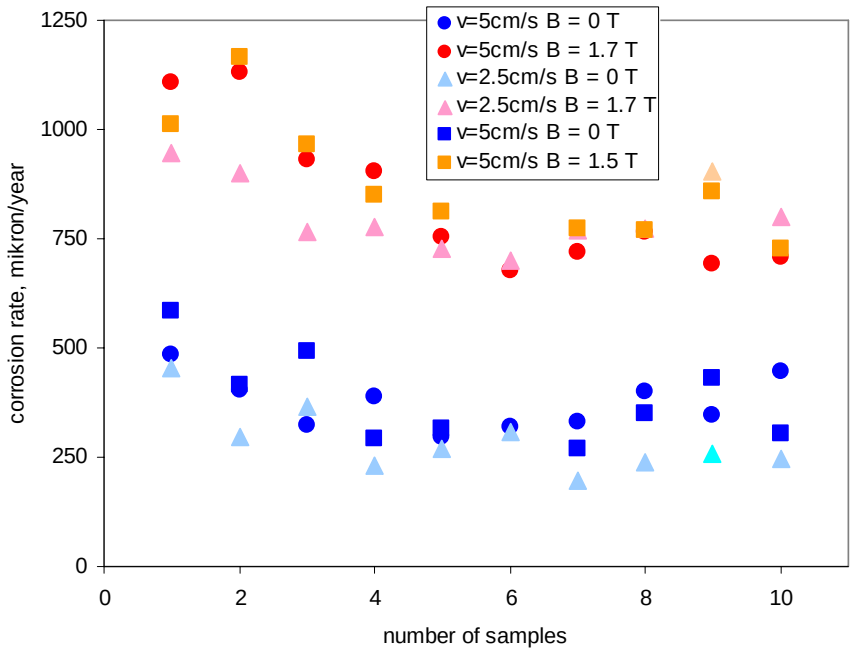


**Figure 14. Comparison of corrosion rate of EUROFER samples in magnetic field and without magnetic field.**

Visual observations of the test samples showed sufficient distinctions in relief on the sample surfaces, suffering corrosion from the zone with B = 0 are rather smooth and, on the contrary, the sample surfaces from the zone exposed to the magnetic field resemble a regular enough wave-like pattern with furrows oriented in the melt flow direction. Such pattern is typical only of the Hartmann (perpendicular to the magnetic field) walls. The side walls remain rather smooth. The same can be attributed to the outer sample surfaces, which exhibit traces of corrosion caused by the EUROFER interaction with the melt that penetrated the gaps between the samples and the outer channel.

The second experimental (2000 hours' session) has been completed successfully and showed that the magnetic field not only generally enhanced the corrosion rate, but showed that magnetic field badly influences corrosion. In the case for samples located in zone (***B*** = 0) all inner surfaces of samples being subjected to the Pb-17Li flow were maintained sufficiently smooth, then in zone with magnetic field (***B*** = 1.7 T) all Hartman surfaces of samples were covered with grooved structure oriented in the flow direction. [1], [49], [55], [56], [64] led to the appearance of regular wave-like patterns on the corroding surfaces perpendicular to the

magnetic field, which were oriented in the melt flow direction and that the corrosion processes on the EUROFER surfaces washed over by **Pb-17Li** and were determined by the surface orientation about the magnetic field direction [55] & [56]

( See figure 15 below)

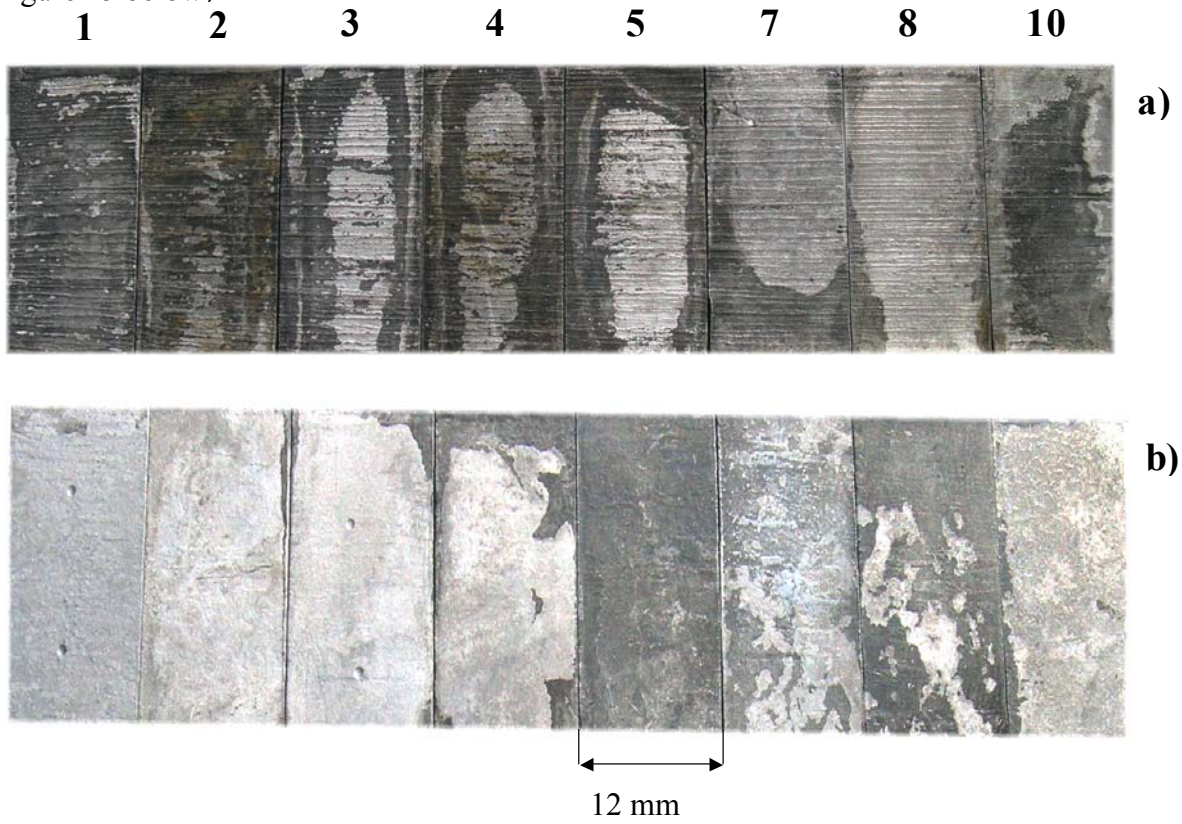


**Figure 15. Surface relief of EUROFER samples subjected to corrosion in Pb17Li during 2000 hours.**

Moreover, in the third experimental session [56] the corrosion rate $h_0$ caused by **Pb-17Li** on the EUROFER steel was investigated and its results of the corrosion rate are shown in the table below)

***Corrosion rate $h_0$ without and with magnetic field.***

| N | $B_0$=0 | $B_0$=1.8T |
|---|---|---|
| | $h_0$, μ meter/year | |
| 1 | 523 | 967 |
| 2 | 458 | 877 |
| 3 | 381 | 694 |
| 4 | 293 | 846 |
| 5 | 388 | 726 |

**Table 2. Corrosion rate of EUROFER steel by Pb-17Li flow** [55], [56]

Hoping that before the end of this century, scientists with all the technologies ans studies available, would be able to achieve success of The ITER project will provide the physics and technological basis for the construction of a demonstration electrically generating power plant in thr future like DEMO and PROTO . Then a new clean and cheap source of energy would be a part of humans' life. [1], [9], [20], [28], [32]-[37] , [40] , [49] , [51], [55] , [56] , [62] , [70] and [73]

## 4. Ginzburg-Landau equation for stability analysis of shallow water in a weakly non-linear regime

Losses due to turbulent friction are often described in hydraulics by means of empirical (or semi-empirical) formulas like Chezy of Manning's formulas [22]. In particular, the Chezy formula is used to represent the bottom friction force $\vec{F}$ in the form

$$\vec{F} = \frac{\rho g A c_f}{h} \vec{v}|\vec{v}|,$$

where $\rho$ is the density of the fluid, $g$ is the acceleration due to gravity, $A$ is the cross-sectional area, $h$ is water depth, $c_f$ is the friction (or roughness) coefficient, $\vec{v}$ is the velocity vector and $\vec{F}$ is the friction force. The coefficient $c_f$ is estimated by means of several empirical formulas which can be found in the literature. One example is Colebrook formula [67] which relates $c_f$ to the Reynolds number of the flow.

Chezy formula is effectively used by hydraulic engineers for many years to estimate the "lumped" effect of a turbulent flow. Examples include computation of flow rate and losses in channels or pipes and design of open channels. Chezy formula is also widely used in cases where more detailed knowledge of the flow field is required [50]. The coherent structures in wake flows are believed to appear as a final product of hydrodynamic instability of the flow [45]. Classical method of analysis of hydrodynamic stability is the linear stability analysis [26]. Linear theory can be used to find the value of the parameters of the problem for which a particular flow becomes unstable. However, the development of instability beyond the threshold cannot be described by the linear theory. Methods of weakly nonlinear theory have been applied in the past to different flows [8, 10, 14-16, 19, 22, 23, 26, 43, 44, 47, and 67] and usually lead to amplitude evolution equations for the most unstable mode. One of such equations is the complex Ginzburg-Landau equation. Weakly nonlinear theory is applied to quasi-two-dimensional flows in [22] with Rayleigh friction (internal friction is assumed to be linearly related to the velocity distribution). It is concluded in [26] that small variations of linear stability characteristics (in

particular, small variations in the base flow profile) led to large changes in the Landau constant (the Landau constant is the real part of one of the coefficients of the Ginzburg-Landau equation).

## 4.1 Shallow flows behind obstacles

Wake flows are quasi-two-dimensional flows behind obstacles (such as islands) in which the horizontal components of the velocity vector are much stronger than the vertical component. A typical measure of shallowness of the flow is the ratio of the transverse length scale of the flow, $D$, and water depth, $H$. The flow is assumed to be shallow if the ratio $D/H$ is large enough: $D/H >> 1$. An excellent example of shallow wake flow is shown in [47] where the leaking oil from the tanker Argo Merchant shows a von Karman vortex street flow pattern. Other examples of aeronautical photographs of island wakes in shallow waters are presented in [37] and [82]. Experimentally observed coherent structures in shallow wakes are believed to appear as a result of flow instability [43], [67]. Linear stability of shallow flows is studied experimentally in [19], [45], [77]. It is shown in [19] that three different flow regimes can be observed in shallow wake flows: steady bubble, unsteady bubble and vortex street. It was found in [24] and [43] that flow patterns behind obstacles depend on shallow wake stability parameter $S = c_f b/H$, where $c_f$ is the bottom friction coefficient and $b$ is length scale (the diameter of the cylinder in [8]).

Theoretical investigation of linear stability of shallow wake flows is performed in [19], [45], [47], and [67]. Linear stability analyses confirm that the stability characteristics of shallow water flows depend on the magnitude of the stability parameter $S$. In particular, a flow becomes more stable as the parameter $S$ increases.

The linear stability theory can be used to determine when a particular flow becomes unstable. The "fate" of the disturbance just above the threshold cannot be predicted by the linear theory. Methods of weakly nonlinear theory are often applied to describe the evolution of the most unstable linear mode when the flow becomes unstable [26], and [67]. Relatively simple amplitude evolution equations such as the Complex Ginzburg-Landau Equation (CGLE) are used in the literature to analyze spatio-temporal dynamics of complex flows [10], [19]. The popularity of the CGLE is based on the following factors: (1) the model is relatively simple but includes such physical effects as nonlinearity and diffusion, (2) the CGLE is a scalar equation, (3) the CGLE can be derived (in some cases) from the equations of motion, (4) the coefficients of the CGLE can be obtained in closed form (in terms of integrals containing the characteristics of the corresponding linear stability problem), (5) the CGLE can exhibit a rich variety of solutions depending on the values of its coefficients.

In many applications (see, for example, the analysis of the dynamics of the flow behind bluff rings [59] and spatio-temporal dynamics in the wakes of a row of 16 circular cylinders placed close to each other in an incoming flow [46]) the CGLE (or the Landau equation) is used as a phenomenological model equation. In such cases the coefficients of the CGLE are obtained from experimental data.

On the other hand, the CGLE can be derived from the equations of motion. Examples include weakly nonlinear analyses of plane Poiseuille flow [67] and problems related to generation of waves by wind [10], shallow flows behind obstacles such as islands [45], and [46] and in the nearshore [44], rapidly decelerated flows in pipes [43] and channels [47].

Despite the fact that the CGLE was successfully applied in practice to model spatio-temporal dynamics of complex flows [46], [47], other sources in the literature suggest that the use of weakly nonlinear theory should be limited. One such an example is introduced in paper [23] where linear and weakly nonlinear theory is applied to the stability analysis of quasi-two-dimensional shear flows such as shallow water flows. It is assumed in [25] that the term representing friction in fluid system is of the form $\vec{f}_R = -\lambda_R \vec{u}$, where $\lambda_R$ is the coefficient of Rayleigh friction and $\vec{u}$ is the velocity vector. The authors compared their theoretical predictions from the linear stability analysis with experimental data. Reasonable agreement was found. On the other hand, it is found in [23] that the Landau constant (the real part of one of the coefficients of the CGLE) is quite sensitive to the shape of the base flow velocity profile. As a result, it is concluded in [23] that it would be impossible to compare directly the theory with experiments since it would be difficult to determine the base flow velocity profile with accuracy up to the third derivative (as it is required by a weakly nonlinear theory). In particular, it is found in [23] that the values of the Landau constant differ by a factor of 3 for two base flow velocity profiles whose linear stability characteristics differ by not more than 20%.

In the present section, linear and weakly nonlinear stability of a one-parametric family of shallow wake flows is investigated [15] and [16]. The parameter used in the study represents a slow longitudinal variation of shallow wake flow behind obstacles such as islands. In contrast to [22] where the internal friction is linearly related to the velocity
distribution, a nonlinear Chezy formula [67] is used to model bottom friction. The base flow profile used in [19] is adopted in our study. Calculations show that the Landau constant as well as other coefficients of the CGLE are not so sensitive to the shape of the base flow
profile. Thus, it is plausible to assume that the CGLE can be used to describe spatio-temporal dynamics of shallow wake flows.

## 4.2 Linear stability analysis

Consider the base flow of the form

$$\vec{U} = (U(y),0) \tag{4.1}$$

where

$$U(y) = 1 - \frac{2R}{1-R}\frac{1}{\cosh^2(\alpha y)}. \tag{4.2}$$

The base flow (4.2) is suggested in [67] after careful analysis of available experimental data for deep water flows behind circular cylinders. The profile (4.2) is also adopted in the present study. The parameter $R$ is the velocity ratio: $R = (U_m - U_a)/(U_m + U_a)$, where $U_m$ is the wake centerline velocity and $U_a$ is the ambient velocity, and $\alpha = \sinh^{-1}(1)$. It is shown in [10] that under the rigid-lid assumption the linear stability of wake flows in shallow water is described by the following eigenvalue problem:

$$\varphi_1''(U - c + SU) + SU_y\varphi_1' + \left(k^2 - U_{yy} - k^2U - \frac{S}{2}kU\right)\varphi_1 = 0 \tag{4.3}$$

$$\varphi_1(\pm\infty) = 0, \tag{4.4}$$

where the perturbed stream function of the flow, $\psi(x,y,t)$, is assumed to be of the form

$$\psi(x,y,t) = \varphi_1(y)\exp[ik(x-ct)] + c.c. \tag{4.5}$$

Here $\varphi_1(y)$ is the amplitude of the normal perturbation, $k$ is the wavenumber, $c$ is the wave speed of the perturbation, and $c.c.$ means "complex conjugate". The linear stability of the base flow (4.2) is determined by the eigenvalues, $c_m = c_{rm} + ic_{im}$, $m = 1,2,...$ of the eigenvalue problem (4.3), (4.4). The flow (4.2) is linearly stable if $c_{im} < 0$ for all $m$ and linearly unstable if $c_{im} > 0$ for at least one value of $m$.

The linear stability problem (4.3), (4.4) is solved by means of a pseudospectral collocation method based on Chebyshev polynomials. The computational procedure is briefly described below (details of the numerical method can be found in [44]). The interval $-\infty < y < +\infty$ is mapped onto the interval $-1 < r < 1$ by means of the transformation $r = \frac{2}{\pi}\arctan y$. The solution to (4.3), (4.4) is sought in the form

$$\varphi_1(r) = \sum_{k=0}^{N} a_k(1-r^2)T_k(r), \tag{4.6}$$

where $T_k(r)$ is the Chebyshev polynomial of degree $k$. The collocation points $r_j$ are

$$r_j = \cos\frac{\pi j}{N}, \quad j = 0,1,...,N. \tag{4.7}$$

The derivatives are transformed by the chain rule:

$$\frac{d\varphi_1}{dy} = \frac{2}{\pi}\cos^2\frac{\pi r}{2}\frac{d\varphi_1}{dr},$$
$$\frac{d^2\varphi_1}{dy^2} = \frac{4}{\pi^2}\cos^4\frac{\pi r}{2}\frac{d^2\varphi_1}{dr^2} - \frac{4}{\pi}\sin\frac{\pi r}{2}\cos^3\frac{\pi r}{2}\frac{d\varphi_1}{dr} \qquad (4.8)$$

Substituting (4.6), (4.8) into (4.3), (4.4) and evaluating the function $\varphi_1(r)$ and its derivatives at the collocation points (4.7) we obtain the following generalized eigenvalue problem:

$$(B - \lambda C)a = 0 \qquad (4.9)$$

where $B$ and $C$ are complex-valued matrices and $a = (a_1 a_2 ... a_N)^T$.

| $R$ | $k$ | $S_c$ | $c$ |
|---|---|---|---|
| -0.3 | 0.892 | 0.11819 | 0.69814 |
| -0.4 | 0.909 | 0.15689 | 0.65964 |
| -0.5 | 0.926 | 0.19548 | 0.62394 |
| -0.6 | 0.944 | 0.23409 | 0.59083 |
| -0.7 | 0.962 | 0.27286 | 0.55925 |
| -0.8 | 0.980 | 0.31189 | 0.52882 |

Problem (4.9) is solved numerically by means of the IMSL routine DGVCCG. The critical values of the stability parameters $k, S$ and $c$ for different values of $R$ are given in Table 3 ( There $S_c = \max_k S$ ).

**Table 3. Critical values of of the stability parameter** $S$

## 4.3 Weakly nonlinear analysis

Following [67], in this section the main steps of the derivation of the amplitude evolution equation for the most unstable mode are briefly described. Consider the two-dimensional shallow water equations of the form :

$$\frac{\partial u}{\partial x} + \frac{\partial v}{\partial y} = 0, \qquad (4.10)$$

$$\frac{\partial u}{\partial t} + u\frac{\partial u}{\partial x} + v\frac{\partial u}{\partial y} + \frac{\partial p}{\partial x} + \frac{c_f}{2H}u\sqrt{u^2 + v^2} = 0, \qquad (4.11)$$

$$\frac{\partial v}{\partial t}+u\frac{\partial v}{\partial x}+v\frac{\partial v}{\partial y}+\frac{\partial p}{\partial y}+\frac{c_f}{2H}v\sqrt{u^2+v^2}=0, \tag{4.12}$$

where $u$ and $v$ are the depth-averaged velocity components in the $x$ and $y$ directions, respectively, $H$ is water depth, $p$ is the pressure.

Suppose that

$$u=\frac{\partial \psi}{\partial y},\ v=-\frac{\partial \psi}{\partial x}, \tag{4.13}$$

where $\psi(x,y,t)$ is the stream function of the flow. Eliminating the pressure and using (4.13) one can rewrite the system (4.10) – (4.12) in the form

$$\begin{aligned}&(\Delta\psi)_t+\psi_y(\Delta\psi)_x-\psi_x(\Delta\psi)_y+\frac{c_f}{2h}\Delta\psi\sqrt{\psi_x^2+\psi_y^2}\\&+\frac{c_f}{2h\sqrt{\psi_x^2+\psi_y^2}}\left(\psi_y^2\psi_{yy}+2\psi_x\psi_y\psi_{xy}+\psi_x^2\psi_{xx}\right)=0\end{aligned} \tag{4.14}$$

Consider a perturbed solution to (4.14) of the form

$$\psi=\psi_0(y)+\varepsilon\psi_1(x,y,t)+\varepsilon^2\psi_2(x,y,t)+... \tag{4.15}$$

The parameter $\varepsilon$ describes a small deviation of the shallow wake stability parameter $S$ from the critical value $S_c$:

$$S=S_c(1-\varepsilon^2) \tag{4.16}$$

Weakly nonlinear theory is applicable in a small neighborhood of the critical point (see Fig. 16):

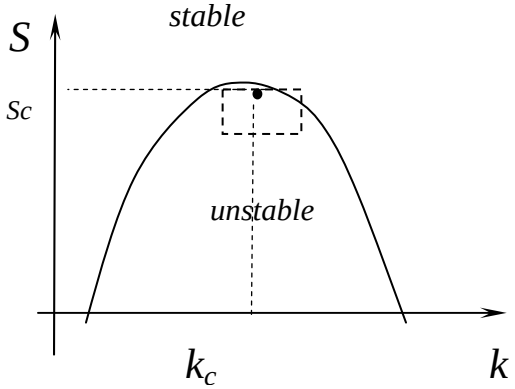


**Figure 16. Neighborhood of the critical point in a weakly nonlinear Region in the $(k,S)$-plane (shown as dashed rectangle) where weakly nonlinear theory is applicable.**

The amplitude evolution equation for the most unstable mode is derived by means of the method of multiple scales. Following [67], the following slow time and longitudinal variables are introduced:

$$\tau = \varepsilon^2 t, \quad \xi = \varepsilon(x - c_g t), \tag{4.17}$$

where $c_g$ is the group velocity.

The function $\psi_1$ in [15] is sought in the form

$$\psi_1(x, y, t) = A(\xi, \tau)\varphi_1(y)\exp[ik(x - ct)] + c.c. \tag{4.18}$$

where $A$ is a slowly varying amplitude.

The linear stability problem (4.3), (4.4) is obtained by substituting (4.15) – (4.18) into (4.14), collecting the terms containing $\varepsilon$ and using (4.5). Collecting the terms containing $\varepsilon^2$ the following equation is obtained:

$$\begin{aligned} L\psi_2 &= c_g(\psi_{1xx\xi} + \psi_{1yy\xi}) - 2\psi_{1x\xi t} - \psi_{0y}(3\psi_{1xx\xi} + \psi_{1yy\xi}) \\ &-\psi_{1y}(\psi_{1xxx} + \psi_{1yyx}) + \psi_{1x}(\psi_{1xxy} + \psi_{1yyy}) + \psi_{1\xi}\psi_{0yyy} \\ &-S[(\psi_{1xx} + \psi_{1yy})\psi_{1y} + 2\psi_{1x\xi}\psi_{0y} + \psi_{1yy}\psi_{1y} - 2\psi_{0y}\psi_{0yy} \\ &+2\psi_{1x}\psi_{1xy}] \end{aligned} \tag{4.19}$$

Here

$$\begin{aligned} L\psi &= \psi_{xxt} + \psi_{yyt} + \psi_{0y}(\psi_{xxx} + \psi_{yyx}) - \psi_{0yyy}\psi_x \\ &+\frac{c_f}{2h}\left[(\psi_{xx} + 2\psi_{yy})\psi_{0y} + 2\psi_y\psi_{0yy}\right]. \end{aligned}$$

Similarly, the equation of order $\varepsilon^3$ has the form

$$\begin{aligned} L\psi_3 &= c_g(\psi_{2xx\xi} + 2\psi_{1x\xi\xi} + \psi_{2yy\xi}) - \psi_{1xx\tau} - \psi_{1yy\tau} - 2\psi_{2x\xi t} \\ &-\psi_{1\xi\xi t} - 3\psi_{0y}(\psi_{2xx\xi} + \psi_{1x\xi\xi}) - \psi_{1y}(\psi_{2xxx} + 3\psi_{1xx\xi}) \\ &-\psi_{2y}(\psi_{1xxx} + \psi_{1yyx}) - \psi_{1y}(\psi_{2yyx} - \psi_{1\xi yy}) - \psi_{0y}\psi_{2\xi yy} \\ &+\psi_{2x}\psi_{1xxy} + \psi_{1\xi}\psi_{1xxy} + \psi_{1x}\psi_{2xxy} + 2\psi_{1x}\psi_{1xy\xi} + \psi_{1x}\psi_{2yyy} \\ &+\psi_{2x}\psi_{1yyy} + \psi_{1\xi}\psi_{1yyy} + \psi_{2\xi}\psi_{0yyy} \\ &-S[\psi_{2y}(\psi_{1xx} + \psi_{1yy}) + 2\psi_{2yy}\psi_{1y} + 1.5\psi_{1xx}\psi_{1x}^2/\psi_{0y} \\ &+\psi_{2xx}\psi_{1y} + 2\psi_{1x\xi}\psi_{1y} + 2\psi_{0y}\psi_{2x\xi} + \psi_{1\xi\xi}\psi_{0y} - \psi_{1xx}\psi_{0y} \\ &-2\psi_{0yy}\psi_{1y} - 2\psi_{0y}\psi_{1yy} + \psi_{1yy}\psi_{2y} - \psi_{1y}\psi_{2yy} + 2\psi_{1x}\psi_{2xy} \\ &+2\psi_{1x}\psi_{1yy} + 2\psi_{2x}\psi_{1xy} + 2\psi_{1\xi}\psi_{1xy}] \end{aligned} \tag{4.20}$$

The function $\psi_2$ is sought in the form

$$\begin{aligned} \psi_2 &= AA^*\varphi_2^{(0)}(y) + A_\xi\varphi_2^{(1)}(y)\exp[ik(x - ct)] \\ &+A^2\varphi_2^{(2)}(y)\exp[2ik(x - ct)] + c.c. \end{aligned} \tag{4.21}$$

The function $\varphi_2^{(0)}(y)$ is the solution of the following boundary value problem

$$\begin{aligned}&2S[u_{0y}\varphi_{2y}^{(0)}+u_0\varphi_{2yy}^{(0)}]=ik[\varphi_{1y}\varphi_{1yy}^{*}-\varphi_{1y}^{*}\varphi_{1yy}\\&+\varphi_1\varphi_{1yyy}^{*}-\varphi_1^{*}\varphi_{1yyy}]-S[k^2\varphi_1\varphi_{1y}^{*}+k^2\varphi_1^{*}\varphi_{1y}\\&+2\varphi_{1y}^{*}\varphi_{1yy}+2\varphi_{1yy}^{*}\varphi_{1y}],\end{aligned}\tag{4.22}$$

$$\varphi_2^{(0)}(\pm\infty)=0.\tag{4.23}$$

The function $\varphi_2^{(1)}(y)$ satisfies the equation

$$\begin{aligned}&(iku_0-ikc)\varphi_{2yy}^{(1)}+(ik^3c-ik^3u_0-iku_{0yy})\varphi_2^{(1)}\\&+S[2u_0\varphi_{2yy}^{(1)}+2u_{0y}\varphi_{2y}^{(1)}-k^2u_0\varphi_2^{(1)}]\\&=(c_g-u_0)\varphi_{1yy}+[-2k^2c+3k^2u_0+u_{0yy}-k^2c_g\\&-iku_0S]\varphi_1,\end{aligned}\tag{4.24}$$

$$\varphi_2^{(1)}(\pm\infty)=0.\tag{4.25}$$

The function $\varphi_2^{(2)}(y)$ is the solution of the boundary value problem

$$\begin{aligned}&2(iku_0-ikc)\varphi_{2yy}^{(2)}+(8ik^3c-8ik^3u_0-2iku_{0yy})\varphi_2^{(2)}\\&+S[2u_0\varphi_{2yy}^{(2)}+2u_{0y}\varphi_{2y}^{(2)}-4k^2u_0\varphi_2^{(2)}]\\&=ik(\varphi_1\varphi_{1yyy}-\varphi_{1y}\varphi_{1yy})-S(2\varphi_{1y}\varphi_{1yy}-3k^2\varphi_1\varphi_{1y}),\end{aligned}\tag{4.26}$$

$$\varphi_2^{(2)}(\pm\infty)=0.\tag{4.27}$$

The amplitude evolution equation for $A$ is obtained from the solvability condition for equation (4.20) and has the form of the complex Ginzburg-Landau equation (the equation is derived in detail in [46]):

$$\frac{\partial A}{\partial\tau}=\sigma A+\delta\frac{\partial^2A}{\partial\xi^2}-\mu|A|^2A\tag{4.28}$$

The coefficients of equation (3.28) are given by

$$\sigma=\frac{\sigma_1}{\gamma},\ \delta=\frac{\delta_1}{\gamma},\ \mu=\frac{\mu}{\gamma},\tag{4.29}$$

where

$$\gamma_1=\int_{-\infty}^{+\infty}\varphi_1^a(\varphi_{1yy}-k^2\varphi_1)dy,\tag{4.30}$$

$$\sigma_1=S\int_{-\infty}^{+\infty}\varphi_1^a(2u_0\varphi_{1yy}+2u_{0y}\varphi_{1y}-k^2u_0\varphi_1)dy,\tag{4.31}$$

$$\delta_1 = \int_{-\infty}^{+\infty} \varphi_1^a [\varphi_{2yy}^{(1)}(c_g - u_0) + \varphi_2^{(1)}(-k^2 c_g - 2k^2 c$$
$$+3k^2 u_0 + u_{0yy} - 2iku_0 S) + \varphi_1(2ikc_g + ikc \qquad (4.32)$$
$$-3iku_0 - US)]dy,$$

$$\mu_1 = \int_{-\infty}^{+\infty} \varphi_1^a \{6ik^3 \varphi_2^{(2)} \varphi_{1y}^* - 2ik\varphi_{1y}^* \varphi_{2yy}^{(2)} + 3ik^3 \varphi_1^* \varphi_{2y}^{(2)}$$
$$+ik^3 \varphi_1(\varphi_{2y}^{(0)} + \varphi^{*(0)}_{2y}) - ik\varphi_{1yy}(\varphi_{2y}^{(0)} + \varphi^{*(0)}_{2y})$$
$$+ik\varphi_{2y}^{(2)} \varphi_{1yy}^* - ik\varphi_1^* \varphi_{2yyy}^{(2)} + ik\varphi_1(\varphi_{2yyy}^{(0)} + \varphi_{2yyy}^{*(0)}) \qquad (4.33)$$
$$+2ik\varphi_{1yyy}^* \varphi_2^{(2)} - 2S[-k^2 \varphi_1(\varphi_{2y}^{(0)} + \varphi^{*(0)}_{2y})$$
$$+3k^2 \varphi_1^* \varphi_{2y}^{(2)} - 1.5k^4 \varphi_1^2 \varphi_1^* / u_0 + 2\varphi_{1yy}(\varphi_{2y}^{(0)} + \varphi^{*(0)}_{2y})$$
$$+2\varphi_{1yy}^* \varphi_{2y}^{(2)} + 2\varphi_{1y}(\varphi_{2yy}^{(0)} + \varphi^{*(0)}_{2yy}) + 2\varphi_{2yy}^{(2)} \varphi_{1y}^*]\}dy$$

In addition, one needs to calculate the adjoint eigenfunction $\varphi_1^a$ of the linear stability problem:

$$(iku_0 + 2Su_0)(\varphi_1^a)'' + (2iku_{0y} + 2Su_{0y})(\varphi_1^a)' \qquad (4.34)$$
$$-(ik^3 u_0 + u_0 k^2 S)\varphi_1^a + ikc[(\varphi_1^a)'' - k^2 \varphi_1^a] = 0$$

$$\varphi_1^a(\pm\infty) = 0. \qquad (4.35)$$

The group velocity $c_g$ is given by

$$c_g = \frac{I_1}{I_2}, \qquad (4.36)$$

where

$$I_1 = \int_{-\infty}^{+\infty} [u_0 \varphi_{1yy} - \varphi_1(3k^2 u_0 + u_{0yy}$$
$$-2k^2 c - 2iku_0 S)]\varphi_1^a dy$$

$$I_2 = \int_{-\infty}^{+\infty} \varphi_1^a(\varphi_{1yy} - k^2 \varphi_1)dy.$$

Solving boundary value problems (4.22) – (4.27), calculating $\varphi_1^a$ and $c_g$ and evaluating integrals in (4.30) – (4.33) numerically, the coefficients of the CGLE (4.28) are obtained for different values of $R$. The results are summarized in Table II.

One of the major conclusions drawn from weakly nonlinear analysis applied to quasi-two-dimensional flows in [22] was the effect of strong dependence of the Landau constant $\mu_r$ on the form of the base flow profile. Calculations presented in [22] showed that the values of the Landau constant differed by a factor of 3 for two base flow velocity profiles whose linear stability characteristics differed by only 20%. As a result, it was concluded in [22] that it would be impossible to apply methods of weakly nonlinear theory in practice since the base flow profile

| $R$ | $\sigma$ | $\delta$ | $\mu$ |
|---|---|---|---|
| -0.3 | 0.063 + 0.004i | 0.060 – 0.206i | 4.673 + 13.294i |
| -0.4 | 0.078 + 0.003i | 0.090 – 0.195i | 3.796 + 10.938i |
| -0.5 | 0.090 + 0.000i | 0.115 – 0.184i | 3.895 + 10.119i |
| -0.6 | 0.100 – 0.003i | 0.136 – 0.172i | 4.375 + 10.109i |
| -0.7 | 0.109 – 0.007i | 0.153 – 0.161i | 5.149 + 10.590i |
| -0.8 | 0.116 – 0.012i | 0.167 – 0.152i | 6.302 + 11.448i |

**TABLE 4**
**Coefficents of the CGLE (4.28)**

cannot be determined very precisely in experiments. In other words, it was concluded in [22] that the problem of determination of the Landau constant from weakly nonlinear theory is ill-posed so that small variations of the base flow profile lead to large changes in the Landau constant.

The calculations presented in Table **3** and **4** in our paper demonstrate that the coefficients of the CGLE are not so sensitive to the variation of the parameter $R$ of the base flow profile (2) as claimed in [22]. In fact, not only the Landau constant is not so sensitive to the changes in the profile (3.2) but all the coefficients of the CGLE do not vary too much.

## CONCLUSIONS

The present thesis is a theoretical work dealing with the roughness elements of MHD problems in strong magnetic fields when taken in rectangular duct and the behavior and conductivities of wall channels in ducts . Besides, we solve the problem that the solutions of certain problems about MHD flow of conducting fluid in the half space are expressed in terms of improper integrals of the product of some strongly oscillating functions at the large x by transforming those functions into integrals of monotone functions using the convolution theorem for product of two Fourier cosine transforms. Besides, we support application to some of the MHD problems. Moreover, we study the stability analysis of shallow water flows in a weakly non-linear regime and that by using the complex form of Ginzberg-Landau equation to getting calculations that showed that the values of the Landau's constants in [12] was found to be quite sensitive to the shape of the base flow profile. In our work we showed that the bottom friction is modeled by a nonlinear Chezy formula [14]. The coefficients of the CGLE do not change much in the interval $-0.8 \le R \le -0.3$. This interval of the $R$ values corresponds to convectively unstable regime [8]. As a result, it is plausible to conclude that the complex Ginzburg-Landau equation can be used for the analysis of shallow wake flows in a weakly nonlinear regime. In addition to that, we report the newest results of the three recently planned experimental sessions (each 2000 hours long) which have been finished successfully in Salaspis LATVIA, where results gained in these investigations demonstrated essential influence of magnetic field on the corrosion processes both in the intensity of corrosion and its character. Besides, new results concerning the profile of corrosion are obtained [56]. The process of investigation of EUROFER corroded samples showed the existence of sufficient distinction of corrosion processes between samples located in the zone outside magnetic field ($\boldsymbol{B}$ = 0) and those located in zone with magnetic field ($\boldsymbol{B}$ = 1.7 T). Such investigations are done for the purpose of fusion control in reactors. Especially, of D-T ( Deutrium- Tritium) plasma fusion concept. One of the main things in this program is the problem of liquid metals breeder blanket behavior. Structural material of blanket should meet high requirements because of extreme operating conditions. Therefore the knowledge of the effect of metals flow velocity, temperatures and also a neutron irradiation and

a magnetic field on the corrosion processes are necessary. At the moment the eutectic lead – lithium (Pb-17Li) is considered as the most suitable tritium breeder material of the reactor. [1], [55], &[56].

The first part is devoted for the description of the principles of MHD flows and to describe two terms that are considered effective to reduce the MHD pressure losses in duct channels, to solve problems of the flow in a strong magnetic field with suitable boundary conditions , to provide an asymptotic evaluation of each problem , to attain numerical results, and to graph the z-components for different Hartmann numbers (low and high values are considered). Besides, Ohm's law was used for describing the equations of Laplacian, fluid velocity, induced current φ(y,z) with its potential and external magnetic field. For example, in the problem introduced in part (1.3.1) we proved that the two dimensional MHD flow arises in the direction opposite to y axis, only if the roughness of the boundary is present. The solutions for the y component of the velocity of the fluid and for the x component of the induced current are obtained in the form of improper integrals of elementary functions. On the other hand, the z component of the induced current is expressed through the Bessel function. The asymptotic solution of the problem at Hartmann number $Ha \to \infty$ is obtained in the form of elementary functions. For Hartmann numbers Ha ≥ 10 the exact and the asymptotic solutions practically coincide.

Moreover, in the problem introduced in this section, it is proved that the induced magnetic field has only a y-component. Solutions for the system of MHD equations for the velocity fluid and for the potential of the induced current are obtained. Also the equations for the x and z components of pressure gradients are obtained. The velocity of the fluid in the core flow at large Hartmann numbers is constant. That means that it does not depend on Ha. With the increase of Hartmann number only the height of the core region is increased. The MHD solutions described in our work facilitate the investigation of the redistribution of the fluid in a region where the magnetic field is strong (The Hartmann number is large). These conclusions are important and can be helpful to other problems dealing with electrically conducting fluid through ducts in various area of Technology and Engineering such as MHD power generation, MHD flow-meters, MHD pumps, etc…

The second part mainly deals with the problem that the solutions of certain problems about MHD flow of conducting fluid in the half space are expressed in terms of improper integrals of the product of some meramorphic function and the function $\exp(-a\sqrt{\lambda^2 + b^2})\cos\lambda\cos\lambda x$. Here $a > 0$ and $b > 0$ are some parameters, $x > 0$ is the x-coordinate in Cartesian coordinate system.

But these functions are strongly oscillating at the large x, what make difficult the calculation of these integrals using package “Mathematica”. In this part these integrals are transformed into integrals of monotone functions using the convolution theorem for product of two Fourier cosine transforms. Besides, we support application to some of the MHD problems. The gotten results facilitate the evaluation of some problems in the field of Mathematics, Engineering, and Engineering Mathematics .

The third part is devoted to the stability analysis of shallow water flows in a weakly non-linear regime and that by using the complex form of Ginzberg-Landau equation to getting the results and conclusion of our study. Calculations presented in [12] showed that the values of the Landau’s constants differ by a factor of 3 for two different velocity profiles with linear stability characteristics In other words, the Landau’s constant in [12] was found to be quite sensitive to the shape of the base flow profile. In our work we showed that the bottom friction is modeled by a nonlinear Chezy formula [13]. The analysis of data from Table 1 and Table 2 shows that for shallow wake flows of the form (3) the changes in the linear stability characteristics resulted in even smaller changes in the coefficients of the CGLE. The coefficients of the CGLE do not change much in the interval $-0.8 \le R \le -0.3$. This interval of the $R$ values corresponds to convectively unstable regime [2]. As a result, it is plausible to conclude that the complex Ginzburg-Landau equation can be used for the analysis of shallow wake flows in a weakly nonlinear regime.

The fourth and last part is devoted of the practical study investigation of EUROFER corrosion in the Pb17Li flow where we introduce the results of the three recently planned experimental sessions which have been finished successfully. Results gained in these investigations demonstrated essential influence of magnetic field on the corrosion processes both in the intensity of corrosion and its character. Besides, new results concerning the profile of corrosion are obtained [56]. The process of investigation of EUROFER corroded samples showed that magnetic field both sufficiently influence on corrosion: visual observation of test samples removed from the test section after experiments showed sufficient distinction of corrosion processes between samples located in the zone outside magnetic field ($\boldsymbol{B}$ = 0) and those located in zone with magnetic field ($\boldsymbol{B}$ = 1.7 T). Search of new energy sources draws the increasing attention to use for this purpose of reactors. EUROATOM program scientists are designing how fusion reactors might properly operate using D-T plasma fusion concept. Starting by JET power plant passing by ITER in the process of DEMO, then reaching PROTO which will be the power plant that all nations around the world longing for, as for being the plant that will

be purely generating a fully controlled power of energy that will be directly connected to electricity networks. Besides, it is one of the very few options potentially acceptable from the environmental safety (Totally free from $CO_2$ emissions) and economic points of view.

Future work can be devoted for the study of liquid metal flow in a cusped spherical magnetic field with the main objective of a better control of the sidewalls of the flow in strong magnetic fields. Morover, another work can be done to proof that the use of the velocity of the fluid in the core flow at large Hartmann numbers is constant. Thus, it does not depend on Ha. With the increase of Hartmann number directly affects only the height of the core region.

Besides, some problems in Engineering Mathematics involve the use of the convolution theorem along the Fourier sine and cosine transforms, these theorems can be used for making up a new book in transforming one class of integrals containing oscillating functions to integrals of monotonic functions. These results are also applicable for transformation of solution of some MHD problems arising in half space $z \geq 0$ in the consequence of the roughness of the space $z$=0. The various boundary layers for induced current in a strong magnetic field can be found and graphed with the use of package

"Matematica" .

At last, the classified information listed in the last part when describing the results of the new experiments done in Salaspils on the magnetic field influence on the corrosion of EUROFER steel in the flow of Pb-17Li and its related D-T plasma confinement in a reactor can be used as a reference for future work related to the use of fusion nuclear energy.

## Appendix 1

## NOMENCLATURE

### List of Latin Symbols

$A$ The cross-sectional area

$\mathbf{B}^{e} = B_0 \mathbf{e}_z$ .the form of the external magnetic field

$B_0$ The potential of the magnetic field

$\vec{B}$ Complex-valued amplitude magnetic induction vector

$\vec{\tilde{B}}$ Magnetic induction vector, $\vec{\tilde{B}} = \vec{B}e^{jwt}$

c Euler conctant, c = 0.577215…

C The flow core, $Ha^{-1} < z < Ha$ ;

*c.c.* Complex conjugate

$c_f$ The friction (or roughness) coefficient,

$\mathbf{C}_r$ The Chromium element (Atomic Number 24)

CGLE The Complex Ginzburg-Landau Equation

$\vec{E}$ Complex-valued amplitude electric field vector

$\vec{\tilde{E}}$ Electric field vector $\vec{\tilde{E}} = \vec{E}e^{jwt}$

EFDA The European Fusion Development Agreement

$\mathrm{erf}(x) = \frac{2}{\sqrt{\pi}} \int_0^x e^{-\xi^2} d\xi$ The probability integral. ( Gauss error function)

$\vec{F}$ The bottom friction force of water flows

$\vec{f}_R = -\lambda_R \vec{u}$ the friction in fluid system $g$ The acceleration due to gravity

$K_\nu(z)$ The modified Bessel function of the second kind of order $(\nu = 1, 2)$

$h$ The water depth

H The Hartmann layer, $0 < z < Ha^{-1}$ ;

Ha The Hartmann number

ITER The International Thermonuclear Experimental Reactor

j Imaginary unit, $j = \sqrt{-1}$

L Length scale

**Li** The Lithium element ( Atomic number 3)

**Pb** The lead element ( Atomic number 82)

**Ni** The Nickel element ( Atomic number 28)

Nu The Nusselt number

$\vec{n}$ The unit normal vector to the surface

*Re* The Reinholds number

$S$ The stability parameter

$S_c$ The critical stability value

**Si** The Silicon Element ( Atomic number 14)

T The temperature in Kelvin.

$\vec{u}$ & $\vec{v}$ Velocity vectors

v The velocity scale

$V_c$ The core velocity constant

X Real part of Z

Y Imaginary part of Z

$Y_\nu(s)$ Bessel function of the second kind of order $\nu$

W The distant wake, $Ha < z < +\infty$.

$\tilde{z} = \tilde{\chi}_0 \tilde{f}(\tilde{x})$ The roughness of the surface of a channel's wall

## List of Greek Symbols

$\Gamma(x)$ Euler Gamma function

$\Delta$ Laplacian , $\Delta f(x,y,z) = \frac{\partial^2 f}{\partial x^2} + \frac{\partial^2 f}{\partial y^2} + \frac{\partial^2 f}{\partial z^2}$

$$\Delta f(r,\phi,z) = \frac{1}{r}\frac{\partial}{\partial r}\left(r\frac{\partial f}{\partial r}\right) + \frac{1}{r^2}\frac{\partial^2 f}{\phi^2} + \frac{\partial^2 f}{\partial z^2}$$

$\delta(\tilde{x})$ The Dirac delta function

$\lambda_R$ The coefficient of Rayleigh friction

$\mu_0$ Magnetic constant

$\rho$ Density of fluid

$\nu$ The Viscosity of fluid

$\tilde{\rho}$ Charge density

$\sigma$ Conductivity

$\psi$ Scalar electric potential intensity

$\tilde{\psi}$ Scalar electric potential, $\tilde{\psi} = \psi e^{jwt}$

$\omega$ Frequency

$\eta(\tilde{x}) = \begin{cases} 0, \tilde{x} < 0, \\ 1, \tilde{x} > 0. \end{cases}$ The Heaviside step function

$\phi$ Potential of current

$$V_y{}^c(\lambda, z) = \sqrt{\frac{2}{\pi}}\int_0^\infty V_y(x,z)\cos\lambda x dx$$ The Fourier cosine transform

$\Phi^s(\lambda,z) = \sqrt{\frac{2}{\pi}}\int_0^\infty \Phi(x,z)\sin\lambda x dx$. The Fourier sine transforms

Coordinate systems

( x,y,z) Cartesian coordinates, $x,y,z \in \Re$

(r, $\phi$,z) Cylindrical polar coordinates , $r \geq 0,\ 0 \leq \phi \leq 2r,\quad z \in \Re$

$(\rho,\theta,\phi)$ Spherical coordinates , $\rho \geq 0$, $0 \leq \theta \leq 2\pi$, $0 \leq \phi \leq \pi$,

**Classes of definite integrals**

$$\int_0^{\infty} \frac{P_n(\lambda^2)}{Q_m(\lambda^2)} e^{-a\sqrt{\lambda^2+b^2}} \frac{\cos\lambda\cos\lambda x}{\lambda^2-\frac{\pi^2}{4}} d\lambda, \quad I_1 = \sqrt{\frac{2}{\pi}} \int_0^{\infty} \frac{P_n(\lambda^2)}{Q_m(\lambda^2)} \frac{\cos\lambda\cos\lambda x\, d\lambda}{\lambda^2-\frac{\pi^2}{4}} = \varphi(x),$$

## Appendix 2

LIST OF FIGURES AND TABLES

## REFERENCES

**( In Alphabetical order )**

[1] Abdou.M. Sawan M. Physics and Technology conditions for attaining Tritium self Sufficiency for the DT fuel cycle . Fusion Engineering & Design, 81:( 8-14), 1131-1144/ (2006).

[2] Antimirov M.Ya., Lielausis O.A., Ligere E.S. Shishko A.Ya. Linear approximation to the flow over roughness elements in a strong magnetic field. Fifth International Pamir Conference on Fundamental and Applied MHD, Volume 1. Ramatuelle, France/ (2002).

[3] Antimirov M.Ya., Kolyshkin, A.A. Vaillancourt, R. Applied Integral Transforms. Springer-Verlag 265 pages, pp,37-234. USA/ (1993).

[4] Antimirov M.Ya. , Kolyshkin, A.A. Vaillancourt, R. Complex variables. pp 23-61 . London, Boston, New-York, Sidney, Tokyo, Toronto. Academic Press / (1998).

[5] Antimirov M.Ya., Kolyshkin, A.A. Journal Heat and Mass Transfer, Effects of MHD free convection and mass transfer on the flow past a vibrating infinite vertical circular cylinder Issue Volume 24, Number 4 , pp.243-250. Publisher Springer/ (1989).

[6] Antimirov.M.Ya, Dzenite I. Evaluation of new classes of Definite Integrals// Scientific

Proceedings at Riga Technical University,5th series: Computer Science,43rd thematic issue Volume 7, pp 32-39. Riga, LATVIA/ (2001).

[7] Antimirov.M.Ya, Dzenite I. Evaluation of new classes of Definite Integrals // Proceeding of the 3rd European Congress of Mathematics, ECM . Barcelona (SPAIN) -July 10-15 / (2000).

[8] Aranson L.S. & Cramer L. The world of the complex Ginzberg-Laundau equation. Review of modern Physics 74:99-143/ ( 2002).

[9] Benamati G., Fazio G, .Ricapito C: Mechanical and corrosion behavior of EUROFER 97 steel exposed to Pb-17Li.J. vol.307-311, 2, pp.1379-1383. Nucl. Mat/ (2002).

[10] Blennerhassett P.J. On the generation of waves by wind , Philosophical transactions of the royal society of London, Ser. A Mathematical and Physical Sciences 298: pp 451-494 / (1980).

[11] Buikis A, Kalis H. Numerical modeling of heat transfer in magnetohydrodynamic flows in a finite cylinder. Computational Methods in Applied Mathematics , vol.2. No.3, pp.243-259/ (2002).

[12] Chaddad I.A., Antimirov M.Ya. Solution of a problem to the flow over the roughness elements of a special form in a strong magnetic field // Scientific Proceedings at Riga Technical University, Computer Science, 45th thematic issue. Vol.11, MHD Riga , LATVIA/ ( 2003).

[13] Chaddad I. A., Antimirov M.Ya. Analytical solution of the MHD problem to the flow over the roughness elements using the Dirac Delta function // Scientific Proceedings at Riga Technical University,5th series: Computer Science, 46th thematic issue.Vol.13, Riga, LATVIA/ (2004).

[14] Chaddad I. A., Kolyshkin A.A. Ginzburg-Landau model: an amplitude evolution equation for shallow wake flows", Proceedings of World Academy of Science, Engineering and Technology, vol. 28, pp. 1 – 5. April/ (2008).

[15] Chaddad, I. A, Kolyshkin A. A Ginzburg-Landau model: an amplitude evolution equation for shallow wake flows", International conference on Mathematics and Statistics, Rome, Italy, April 25 – 27/ (2008).

[16] Chaddad I. A., Kolyshkin A. Ginzburg-Landau model: an amplitude evolution equation for shallow wake flows", International Journal of Mathematical, Physical and Engineering Sciences, vol. 2, no. 3, pp. 126 – 130/ (2008).

[17] Chaddad I. A, Ligere E.S.The transformation of one class of integrals containing oscillating functions and its application to some MHD problems// Proceeding of Riga Technical University, 5th series: Computer Science, 45th issue.Vol.7, Riga, LATVIA/ ( 2003).

[18] Chaddad.I.A. On the form of magnetic field of fully developed MHD equations. Proceeding of Riga Technical University,6th series: Computer Science, 46th issue.Vol.9, Riga LATVIA/ ( 2004).

[19] Chen D., & Jirka G.H. Absolute and convective instabilities of plane turbulent wakes in shallow water, Journal of fluid Mechanics 338: pp, 157-172/ (1997).

[20] Cross M.C. & Honenberg P.C . Thermodynamic properties of fusion reactor breeding materials, reviews of Modern Physics 65: pp.851-1112/ (1993).

[21] Davidson P.A. An introduction to Magnetohydrodynamics. Cambridge Univ Press, pp.56-61/ ( 2001).

[22] Dolzhanskii F.V. Krymov V.A., & Manin D. Yu. Stability and vertex structures of quasi-two-dimentional shear flow, Soviet Physics Uspekhi. 33: pp.495-520/ (1990).

[23] Dufrenoy T, Rodi W. Developments in computational modelling of turbulent flows. In 'ERCOFTAC'. Workshop on numerical simulation of unsteady flows. Cambridge Univ. Press.1-76.(Updated and shortened version ) , Presses Ponts, pp 13-38 Paris/ (1996).

[24] Drazin, P.G & reid W.H. Hydrodynamic stability (second edition) Cambridge University Press/ (2004).

[25] EFDA ( European Fusion Development Agreement) The European Fusion Research Programme:Strategic outlook for infrastructure towards DEMO. EFDA associates and F4E/ (2008).

[26] Fedderson F. Weakly nonlinear shear waves, Journal of Fluid Mechanics, 372: pp.71-91 Cambridge University Press/ (1998).

[27] Gazzola F., Secchi P. Some results about Stationary Navier-Stokes equations with a pressure dependent viscosity // Proceedings of the International Conference on Navier- Stokes. Equations, Theory and Numerical Methods, Varenna 1997, Pitman Research Notes , pp 131-137.Math. 388/ (1998).

[28] Gelfgat YM., Lielausis O.A., Shcherbinin E.V. Liquid metal under influence of electromagnetic forces. pp.76-91 . Riga, LATVIA/ (1975).

[29] Hartmann J. Theory of the laminar flow of an electrically conductive liquid in a homogenous magnetic field. MathFys Med 15 (6) . Cambridge University press/ (2004).

[30] Hunt, J.C.R. Magnetohydrodynamic flow in a rectangular duct.J. Fluid Mechanics (fourth edition ), pp 577-590/ (1988).

[31] Hunt, J.C.R. Liquid metal magnetohydrodynamics with strong magnetic fields: a report on Euromech 70-78(2), pp.261-288/ (1992).

[32] Ihle H., Wu C. Chemical thermodynamics of fusion reactor breeding materials and their interaction with tritium. - Nuclear.Materials. Vol.130, No.3, pp 454-464/ (1985).

[33] ITER Physics basis, Nuclear Physics Documentation vol.47, Number 6 pp. S1-414/ (2007).

[34] ITER EDA Agreement and Protocol 2. Documentation series Number 5.IAEA Vienna/ (1999).

[35] ITER special working group report on task 1 results. ITER Council proceeding/ (1998).

[36] ITER technology R&D.Fusion Engineering and design.Vol 5597-358/ (2001).

[37] ITER Council proceeding: ITER DEMO Documentation series Number 20. IAEA Vienna/ (2007).

[38] Jackson J.D. Classical electrodynamics.New York, London.John Wiley and sons,inc. pp. 131-153 vol.7/ (1986).

[39] Jefrey. P., Freidberg H. Plasma Physics and Fusion energy . Cambridge University Press 690, pp.344- 354 / (2006).

[40] Kallenrode May & Britt Space Physics, An introduction to Plasmas and particles in Magnetospheres. Second Edition. pp. 78- 82.Springer/ ( 2001 ).

[41] Kalis.H, Buikis.A, cepitis.J, Reinfelds.A) Numerical modeling of heat and Magnetohydrodynamics (MHD) flows in a finite cylinder. pp 45-50. vol. 4/ (2001).

[42] Kalis H., Kangro I. Numerical simulation of liquid-metal MHD flows in rectangular ducts. Mathematical Modelling and Analysis, Vilnius, Technika, , 6, pp. 85-96 / (2001).

[43] Kolyshkin A.A., Ghydaoui M.S. A quasi-steady approach to the stability of time-dependent flows in pipes. Journal of fluid mechanics. 465: pp. 301-330/ (2002).

[44] Kolyshkin A.A., Ghydaoui M.S. Stability analysis of shallow weak flows, journal of Fluid Mechanics 494: pp.355-377/ ( 2003).

[45] Kolyshkin A.A.,& Nazarovs S. Influence of averaging coefficients on weakly nonlinear stability of shallow flows, IASME transactions. Issue 1, vol.2:pp.86-91/ (2005).

[46] Kolyshkin A.A., Vaillancourt, R& Volodko, I. weakly nonlinear analysis of rapidly decelerated flow, IASME transactions. Issue 7, vol. 2 pp.1157-1165/ (2005).

[47] Kolyshkin A.A. Chaddad I.A., Ginzberg- Landau equation for stability of water flow in a weak nonlinear regime. Riga Technical University/ (Feb. 2008).

[48] KYOTO Protocol to the United Nations framework convection on climate change By United States Congress. House. Committee on Science United Nations Framework Convention on ClimateChange/ (2007).

[49] Leavenworth H.W., Clealy R.E. The solubility of Ni, Cr, Fe, Ti and Mo in lithium. Acta Metallurgica, vol.9, No.5, p.519-520/ (2002).

[50] Lorrain P., Lorrain F., Haule S. Magneto-fluid dynamics. Fundamentals and case studies of natural phenomena. Springer/ (2006).

[51] Max-Plank Institute for Plasma Physics- Research for Energy of the Future. Vol.2 Issue3. Berlin/ (2005).

[52] Micheal I. Liquid metal blanket reactor , Vol.7 , pp.33-36. New jersey/ (1996).

[53] Moreau R. Magnetohydrodynamics , Vol.3. pp 36-45.Kluwer academic publisher/ (1990).

[54] Muller U., Buhler L. Magnetofluiddynamics in channels and containers. Spinger/ (2001).

[55] Platacis.E, Shishko.A, Bucenieks.I., Krishbergs R., Lipsbergs G, Zik A., & Muktepāvela F., Assessement of Magnetic field effects on EUROFER Corrosion in Pb.17 Li at 550°C, EFDA, final report TTBC-006-D1, Salaspils, LATVIA/ ( 2006).

[56] Platacis.E, Shishko.A, Bucenieks.I., Krishbergs R. Analysis of the strong magnetic field influence on the Corrosion of EUROFER steel in Pb.17 Li flows, Salaspils, LATVIA /( 2008).

[57] Porleon L., Miyazaki,K. Reed C. Present understanding of MHD and heat transfer phenomena for liquid metal blankets. Report 8 ANL/TD/CP--83938; CONF-940664-27, Washington, DC , USA/ (1998).

[58] Priest & Forbes, MHD Theory and Applications. Cambridge University Press , vol2, pp 121-129/ ( 2000).

[59] Ramos J.I, Picologlu Numerical simulation of liquid metal MHD in rectangular ducts. Physics of Fluids 29, pp.34-42/ ( 1996).

[60] Ramos J. Report of of the PROTO Project on joint implementastion of ITER : Documentation series. Number 20. IAEA Vienna/ (2007).

[61] Schultz B. Thermophysical properties of the Li17Pb83 alloy. Fusion Engineering and Design activities . Vol. 14, Issues 3-4, pp.199-205/ (2005).

[62] Shimomura . yu. Simulation of turbulent flows in strong magnatic fields, American Mechanics Society & Intitute of Nuclear Physics, pp 23-28/ ( 2004).

[63] Shimomura . yu. Numerical Simulation on Magnetohydrodynamic Flow in the Disk MHD Generators . pp. 8-16/ (1991).

[64] Simon N., Terlain A., Flament T. Nuclear Materials 254 . pp 185-194/ (1998).

[65] Singh B. & Lal J. Heat transfer in an MHD channel flow with boundary conditions: Applied scientific research, Springer, ISSN 0003-6994, volume 48, number 1/ (1991) .

[66] Streeter V.L., Wylie E.B., & Bedford K.W. Fluid Mechanics ( 9th edition) McGraw Hill Vol. 3/ ( 1998).

[67] Stewartson, K. & Stuart J.T. A nonlinear instability theory for a wave system in plane Poiseuille flow. Journal of Fluid Mechanics 48:pp 529-545/ (1971).

[68] Stott G., PeterE. Diagnostics for thermonuclear Fusion reactors part 2, Proceedings of the International School of Plasma Physics "Piero Caldirola" Workshop on Diagnostics for Experimental Fusion Reactors, held September 4-12, in Varenna, Italy / (1997).

[69] Valdmanis J., Shishko A., & Krishbergs R. MHD flow pattern near the rough Hartmann wall subjected to corrosion process. 4th International conference of electromagnetic

proceeding of materials. FRANCE/ (2007).

[70] Yamada M., Zanstorff M.C. Plasma Physics, Princeton University, New Jersey Vol.5 pp. 123-126/ ( 1993).

[71] Antimirov M. Ya., Kremenetsky V.N. Magnetohydrodynamical flow of a flat submerged jet into semi-space in a strong magnetic fields . Magnitnaya Gidrodinamika, 32(1):56-62, (in Russian)/ (1996).

[72] Ditkin V.A., Proudnikov A. P. Integral transforms and operational calculus Moscow , FizMatGiz pp.524 (In Russian)/ (1979).

[73] Gryaznov G.M., Evtikhin V.A., Zavyalsky L.P. et al. Material science of liquid metal systems for thermonuclear reactors. - pp. 239-240. Energoizdat Publishing House, Moscow, (In Russian) / (1989).

[74] Prudnikov A.P., Brichkov Yu.A., Marilev O.I. Integrals and lines, Science journal, Moscow, (In Russian) / (1981).